A 001 293 368 5
UC SOUTHERN REGIONAL LIBRARY FACILITY

...mber 32 Price $1.00

...EPRINT AND CIRCULAR SERIES
OF THE
NATIONAL RESEARCH COUNCIL

MOMENTS AND STRESSES IN SLABS

By H. M. Westergaard
Assistant Professor of Theoretical and Applied Mechanics
University of Illinois

and

W. A. Slater
Engineer Physicist, U. S. Bureau of Standards

...IVERSITY OF CALIFORNIA
AT LOS ANGELES
NOV 27 19...
LIBRARY

Reprinted from *Proceedings of the American Concrete Institute*, vol. 17, 1921
By permission of the American Concrete Institute

Digitized by the Internet Archive
in 2007 with funding from
Microsoft Corporation

http://www.archive.org/details/momentsstressesi00westiala

MOMENTS AND STRESSES IN SLABS.

By H. M. Westergaard * and W. A. Slater.†

I.—INTRODUCTION.

1. The subject of the strength of flat slabs has received considerable attention during the past ten years. In November, 1910, the floor of the Deere and Webber Building ‡ at Minneapolis was tested. This was the first field test of a reinforced-concrete building floor in which strain measurements in the reinforcement and in the concrete were taken at various places in the building. Since that time many other tests have been made and much study has been given to the analytical side of the problem.

While considerable work has been done on the correlation of the analytical and the experimental results, it does not seem that the possibilities of useful work in this direction have been exhausted. It is the purpose of this paper to present information which correlates the results of tests of a fairly large number of slab structures with the results of analysis, so that the report may aid in the formulation of building regulations for slabs.

The field of this report may be divided into three parts: (a) analysis of moments and stresses in slabs, (b) study of the relation between the observed and the computed steel stresses in reinforced-concrete beams, made for the purpose of assisting in the interpretation of slab tests, (c) a study of the test results for flat slabs with a view of comparing the moments of the observed steel stresses with the bending moments indicated by the analysis, and of estimating the factor of safety.

The mathematical analysis is the work of Mr. Westergaard. The analysis of the beam tests to show the relation between the computed and the observed stresses is the work of Mr. Slater.

2. Acknowledgment. The expense of the report has been borne jointly by the American Concrete Institute and the United States Bureau of Standards.

The Corrugated Bar Co., of Buffalo, N. Y., and A. R. Lord, of the Lord Engineering Company, of Chicago, have furnished the results of a number of tests which had not been published, or which had been published only in part.

Acknowledgment is made to M. C. Nichols, graduate student, and to J. P. Lawlor and K. H. Siecke, seniors in engineering, in the University of Illinois, for their assistance in working up the data of the tests.

---

* Assistant Professor of Theoretical and Applied Mechanics, University of Illinois.

† Engineer Physicist, U. S. Bureau of Standards.

‡ A. R. Lord, Test of a Flat Slab Floor in a Reinforced-concrete Building, National Association of Cement Users, v. 6, 1910.

II.—ANALYSIS OF HOMOGENEOUS ELASTIC PLATES.

By H. M. Westergaard.

3. Scope of the Analysis. A slab is sometimes analyzed by considering it as divided into strips, each carrying a certain portion of the total load. One may expect to obtain, by this method, an exact analysis of a structure consisting of strips which cross one another and carry the loads as assumed. This structure, however, is quite different from the slab. The degree of approximation obtained may be judged by the resemblance or lack of resemblance between the strip-structure and the actual slab. As the resemblance is not very close, the approximation, naturally, is not very satisfactory. The ordinary theory of beams, too, is approximate, not exact, when applied to actual beams. Assumptions are introduced in the beam theory: for example, the plane cross-sections remain plane after the bending, and the material is perfectly elastic. But the approximation in the beam theory is much closer than in the strip analysis of plates. The explanation is simple: the beam to which the beam theory applies exactly has a closer resemblance to actual beams than the strip-structure has to slabs. It is possible, however, to analyze slabs more exactly than can be done by the strip method. If an analysis of slabs is to compare in exactness with beam analysis, then it must be based on a structure which resembles actual slabs more closely than does the strip structure. It is hardly possible at present to cover by analysis the whole range of designs of reinforced-concrete slabs. It is expedient, therefore, to confine this investigation to a single type. The homogeneous slab of perfectly elastic material is selected; homogeneous slabs have a fairly close resemblance to other slabs, and exact methods exist by which they may be analyzed. The selection of a homogeneous elastic material agrees with common practice in the investigation of statically indeterminate structures. For example, the distribution of bending moments in a reinforced-concrete arch or frame is often determined by replacing the structure by one of homogeneous material. The plan is then to investigate distributions of moments in homogeneous slabs. These distributions may be used as a basis for the study of the experimental data.

Theoretical analysis is under the disadvantage that its processes are often rather more remote from the actual phenomena which are studied, than are the processes of direct physical tests. For this reason alone it would be out of the question to rely on the results of theoretical analysis only. There are, on the other hand, advantages of theoretical analysis which fully warrant its extensive use in conjunction with physical tests. One may appreciate these advantages by looking upon the theoretical analysis as being, in a sense, a test in which the testing apparatus consists of the principles of statics and geometry, expressed in equations, and in which the structure tested is the structure assumed in the analysis. The equations may be solved with any desired exactness, and the structure has dimensions

and properties exactly as assumed, and is not subject to the incidental variations which so often have made it impossible to draw definite conclusions from physical tests. Besides, by the analysis one may cover whole ranges of variations of the structure or at least a great number of individual structures, while a physical test can deal with only a limited number of cases. For these reasons the analysis is of particular value as a basis of comparison and as a method of establishing continuity between results of separate, individual tests.

It will be seen from the historical summary which follows that the problem of flexure of plates is one on which scientists have been at work for more than a century. The methods, which have been developed by such men as Navier, St. Venant, Kirchhoff, and Lord Kelvin, have found their way into engineering literature in Europe. It has been possible, therefore, to build the present report, in part, on the work of previous investigators. The agreement between the results of different analyses of rectangular slabs supported on four sides, serves as evidence that the methods are dependable.

It has been thought desirable to follow the method of presenting the results first, and details of the processes afterwards. A historical summary, a statement of the limitations of the theory, and a derivation of the fundamental equations are followed by the report of results. The results deal with rectangular slabs supported on four edges, and with flat slabs supported on round column capitals. Details of the analysis will be given in the appendix A.

4. HISTORICAL SUMMARY. The incentive to the earliest studies of the flexure of plates appears to have been an interest in their vibrations, in particular those producing sound, rather than an interest in the stresses and strength. Euler, after having developed his theory of the flexure of beams, attempted to explain the tone-producing vibrations of bells by assuming a division into narrow strips (or rings), each of which would act as a beam,[1] but this application of the strip method was not satisfactory. Jacques Bernouilli (the younger), in a paper presented in 1788,[2] treated a square plate as if it consisted of two systems of crossing beams or strips, and he attempted in this way to explain the results of Chladni's experiments with vibrating plates,[3] in particular the so-called nodal figures. As might be expected, the results of this theory did not agree very well with the experimental data. In 1809 the French Institut, at the instigation of Napoleon, proposed as a prize subject a theoretical analysis of the tones of a vibrating plate. Mlle. Sophie Germain [4] made some unsuccessful attempts to win this prize, but won it in 1815, when she arrived finally at a

[1] Euler, De sono campanarum, Novi Commentarii Academiae Petropolitanae, v. 10, 1766.

[2] Jacques Bernouilli, Essai théorétique sur les vibrations des plaques élastiques rectangulaires et libres, Nova Acta Academiae Scientarum Petropolitanae, v. 5, 1787 (printed 1789).

[3] E. F. F. Chladni, Entdeckungen über die Theorie des Klanges, Leipzig, 1787.

[4] See Todhunter and Pearson, A History of the Theory of Elasticity, Cambridge, 1886, p. 147.

fairly satisfactory, though not faultless derivation of a fundamental equation for the flexural vibrations. But in the meantime, in 1811, Lagrange, who was a member of the committee to pass on the papers, had indicated in a letter this equation, which is known, therefore, as Lagrange's equation for the flexure and the vibration of plates (with the term depending on the motion omitted, it is the same as (11) in Art. 6).

In 1820, Navier,[5] in a paper presented before the French Academy, solved Lagrange's equation for the case of a rectangular plate with simply supported edges. By this solution one may compute the deflections and, therefore, also the curvatures and the stresses at any point of a plate of this kind, under any distributed uniform or non-uniform load. Navier's solution could be applied only to plates of this particular shape and with this type of support. Furthermore, a really acceptable derivation of Lagrange's equation, a derivation based on the stresses and deformations at all points of the plate, had not been found so far. Poisson,[6] in his famous paper on elasticity, published in 1829, obtained such a proof. With it, he derived a set of general boundary conditions (conditions of equilibrium and of deformation at the edge of the plate), and was then able to obtain solutions for circular plates, both for vibrations and for static flexure under a load which is symmetrical with respect to the center. Poisson's theoretical results were compared with results of tests, namely, with the experimental values, found by Savart for the radii of the nodal circles of three vibrating circular plates. A close agreement was found.

In a paper, published 1850, Kirchhoff[7] derived Lagrange's equation and the corresponding boundary conditions by using the energy principle, or the principle of least action. He found one boundary condition less than Poisson, namely, four at each point instead of Poisson's five. This difference gave rise to some discussion, but finally, in 1867, Kelvin and Tait[8] showed that there was only an apparent discrepancy, due to an interrelation between two of Poisson's conditions. This conclusion, as well as Kirchhoff's and Poisson's theories as a whole, applies, as might be expected, with limitations which are analogous to the limitations of the ordinary theory of beams. For example, the plate-theory ceases to apply when the span becomes small compared with the thickness of the plate, but, of course, in that case the structure has really ceased to be a plate in the ordinary sense. The question of the exact nature of the limitations called for further researches. Such were made by Bouissinesq.[9] His investigations have established the applicability of Poisson's and Kirchhoff's theories to

---

[5] See Saint-Venants annotated edition of Clebsch's Theory of Elasticity, Paris, 1883. Note by Saint-Venant, pp. 740-752.

[6] S. D. Poisson, Mémoire sur l'équilibre et le mouvement des corps élastique, Memoirs of the Paris Academy, v. 8, 1829, pp. 357-570. See Todhunter and Pearson, History of the Theory of Elasticity, 1886, pp. 241, 272.

[7] G. Kirchhoff, Ueber das Gleichgewicht und die Bewegung einer elastischen Scheibe, Crelles Journal, 1850, v. 40, pp. 51-88.

[8] Kelvin and Tait, Natural Philosophy, ed. 1, 1867. See A. E. H. Love, Mathematical Theory of Elasticity, ed. 1906, p. 438.

[9] J. Boussinesq, Étude nouvelle sur l'equilibre et le mouvement des corps solides élastiques dont certaines dimensions, sont très-petites par rapport a d'autres, Journal de Mathématiques, 1871, pp. 125-274, and 1879, pp. 329-344.

homogeneous elastic plates whose ratio of the thickness to the span is neither very large nor very small, that is, plates whose dimensions are not extreme.

With a theoretical foundation thus laid, the time was ready for efforts to obtain numerical results by application of the theory, that is, by solution of the general differential equation in specific cases of technical, or otherwise scientific importance. There was due also a change of chief interest in the problem from the question of vibrations to that of stresses and strength, that is, the time had come for the structural, rather than the acoustic problem to stand in the foreground. Lavoinne,[10] in 1872, tackled the question of a plane boiler bottom supported by stay-bolts. The problem is essentially the same as that of the flat slab (of homogeneous material) supported directly on column capitals, without girders, and carrying a uniform load. Lavoinne's solution is for the case in which Poisson's ratio of lateral contraction is equal to zero, but, as will be shown later, a correction for this lateral effect may be made afterward without any difficulty. Lavoinne, by the use of a double-infinite Fourier series, solves Lagrange's equation for a uniformly loaded, infinitely large plate which is divided by the supports into rectangular panels, and which has its supporting forces uniformly distributed within small rectangular areas around the corners of the panels. The series for the load become divergent when the size of the rectangles of the supporting forces becomes zero, that is, when the supports are point-supports. The same problem was treated by Grashoff,[11] whose solution, however, is incorrect, since it disregards some of the boundary conditions. G. H. Bryan,[12] in 1890, made an analysis of the buckling of a rectangular elastic plate, due to forces in its own plane. Maurice Lévy [13] showed how Lagrange's equation, when applied to rectangular plates with various types of supports, may be integrated by a single-infinite series depending on hyperbolic functions, instead of the double-infinite Fourier series in Navier's solution.

In the meantime, a different path of investigation, namely, that of semi-empirical methods, had been entered into by Galliot and by C. Bach. Galliot [14] compared observed deflections of plates in lock-gates (under hydraulic pressure) with the results of an approximate theory, which, in this manner, he found applicable as a basis of design. Bach's [15] empirical formulas are based on laboratory tests in connection with some very simple theoretical considerations. An example will illustrate his method. He found by test that the line of failure, the danger section, of a square plate,

---

[10] Lavoinne, Sur la résistance des parois planes des chaudières a vapeur, Annales des Ponts et Chaussées, v. 3, 1872, pp. 276-303.

[11] F. Grashof, Elasticität und Festigkeit, ed. 1878, p. 351.

[12] G. H. Bryan, On the stability of a plane plate under thrusts in its own plane, London Math. Soc., v. 22, 1890, pp. 54-67.

[13] Maurice Lévy, Sur l'équilibre élastique d'une plaque rectangulaire, Comptes Rendus, v. 129, 1899, pp. 535-539.

[14] Galliot, Étude sur les portes d'écluses en tôle, Annales des Ponts et Chaussées, 1887, v. 14, pp. 704-756.

[15] C. Bach, Versuche über die Widerstandsfähigkeit ebener Platten, Zeitschr. d. Ver. deutscher Ingenieure, v. 34, 1890, pp. 1041-1048, 1080-1086, 1103-1111, 1139-1144.

simply supported along the edges, is along the diagonals. It happens that the average bending moment per unit length across the diagonal can be determined by a simple analysis based on elementary principles of statics (the result is $1/24\ wl^2$ where w is the load per unit-area, l the span). But this analysis gives no information as to the distribution of the bending moment. Bach, then, multiplies the average moment by an empirical constant, found by comparison with the tests. The investigation included cases of rectangular and circular plates, with distributed or concentrated loads. Bach's formulas, because of their simplicity and sound empirical basis, have been used rather extensively. A similar treatment of the problem of the plane boiler-bottom, supported by stay-bolts, was added later.[16] The analysis of flat slabs, which was indicated in 1914 by Nichols,[17] may be recognized as falling into the same category as Bach's analyses. Since its first appearance, Nichol's analysis has been used by many as a basis of comparison between results of tests and rules of design.

Since the close of the nineteenth century the investigators of the theoretical side of the question have been confronted with three definite tasks. Analyses which would cover the extreme cases in which the plate is either very thick or very thin were called for; new theoretical methods were needed, for example, for the solution of Lagrange's equation; and numerical results applying to specific cases had to be worked out.

Theories applying to plates of ordinary thickness, as well as to thick plates with a short span, have been developed by Michell,[18] Love,[19] and Dougal.[20] The latter, when he applied the exact theory to plates of ordinary thickness, found agreement, in a number of specific cases, with the results derived by Lagrange's equation. Thin plates, whose deflections have become so large compared with the thickness that the curving of the cross-section must be considered, have been treated by A. Föppl.[21]

As an example of the development of methods, mention may be made again of Lévy's solution of hyperbolic functions. Dougall, in the paper just quoted, used Bessel-functions, and obtained thereby some rapidly converging solutions. Other solutions by various series have been contributed by Hadamard,[22] Lauricella,[23] Happel, [24] and Botasso.[25] The modern theory

---

[16] C. Bach, Die Berechnung flacher, durch Anker oder Stehbolzen unterstützer Kesselwandungen und die Ergebnisse der neuesten hierauf bezüglichen Versuche, Zeitschr. d. Ver. deutscher Ingenieure, 1894, pp. 341-349.

[17] J. R. Nichols, Statical limitations upon the steel requirement in reinforced-concrete flat slab floors, Am. Soc. C. E., Trans., v. 77, 1914, pp. 1670-1681.

[18] J. H. Michell, On the direct determination of stress in an elastic solid, with application to the theory of plates, London Math. Soc. Proc., v. 31, 1899, pp. 100-124.

[19] A. E. H. Love, Mathematical Theory of Elasticity, ed. 1906, pp. 434-465.

[20] J. Dougall, An analytical theory of the equilibrium of an isotropic elastic plate, Edinburgh Royal Soc. Trans. v. 41, 1903-4, pp. 129-227.

[21] A. Föppl, Technische Mechanik, v. 5, ed. 1918, pp. 132-144; also: A. and L. Föppl, Drang und Zwang, v. 1, 1920, pp. 216-232.

[22] J. Hadamard, Sur le problème d' analyse relatif à l'équilibre des plaques élastiques encastrées, Institut de France, Acad. des Sciences, Mémoires presentes par divers savants, v. 33, 1908, No. 4, 128 pp.

[23] G. Lauricella, Sur l'intégration de l'équation relative a l'équilibre des plaques élastiques encastrées, Acta Mathematica, v. 32, 1909, pp. 201-256.

[24] H. Happel, Ueber das Gleichgewicht rechteckiger Platten, Göttinger Nachrichten, Math. phys. Klasse, 1914, pp. 37-62 (rectangular plate with fixed edges and with a concentrated load at the center).

[25] Matteo Botasso, Sull'equilibrio delle piastre elastiche piane appoggiate lungo il contorno, R. Accademia della scienze di Torino, Atti, v. 50, 1915, pp. 823-838.

of integral equations has opened the way for new solutions, by series which may fit almost any type of plate (see, for example, Hadamard's and Happel's works, which were just quoted). A method of a different type is Ritz's[26] approximate method, which was indicated in 1909, which may be applied to any elastic structure, and which was applied by Ritz himself to plate problems, and after him, by other writers, to water tanks, domes, etc., and to plates. The method makes use of series of properly chosen functions, each of which must satisfy the boundary conditions of the problem, and each of which is introduced in the series with a variable coefficient which is unknown beforehand. Then one determines a suitable, finite number of these coefficients by the principle of energy-minimum. Ritz's method has proved itself an effective addition to our analytical equipment. Another approximate method is that of difference equations which was used by N. J. Nielsen[27] in a work on stresses in plates. His results will be mentioned later. By the method, the differentials of the differential equations are replaced by finite differences, and the problem is then reduced to the solution of a set of linear equations, in which, for example, the deflections at a finite number of points enter as variables. The method is used, in fact, when string curves for distributed loads (for example, in the investigation of beams) are replaced by string polygons.

Investigations in the theory of plates, made with the purpose of obtaining definite results in specific cases, have appeared in a fairly great number during recent years. Estanave,[28] in a thesis in Paris, 1900, analyzed various cases of the flexure of rectangular plates. Simic,[29] in 1908, gave an approximate solution for rectangular plates with simply supported edges. He used a rather short series of polynomials. The results agree fairly well with those found by later investigations. Hager,[30] in a work published in 1911, applied trigonometric series, and used Ritz's method, in an investigation of rectangular slabs. His results are incorrect, in so far as they apply to homogeneous plates, because the torsional moments in the sections parallel to the edges are not considered; the results may, however, have some interest with reference to two-way-reinforced concrete slabs, which have a reduced torsional resistance in these sections. The same criticism applies to an investigation, first published in 1911, by Danusso.[31] He

[26] Walter Ritz, Ueber eine neue Methodé zur Lösung gewisser Variationsprobleme der mathematischen Physik, Crelles Journal, v. 135, 1909, pp. 1-61. See also H. Lorenz, Technische Elastizitätslehre, 1913, p. 397.

[27] N. J. Nielsen, Bestemmelse af Spaendinger i Plader ved Anvendelse af Differensligninger, Copenhagen, 1920.

[28] E. Estanave, Contribution a l'étude de l'équilibre élastique d'une plaque mince, Paris, 1900.

[29] Jovo Simie, Ein Beitrag zur Berechnung der rechteckigen Platten, Zeitschr. des oesterr. Ingenieur- und Architekten-Vereines, v. 60, 1908, pp. 709-714. Another paper by Simic (Oesterr. Wochenschrift für den offentlichen Baudienst, 1909), was criticized by Mesnager (see the paper quoted later, of 1916, p. 417) on the ground that torsional moments had not been duly considered.

[30] Karl Hager, Berechnung ebener rechteckiger Platten mittels trigonometrischer Reihen, Munich and Berlin, 1911. For criticism, see Mesnager's paper of 1916, which is quoted below, pp. 414-418.

[31] See Arturo Danusso, Beitrag zur Berechnung der kreuzweise bewehrten Eisenbetonplatten und deren Aufnahmeträger. Prepared in German by Hugo von Bronneck after the articles by Danusso in Il Cemento, 1911, No. 1-10; Forscherarbeiten auf dem Gebiete des Eisenbetons, v. 21, 1913, 114 pp.

replaces the rectangular slab, as Jacques Bernouilli had done in 1789, by two systems of crossing beams which are connected at the points of intersection, only he considers a finite, instead of an infinite number of such beams. This structure, again, has no torsional resistance in the sections parallel to the sides. A structure consisting of three closely spaced systems of crossing beams in three different directions would, on the other hand, have both torsional and bending resistance in all directions. Such a structure was used by Danusso in the analysis of a triangular plate, and his results may be expected to be approximately correct in this special case, as long as Poisson's ratio may be assumed equal to zero.

In a note issued in 1912 by the French Council on Bridges and Roads [32] some design formulas were presented, together with various analyses based on the differential equation of flexure. The years 1913 to 1916 brought forth a rather valuable collection of exact or approximately exact studies of rectangular slabs supported on four sides. The authors referred to are Hencky,[33] Paschoud,[34] Leitz,[35] Nádai,[36] and Mesnager,[37] and they appear to have worked entirely independently of each other. Their numerical results agree, on the whole, very well. A treatment of flat slabs by Eddy,[38] published in 1913, was, unfortunately, not free from faults. Incorrect boundary conditions, inconsistencies in the consideration of the negative moments across the rectangular belts, and the use of an abnormally high value of Poisson's ratio, namely, one-half, led, naturally, to incorrect results. One may also object to his use of the terms "true" and apparent" stresses and bending moments in a manner which is contrary to common usage.

N. J. Nielsen's[27] investigation, published in 1920, was mentioned on account of the use of difference equations. He proved the applicability of the method by applying it to known cases, where the results found by previous investigators had shown approximate agreement. Analyses of rectangular slabs supported on four sides served this purpose. He then analyzed the action of flat slabs with different loading arrangements, with square or rectangular panels, stiff or flexible columns, etc., and he made special studies of the stresses in exterior panels and corner panels. The approximation obtained does not seem to be quite satisfactory in all the

---

[32] Conceil Général des Ponts et Chaussées, Calcul des hourdis en béton armé, Annales des Ponts and Chaussées, 1912, VI, pp. 469-529.

[33] H. Hencky, Ueber den Spannungszustand in rechteckigen ebener Platten, 1913, 94 pp. (thesis in Darmstadt).

[34] Maurice Paschoud, Sur l'application de la méthode de Walter Ritz à l'étude de l'équilibre élastique d'une plaque carrée mince, thesis in Paris, 1914, 56 pp. (See Mesnager's paper, quoted later.)

[35] H. Leitz, Die Berechnung der frei aufliegenden, rechteckingen Platten, Forscherarbeiten auf dem Gebiete des Eisenbetons, v. 23, 1914, 59 pp. He added later an analysis of rectangular plates with fixed edges, see his paper: Die Berechnung der eingespannten, rechteckigen Platte, Zeitschr. f. Math. u. Phys., v. 64, 1917, pp. 262-272.

[36] Arpád Nádai, Die Formänderungen und die Spannungen von rechteckigen elastichen Platten, Forschungsarbeiten auf dem Gebiete des Ingenieurwesens, v. 170-171, 1915, 87 pp. Also, in a shorter presentation, in Zeitschr. d. Ver. deutscher Ingenieure, 1914, pp. 487-494, 540-550.

[37] Mesnager, Moments et flèches des plaques, rectangulaires minces, portant une charge uniformément répartie, Annales des Ponts et Chaussées, 1916, IV, pp. 313-438.

[38] H. T. Eddy, The theory of the flexure and strength of rectangular flat plates applied to reinforced-concrete floor slabs, 1913.

cases. This deficiency might have been remedied by the use of a greater number of terms, but thereby the complexity of the work would, of course, have increased. Nielsen's analysis is the first in which approximately exact methods of analysis are applied, on an extensive scale, to the flat-slab problem. His results will be quoted later, on various occasions.

The experimental work on steel plates had been continued, in the meantime, by Bach.[39] Another contribution of the sort is due to Crawford.[40] A test of a rubber model, designed to represent a flat-slab structure, was made by Trelease [41] for the Corrugated Bar Co. The experimental work on concrete slabs is mentioned at other places in this report.

Among the treatises in which the slab-problem is dealt with extensively may be mentioned those by Love, Föppl, and Lorenz.[42]

5. LIMITATIONS OF THE THEORY. The properties of the plates dealt with in the following analysis will now be defined.

a. In order to simplify the discussions the plates will be assumed to be horizontal, the applied forces vertical.

b. The plates are medium-thick. A medium-thick plate is defined here as one which is neither so thick in proportion to the span that an appreciable portion of the energy of deformation is contributed by the vertical stresses (shears, tensions, and compressions), nor so thin that an appreciable part of the energy is due to the stretchings and shortenings of the middle plane when the plate is bent into a double-curved surface. All plates and plate-like structures may be divided into four groups according to thickness: thick plates, in which the vertical stresses are important; medium-thick plates, to which the present analysis applied; thin plates, whose resistance to transverse loads depends in part on the stretching of the middle plane; and membranes, which are so thin that the transverse resistance depends exclusively on the stretching. The membrane, of course, is not a plate in the ordinary sense, any more than a suspended cable is a beam. The thick and the thin plates require special theories, such as those developed by Michell, Love, Dougall, and Föppl (see Art. 4). These extreme cases are eliminated by definition. Plates of such proportions as are generally used in reinforced-concrete floor slabs may be classified as medium-thick, and fall within the scope of the analysis.

c. The plates are homogeneous and of uniform thickness. Since the vertical stresses do not contribute directly to the work of deformation or to the deflections, it is sufficient to specify the elastic properties with regard

---

[39] C. Bach, Versuche über die Formänderung und die Widerstandsfähigkeit ebener Wandungen, Zeitschr. d. Ver. deutscher Ingenieure, 1908, pp. 1781-1789, 1876-1881.

[40] W. J. Crawford, The elastic strength of flat plates, an experimental research, Edinburgh Roy. Soc. Proc., v. 32, 1911-1912, pp. 348-389. Additional note by C. G. Knott, pp. 390-392.

[41] Corrugated Bar Co., Bulletin on flat slabs, Buffalo, 1912.

[42] A. E. H. Love, Mathematical Theory of Elasticity, ed. 1906, Chapter XXII.
A. Föppl, Technishe Mechanik, v. 3 and v. 5 (ed. 1919 and 1918).
A. and L. Föppl, Drang und Zwang, v. 1, 1920.
H. Lorenz, Technische Elasticitätslehre, 1913, Chapter VII.
See also: Todhunter and Pearson, History of the theory of elasticity, 1886-1893; and: Encyclopädie der mathematischen Wissenchaften, Vol. IV, 25, 1907, pp. 181-190, and 27, 1910, pp. 348-352.

to the horizontal strains. Hooke's law is assumed to apply to the horizontal strains, and the elastic properties, then, depend on two constants; namely,

E = modulus of elasticity for horizontal tensions and compressions, and

K = Poisson's ratio of lateral horizontal contraction to longitudinal horizontal elongation.

d. A straight line, drawn vertically through the plate before bending, remains straight after bending. This assumption is consistent with the preceding specifications that the plate is medium-thick, and is homogeneous and of uniform thickness, and it is entirely analogous to the assumption in the theory of beams that a plane cross-section before bending remains plane after bending. It follows that the horizontal unit-stresses, tensions, compressions, and shears, in vertical sections are distributed according to straight-line diagrams, as the tensions and compressions in the cross-section of a beam.

e. The zero-points in these diagrams for the horizontal stresses in vertical sections are in the middle plane, which is therefore a neutral plane.

As to the question of the consistency of these assumed properties reference may be made to the theoretical works mentioned in the historical summary (Art. 4).

6. THE EQUATIONS APPLYING TO A SMALL RECTANGULAR ELEMENT OF THE SLAB.

The following notation is used:

x, y = horizontal rectangular coördinates (see Fig. 1).

z = vertical deflection, positive downward.

V_x = vertical shear per unit length in the section perpendicular to x at point (x, y); the positive direction of V_x is indicated by the arrow in Fig. 1.

V_y = same in section perpendicular to y.

M_x = bending moment per unit length in the section perpendicular to x at point (x, y); M_x is positive when causing compression at the top and tension at the bottom.

M_y = same in section perpendicular to y.

M_z = torsional moment per unit length in sections perpendicular to x and y at point (x, y); the positive directions are indicated by the arrows in Fig. 1; that is, the torsional moment is considered positive when it causes shortenings at the top along the diagonal through the corner (x, y) of the element.

E = modulus of elasticity of the material.

K = Poisson's ratio of lateral contraction to longitudinal elongation. Concerning E and K, see the preceding article.

I = moment of inertia per unit length; $I = \frac{1}{12} d^3$ when d is the thickness of the slab.

Fig. 1 shows a small rectangular element of the slab with the forces and couples acting on it. The location of the element is defined by the horizontal coördinates x and y of the midpoint of the lower left-hand edge

in the figure. The dimensions are dx and dy in the x- and y-directions, and the thickness of the slab in the z-direction. The deflection at point (x, y) is measured by z, which is positive downward.

The loads are: first, the applied surface load w per unit-area, in the z-direction; that is, a total load of $w\,dx\,dy$; secondly, the internal vertical

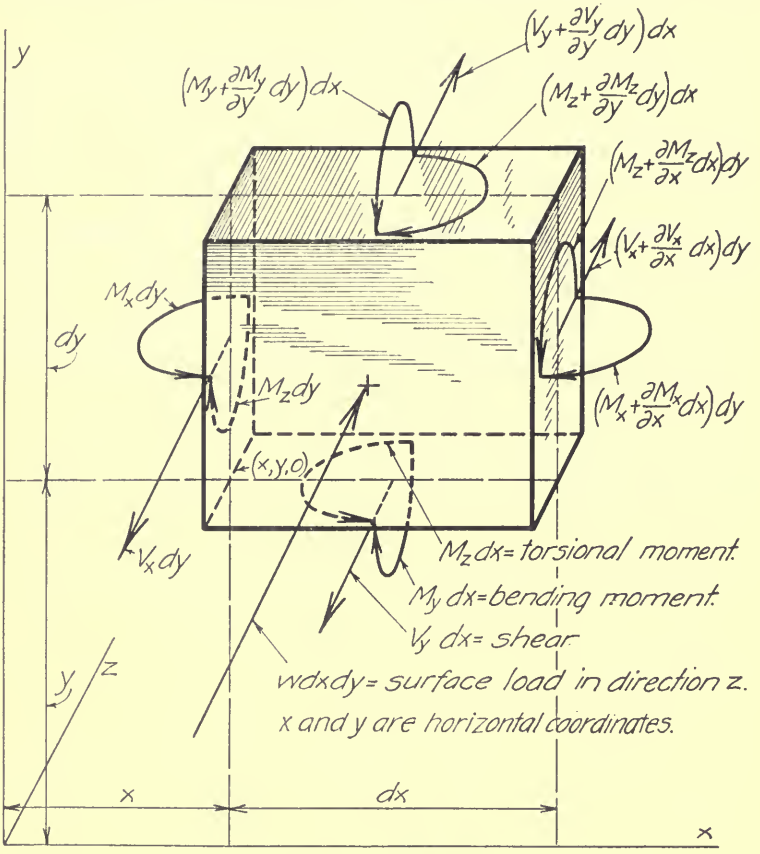

FIG. 1.—RECTANGULAR ELEMENT OF SLAB.

shears, bending moments and torsional moments which are listed in Table 1. The values per unit-length are V_x, $V_x + \frac{\delta V_x}{\delta x}dx$, V_y ..... etc., hence the total values are $V_x\,dy$, $(V_x + \frac{\delta V_x}{\delta x}dx)\,dy$, $V_y dx$ ....., etc. The vertical shears and the bending moments are of the same nature as the vertical shears and the bending moments in beams. The torsional moments

M_z are resultants of the horizontal shears in the vertical faces. The values of M_z for the lower and left-hand faces in Fig. 1 are equal on account of the law of equality of shears in sections perpendicular to one another.

TABLE I.—FORCES AND COUPLES IN FIG. 1.

TABLE I.

Face	Vertical shear		Bending moment		Torsional moment	
	Value	Direction	Value	Direction	Value	Direction
Left face	$V_x dy$	$-z$	$M_x dy$	xz	$M_z dy$	yz
Right face	$(V_x + \frac{\partial V_x}{\partial x} dx) dy$	$+z$	$(M_x + \frac{\partial M_x}{\partial x} dx) dy$	zx	$(M_z + \frac{\partial M_z}{\partial x} dx) dy$	zy
Lower face in Fig. 1.	$V_y dx$	$-z$	$M_y dx$	yz	$M_z dx$	xz
Upper face in Fig. 1.	$(V_y + \frac{\partial V_y}{\partial y} dy) dx$	$+z$	$(M_y + \frac{\partial M_y}{\partial y} dy) dx$	zy	$(M_z + \frac{\partial M_z}{\partial y} dy) dx$	zx

The directions indicated are the positive directions of the loads.

The forces shown in Fig. 1 must hold the element of the slab in equilibrium. By equating the sum of the vertical components (in the z-direction) to zero and dividing by $dx\,dy$ we find

$$\frac{\delta V_x}{\delta x} + \frac{\delta V_y}{\delta y} + w = 0 \quad . \tag{1}$$

By equating to zero the sum of the moments about a line parallel to y through the center of the element, and dividing by $dx\,dy$, we find

$$\frac{\delta M_x}{\delta x} + \frac{\delta M_z}{\delta y} = V_x \quad , \tag{2}$$

and by analogy,

$$\frac{\delta M_y}{\delta y} + \frac{\delta M_z}{\delta x} = V_y \quad . \tag{3}$$

By differentiating (2) and (3) with respect to x and y, respectively, and substituting in (1), we find

$$\frac{\delta^2 M_x}{\delta x^2} + 2\frac{\delta^2 M_z}{\delta x \delta y} + \frac{\delta^2 M_y}{\delta y^2} = -w \quad . \tag{4}$$

The equations (1) to (4) are equations of equilibrium. If the slab is bent, say, in the x-direction only, so that the lines parallel to y remain straight and parallel to y, then the slab acts as a beam, V_y, M_y, and M_z become zero, and the formulas (1) to (4) are reduced to the well-known equations from beam theory:

$$w = -\frac{dV_x}{dx}; \quad V_x = \frac{\delta M_x}{\delta x}; \quad w = -\frac{d^2 M_x}{dx^2}$$

The terms containing M_z represent the effect of the torsional resistance.

The equations (1) to (4) were derived by the statical conditions of equilibrium without reference to the deformations. That is, (1) to (4) apply without reference to the particular elastic properties. Since they are merely equations of equilibrium, they apply to non-homogeneous slabs, such as reinforced-concrete slabs, and to slabs with reduced torsional resistance, as well as to the homogeneous elastic plates.

We now consider the deformations and their relations to the loads. The plate is again assumed to be homogeneous. Fig. 2 illustrates three types of deformation: bending in the x-direction shown in Fig. 2(a); in the y-direction shown in Fig. 2(b); and torsion in the xy-directions shown in Fig. 2(c). Any state of flexure of an element of the slab may be resolved into component parts of these three types. The amounts of deformation are measured in Fig. 2(a) and Fig. 2(b) by the curvatures $-\frac{\delta^2 z}{\delta x^2}$ and $-\frac{\delta^2 z}{\delta y^2}$ (as in beams), and in Fig. 2(c) by the rate of change of slope, that is, by $-\frac{\delta\left(\frac{\delta z}{\delta x}\right)}{\delta y} = -\frac{\delta\left(\frac{\delta z}{\delta y}\right)}{\delta x} = \frac{\delta^2 z}{\delta x \delta y}$

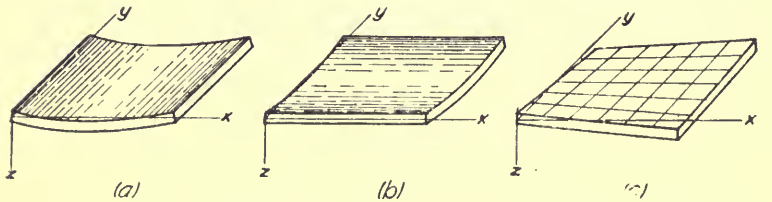

FIG. 2.—DEFORMATIONS OF ELEMENT OF SLAB.

A bending moment M_x, acting alone, produces the curvatures $-\frac{\delta^2 z}{\delta x^2} = \frac{M_x}{EI}$ in the x-direction, $-\frac{\delta^2 x}{\delta y^2} = K\frac{M_y}{EI}$ in the y-direction, and no twist; these results may be taken directly from the theory of beams. The torsional couples M_z produce a twist $-\frac{\delta^2 z}{\delta x\, \delta y}$ which may be determined by introducing temporarily another system of coördinates, x', y', making angles of 45° with the system of x, y. The couples M_z are replaced by an equivalent combination of couples consisting of the bending moments $M_{x'} = M_z$ in the x'-direction and $M_{y'} = -M_z$ in the y'-direction. These bending moments produce the curvatures $-\frac{\delta^2 z}{\delta x'^2} = \frac{M_{x'} - KM_{y'}}{EI} = \frac{M_z(1+K)}{EI}$, $-\frac{\delta^2 z}{\delta y'^2} = -\frac{M_z(1+K)}{EI}$, in terms of which the twist may be expressed by the transformation formula

$$-\frac{\delta^2 z}{\delta x \delta y} = \frac{1}{2}\left(-\frac{\delta^2 z}{\delta x'^2} + \frac{\delta^2 z}{\delta y'^2}\right), \text{ that is } -\frac{\delta^2 z}{\delta x \delta y} = \frac{M_z(1+K)}{EI}.$$

In the general case the bending moments M_x and M_y, and the torsional moment M_z are all present, and the resultant deformations are then

$$-\frac{\delta^2 z}{\delta x^2} = \frac{M_x - KM_y}{EI} , \tag{5}$$

$$-\frac{\delta^2 z}{\delta y^2} = \frac{-KM_x + M_y}{EI} , \tag{6}$$

$$-\frac{\delta^2 z}{\delta x \delta y} = \frac{(1+K)M_z}{EI} . \tag{7}$$

Equations (5), (6), and (7) express the deformations in terms of the moments. By solving them with respect to the moments, the moments are found in terms of the deformations:

$$M_x = \frac{EI}{1-K^2}\left(-\frac{\delta^2 z}{\delta x^2} - K\frac{\delta^2 z}{\delta y^2}\right) , \tag{8}$$

$$M_y = \frac{EI}{1-K^2}\left(-K\frac{\delta^2 z}{\delta x^2} - \frac{\delta^2 z}{\delta y^2}\right) , \tag{9}$$

$$\text{and} \quad M_z = \frac{EI}{1+K}\left(-\frac{\delta^2 z}{\delta x \delta y}\right) . \tag{10}$$

By substituting these values of the moments in equation (4), which is a relation between the moments and the applied load, a direct relation is found between the applied load w and the deformations, z. The result is Lagrange's equation for the flexure of plates, or, the "plate equation,"

$$\frac{\delta^4 z}{\delta x^4} + 2\frac{\delta^4 z}{\delta x^2 \delta y^2} + \frac{\delta^4 z}{\delta y^4} = \frac{1-K^2}{EI} w . \tag{11}$$

We may introduce Laplace's operator

$$\Delta = \frac{\delta^2}{\delta x^2} + \frac{\delta^2}{\delta y^2} ,$$

which gives

$$\Delta\Delta = \frac{\delta^4}{\delta x^4} + 2\frac{\delta^4}{\delta x^2 \delta y^2} + \frac{\delta^4}{\delta y^4}$$

Then Lagrange's equation (8), may be written in the simpler form

$$\Delta\Delta z = \frac{1-K^2}{EI} w . \tag{12}$$

One may determine, in a similar manner, a direct relation between the shear V_x and the deflections z, by combination of the equations (2), (5), (6), and (7). One finds:

$$V_x = \frac{EI}{1-K^2}\left(-\frac{\delta^3 z}{\delta x^3} - \frac{\delta^3 z}{\delta x \delta y^2}\right) = -\frac{EI}{1-K^2}\frac{\delta \Delta z}{\delta x} , \tag{13}$$

$$V_y = -\frac{EI}{1-K^2}\frac{\delta \Delta z}{\delta y} . \tag{14}$$

Calculations are sometimes made under the assumption that Poisson's ratio is equal to zero. Let M_x, M_y, M_z, V_x, V_y, and z, denote the moments, shears, and deflections when Poisson's ratio is equal to zero, while $M'_x \ldots$, $V'_x \ldots$, $z' \ldots$ are the corresponding values, for the same load, when Poisson's ratio has a value K which is different from zero. There are

certain relations between the two sets of values which apply when the boundary of the area under consideration, as marked by the supports and by the edges of the plate, is fixed, or consists of simply supported straight edges, or consists of parts which are fixed and parts which are simply supported along straight edges. These relations apply to the slabs dealt with in this report, but they do not apply, in general, when the supports are elastic, or when there are unsupported edges, or simply supported curved edges. The relations may be verified by inspection of equations (11) or (12), (8) and (9), (10), and (13) and (14), respectively. The relations are:

$$z' = (1 - K^2) z \; ; \tag{15}$$

$$M_x' = M_x + K M_y \; , \quad M_y' = M_y + K M_x \; ; \tag{16}$$

$$M_z' = (1 - K) M_z \; ; \tag{17}$$

$$V_x' = V_x \; , \quad V_y' = V_y \; . \tag{18}$$

Since Poisson's ratio K varies according to the material used, it is expedient to make the calculations of z, M_x, M_y....., etc., on the basis of $K = 0$. The values z', M'_x, M'_y....., etc., for any particular value of K may then be determined afterward by formulas (15 to (18).

When $K = 0$, then the equations (12), (5) to (10), (13) and (14) assume the simplified forms:

$$\Delta\Delta z = \frac{w}{EI} \; , \tag{19}$$

$$M_x = EI\left(-\frac{\delta^2 z}{\delta x^2}\right) \; , \quad M_y = EI\left(-\frac{\delta^2 z}{\delta y^2}\right) \; , \tag{20}$$

$$M_z = EI\left(-\frac{\delta^2 z}{\delta x \delta y}\right) \; , \tag{21}$$

$$V_x = EI\left(-\frac{\delta \Delta z}{\delta x}\right) \; , \quad V_y = EI\left(-\frac{\delta \Delta z}{\delta x}\right) \; , \tag{22}$$

$$\text{where} \quad \Delta z = \frac{\delta^2 z}{\delta x^2} + \frac{\delta^2 z}{\delta y^2} \; , \quad \Delta\Delta z = \frac{\delta^4 z}{\delta x^4} + 2\frac{\delta^4 z}{\delta x^2 \delta y^2} + \frac{\delta^4 z}{\delta y^4} \; .$$

Equations (19) to (22), in connection with equations (15) to (18), constitute a set of fundamental relations, by which plates may be analyzed. The most difficult part of the problem lies in the solution of Lagrange's equation, (19). This equation must be solved in each case with due consideration of the particular boundary conditions.

The reactions in a beam are expressed by the end shears, and end moments. In a similar way, the reactions in a slab may be expressed in terms of the shears, bending moments, and torsional moments at the edge. The torsional moments along a straight simply supported outer edge may be replaced by an equivalent vertical reaction by the method indicated by Kelvin and Tait. The method is described fully in Nádai's work on rectangular plates (see the historical summary).

The above differential equations in rectangular coördinates have furnished the larger number of the results which are indicated in the following articles. Polar coördinates may be introduced instead of rectangular coördinates by transformation of the above equations; they have been used with advantage in the analysis of circular slabs (see for example Föppl's treatment). Beside the method of differential equations two other methods stand out as effective in analysis, and they have furnished some of the results which are quoted and used in the following articles. These methods are: Ritz's method, which is based on the energy variations for the whole plate; and the method of difference equations, which was used by Nielsen (see Art. 4).

7. MOMENTS IN RECTANGULAR PLATES SUPPORTED ON FOUR SIDES.

The following notation is used:

a = longer span.

b = shorter span.

α = b/a = ratio of shorter span to longer span.

w = uniformly distributed load per unit-area.

M_{bc} = positive moment per unit-width at the center of the panel, in the direction of the short span. M_{bc} is referred to as the "positive moment in the short span."

M_{ac} = maximum positive moment per unit width in the direction of the long span, or "maximum positive moment in the long span." This maximum moment occurs somewhere on the center line parallel to the long sides, but not necessarily at the center of the panel (see the small diagrams at the top in Fig. 3).

M_{be} = negative moment per unit-width at the center of the long edge, in the direction of the short span, or "negative moment in the short span."

M_{ae} = negative moment per unit-width at the center of the short edge, in the direction of the long span, or "negative moment in the long span."

M_{diag} = moment per unit-width at the corner across a line through the corner, making angles of 45 degrees with the sides (see the sketches at the top of Fig. 3).

Fig. 3 to Fig. 11 show results of analyses of rectangular slabs supported on four sides. The slabs are single panels. The edges are assumed to remain undeflected in their original plane. The edges are either simply supported or fixed, as indicated in titles of the figures. The load is uniformly distributed.

In Fig. 3 to Fig. 10 the abscissas represent the ratio, α, of the shorter span b to the longer span a. The right-hand edge of each diagram corresponds to $\alpha = 1$, that is, to a square slab, while the left-hand edge corresponds to $\alpha = 0$, or $a = \infty$, that is, to an infinitely long slab supported along the two parallel edges. The ordinates in Fig. 3 to Fig. 10 are coefficients, M/wb^2, of moment per unit width. The diagrams (a), to

the left in Fig. 3 to Fig. 8, show moments coefficients calculated by analysis, while the diagrams (b), to the right, consist of simplified curves of approximately the same shape as the curves to the left. The values indicated in the diagrams to the left in Fig. 3 to Fig. 8, are based on a Poisson's ratio, K, equal to zero. The points marked by small squares and triangles are based on results found by Nádai and by Hencky, respectively.* The points marked by circles were determined in the present investigation by independent calculations. In these calculations infinite series were used which are based on Navier's and Lévy's solutions† of Lagrange's equation ((11), (12), or (19), in Art. 6). The series are similar, but not identical, to those used by Nádai and Hencky. Each coeffi-

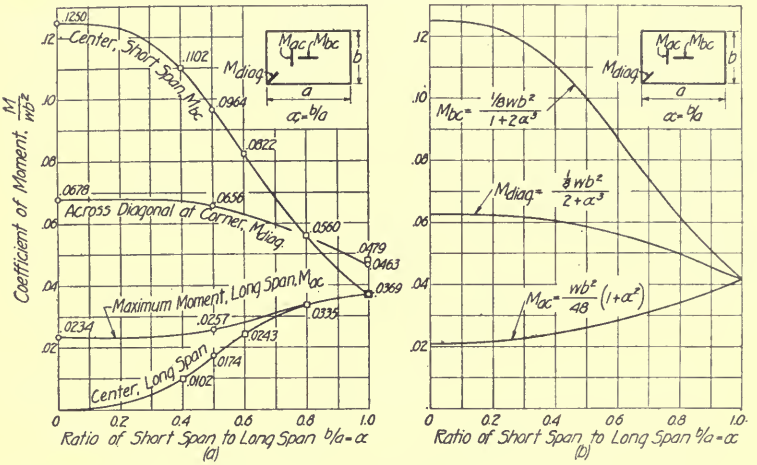

FIG. 3.—BENDING MOMENTS PER UNIT WIDTH IN RECTANGULAR SLABS WITH SIMPLY SUPPORTED EDGES.

Poisson's ratio equal to zero; (a) calculated values; (b) simplified curves.

cient indicated in Fig. 3 to Fig. 8 is the outcome of a rather large amount of numerical work. The results shown in Fig. 3 to Fig. 8 might be supplemented by coefficients which have been determined by Leitz, Mesnager, and Nielsen,‡ some of whose results will be quoted later. On the whole, the results obtained in the different investigations are very consistent.

The results stated by Nádai and Hencky are based on a Poisson's ratio $K = 0.3$, while the values given in Fig. 3 to Fig. 8 are for Poisson's ratio equal to zero. Coefficients which apply when Poisson's ratio is zero may be derived by formulas (16) in Art. 6, from the corresponding coefficients which apply when Poisson's ratio has some other value. Nádai's and

* See Art. 4, footnotes 36 and 33, respectively.
† See Art. 4, footnotes 5 and 13; also, A. E. H. Love, Mathematical theory of elasticity, 1906, p. 468.
‡ See Art. 4, footnotes 35, 37, and 27, respectively.

Heneky's results were transformed in this manner, as will be shown by an example. Take the moments at the center of a simply supported slab with $b/a = 0.6$. Nádai, in his Table 6, p. 38, indicates the values $M'_y = 0.1289\, w(a/2)^2$ for the short span, and $M'_x = 0.0704 w(a/2)^2$, for the long span. Formulas (16), in Art. 6, then determine the corresponding values for $K = 0$:

$$M_y = M_{bc} = \frac{M'_y - KM'_x}{1 - K^2} = \frac{0.1289 - 0.3 \times 0.0704}{1 - 0.3^2} \cdot \frac{wb^2}{0.6^2 \cdot 2^2} = 0.0822 wb^2$$

and, in the same way, $M_x = 0.0243 wb^2$ These values of the moments at the center, for $\alpha = 0.6$, are indicated in Fig. 3 (a). The coefficients given in Fig. 3 to Fig. 8 are for Poisson's ratio equal to zero.

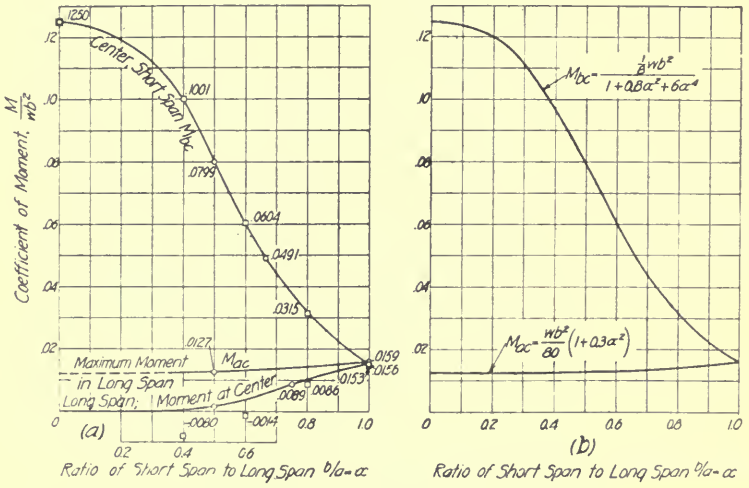

FIG. 4.—BENDING MOMENTS PER UNIT WIDTH IN SIMPLE SPAN OF RECTANGULAR SLABS; TWO PARALLEL EDGES FIXED AND TWO EDGES SIMPLY SUPPORTED.

Poisson's ratio equal to zero; (a) calculated values; (b) simplified curves.

Fig. 3 deals with rectangular slabs with simply supported edges. When $a = \infty$, that is, $\alpha = 0$, the slab acts as a beam, and the moment coefficient for the span b becomes one-eighth. When α increases from zero to one, then the moment coefficient M_{bc}/wb^2 decreases from 0.1250 to 0.0369, and the corresponding coefficient for the center of the long span increases from 0 to 0.0369. The value 0.0369 applies to the square slab ($b = a$, $\alpha = 1$). For this case Hencky's analysis gives the coefficient 0.0365, Leitz's analysis of 1914 gives 0.0368, Mesnager's 0.0368, and Nielsen's 0.0366.* In Fig. 3(a) there is a separate curve for the maximum

* See the investigations quoted in Art. 4 in footnotes 33 (Hencky, p. 34); 35 (Leitz, p. 27); 37 (Mesnager, p. 369); and 27 (Nielsen, p. 132).

moment in the long span. This curve defines coefficients which are greater than the corresponding values at the center of the long span; that is, the maximum moment in the long span of a rectangular panel does not occur at the center, except when the slab is nearly square. Moment diagrams for the center line of the long span are shown in Fig. 11. Two cases are represented, namely, $\alpha = \frac{1}{2}$ and $\alpha = 0$. The coefficients 0.0257 and 0.0234, which are indicated in Fig. 3(a), appear as maximum ordinates in Fig. 11; and the coefficient 0.0174, for $\alpha = \frac{1}{2}$, appears in both figures, as applying to the moment at the center, in the direction of the long span.

A simply supported square or rectangular slab (simply supported on four sides), when loaded, has a tendency to bend up at the corners. In the slabs treated here the corners are assumed to be anchored, that is, the supports provide for a concentrated downward reaction at each corner. With this force acting, stresses and moments are set up at each corner: there is a positive moment, M_{diag}, across the line which makes angles of 45 deg. with the sides, that is, across the diagonal in the square slab; there is

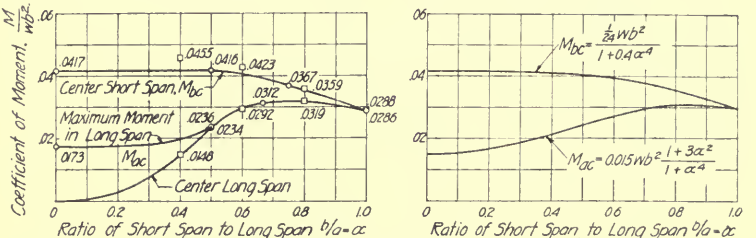

FIG. 5.—POSITIVE BENDING MOMENTS PER UNIT WIDTH IN FIXED SPAN OF RECTANGULAR SLAB; TWO PARALLEL EDGES FIXED AND TWO EDGES SIMPLY SUPPORTED.

Poisson's ratio equal to zero; (a) calculated values; (b) simplified curves.

an equally large negative moment in the direction of this line, and there is an equally large torsional moment in the sections parallel to the sides. The presence of negative moments in the direction of the diagonal of a square slab may be understood easily when one considers the curve of deflections along the whole diagonal. This curve has a horizontal tangent at the corner, because the deflected surface has a horizontal tangential plane at this point. The convex side of this elastic curve, therefore, is upward; that is, the moment is negative. The following values of the coefficients, M_{diag}/wb^2, in a square slab were determined: by Nádai's analysis, 0.0479; by Mesnager (his paper, p. 369), 0.0464; and by the present investigation, 0.0463. The concentrated downward reaction is equal to twice the diagonal or torsional moment per unit width; that is, the present analysis leads to a corner reaction equal to $2 \times 0.0463wb^2 = 0.0926wb^2$. Leitz indicates this reaction as $0.092wb^2$.

The average coefficient of moment across the diagonal in a simply sup-

ported square slab may be determined by simple statical principles.* It is $1/24 = 0.0417$; that is, practically the average of the extreme values, 0.0463 and 0.0369, occurring at the corner and at the center, respectively. The coefficient 1/24 has been used frequently as a basis of design. This value, 1/24, may be justified on the ground that when the proportional limit is exceeded, or when the material begins to yield, in a part of the diagonal section, the stresses will be redistributed so that they become more nearly uniformly distributed.

The curves in Fig. 3(a) do not have equations which can be expressed by simple algebraic formulas. It is possible, however, to indicate simple

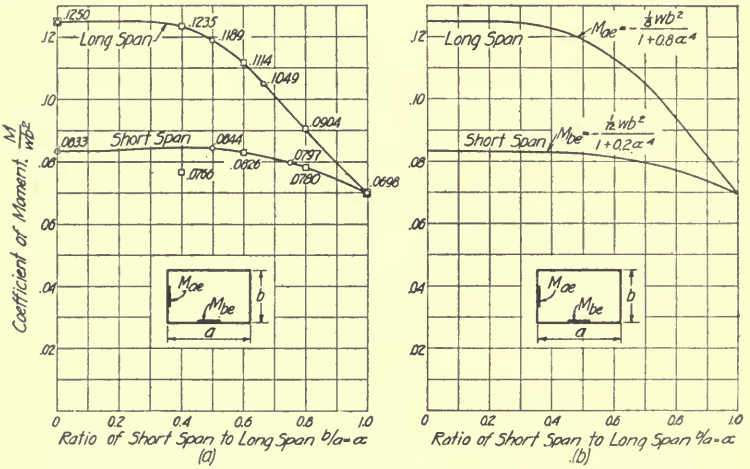

FIG. 6.—NEGATIVE BENDING MOMENTS PER UNIT WIDTH IN FIXED SPAN OF RECTANGULAR SLABS; TWO PARALLEL EDGES FIXED AND TWO EDGES SIMPLY SUPPORTED.

Poisson's ratio equal to zero; (a) calculated values; (b) simplified curves.

formulas which give nearly the same values as are found in Fig. 3(a). Such formulas, and the curves which represent them graphically, are indicated in Fig. 3(b). The formulas and the curves give the coefficient 1/24 for the square slab. The curve for M_{diag} lies lower in Fig. 3(b) than in Fig. 3(a). The decrease for $\alpha = 0$ from 0.0678 in Fig. 3(a) to 0.0625 in Fig. 3(b) may be defended on the ground that in very long slabs the stresses at the corner, due to M_{diag} are local stresses upon which the safety of the slab as a whole does not depend. And in the case of $\alpha = 1$ the probable redistribution of moments and stresses across the diagonal, when the material begins to yield at one point, will account for the proposed reduction of the coefficient, from 0.0463 to 1/24. In selecting the formulas

*Used by Bach in his plate theory, see the paper quoted in Art. 4, footnote 15.

indicated in Fig. 3(b) some weight was given to the desirability of having simple formulas, upon which design computations might be based.

Fig. 4, Fig. 5, and Fig. 6 deal with rectangular slabs which have two fixed opposite edges and two simply supported opposite edges. In a uniformly loaded single continuous row of simply supported panels each panel acts, on account of the continuity, in the same way as the single panel with two fixed and two simply supported edges. The torsional moments and bending moments are zero at the corners in these slabs. As in Fig. 3(a), separate curves are indicated in Fig. 4(a) and Fig. 5(a) for the maximum moments in the long span; these curves lie, in part, above the corresponding curves for the moment at the center. Certain individual points, which were derived from Nádai's work (p. 62, Table 9, in his work), lie at a distance from the curves drawn through the rest of the points. There are three such points lying below the bottom curve in Fig. 4(a), and

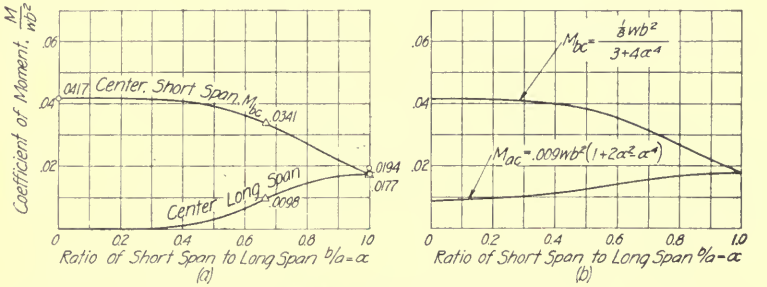

FIG. 7.—POSITIVE BENDING MOMENTS PER UNIT WIDTH IN RECTANGULAR SLABS WITH FIXED EDGES.

Poisson's ratio equal to zero; (a) calculated values; (b) simplified curves.

three points, belonging to the same cases, lying above the top curve in Fig. 5(a). In Fig. 6(a) one point lies below the bottom curve. There is a possibility of an error in these points. Fig. 6(a) shows the peculiar result that greater negative moments are produced when the long span is fixed than when the short span is fixed. The simplified curves to the right in Fig. 4, Fig. 5 and Fig. 6 follow rather closely the curves to the left.

Fig. 7 and Fig. 8 deal with slabs fixed on four sides. Unfortunately, this case, on account of the greater difficulties involved, has been treated less extensively than the preceding cases. Navier's and Levy's solutions do not apply to these slabs. Ritz's method, which was applied to these slabs, for example, by Nádai, leads to a fairly satisfactory analysis. The curves in Fig. 7(a) are drawn according to Hencky's results. For the moments at the center of a square plate various writers have indicated values, which lead to the following coefficients: Hencky, 0.0177; Nádai, 0.0177; Mesnager, 0.018; Leitz, 0.0184; Nielsen, 0.0171; the present investigation, by an approximate method, 0.0194. For the negative moments at the center of the edge of a square panel the same writers have indicated

the following coefficients: * Hencky, —0.0513; Nádai, —0.0487; Mesnager, —0.0474; Leitz, —0.0515; Nielsen, —0.0511; the present investigation, by an approximate method, —0.0493. The curve for M_{ac}, in Fig. 7(b), and the line for M_{ae} in Fig. 8(b), have been drawn according to an estimate, and they may have to be revised later.

Fig. 9 contains a summary of all the simplified curves in Fig. 3 to Fig. 8. The curves for the negative moments are shown to the left, those for the positive moments to the right. Table II gives a summary of the formulas represented by these curves. A corresponding set of formulas, applying exactly to an elliptic plate with fixed edges and with Poisson's ratio equal to zero,† is indicated, for the purpose of comparison with the other formulas, in the bottom line in the table.

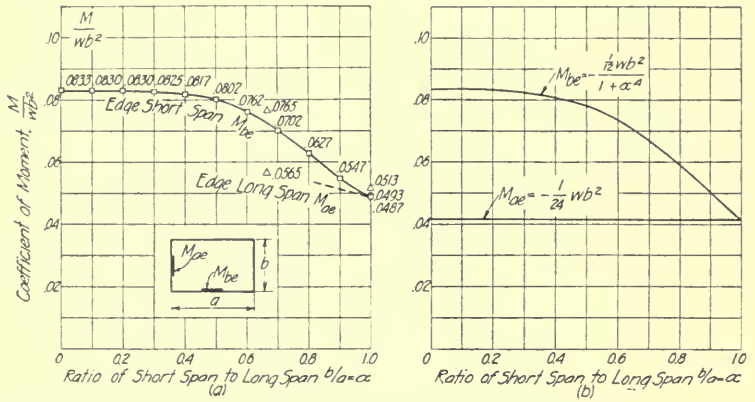

FIG. 8.—NEGATIVE BENDING MOMENTS PER UNIT WIDTH IN RECTANGULAR SLABS WITH FIXED EDGES.

Poisson's ratio equal to zero; (a) calculated values; (b) simplified curves.

Fig. 10(a) illustrates the influence of change in Poisson's ratio. Such a change causes a redistribution of the moments in the slab. The case dealt with is again that of the slab with simply supported edges. Two of the curves in Fig. 3(a) are reproduced, namely, the curve for the moment in the short span at the center, and the curve for the moment at the corner, in a section making angles of 45 degrees with the sides; that is, the curves for M_{bc} and M_{diag} respectively. These curves are marked $K = 0$; those for $K = 0.3$ are indicated in the figure. The computations of the changed moment coefficients were made according to formulas (16) in Art. 6. They apply when Poisson's ratio, K, is equal to zero. The corresponding curves

* See the investigations quoted in Art. 4 in footnotes 33 (Hencky, p. 53); 36 (Nádai, p. 86); 37 (Mesnager, p. 413); 35 (Leitz); 27 (Nielsen, p. 139). Leitz's paper of 1917, unfortunately was not available to the writer. Leitz's results for the square slab are quoted from Nielsen.

† See A. Föppl, Technische Mechanik, Vol. 5, ed. 1918, p. 106.

change from $K = 0$ to $K = 0.3$ is seen to increase the moment at the center, and to decrease the moment at the corner. In the square slab the moments across the diagonal are redistributed; the point of maximum moment across the diagonal is moved from the corner to the center.

The stresses at a point in a homogeneous slab are directly proportional to the moments at the point. But the maximum stress at a point does not necessarily define the "nearness of rupture" or "tendency to failure" at the point. This tendency depends on the whole "state of stress" at the point, or, in the slab, on the state of moments at the particular point. In a square slab the moments at the center are equal in all directions, while at the

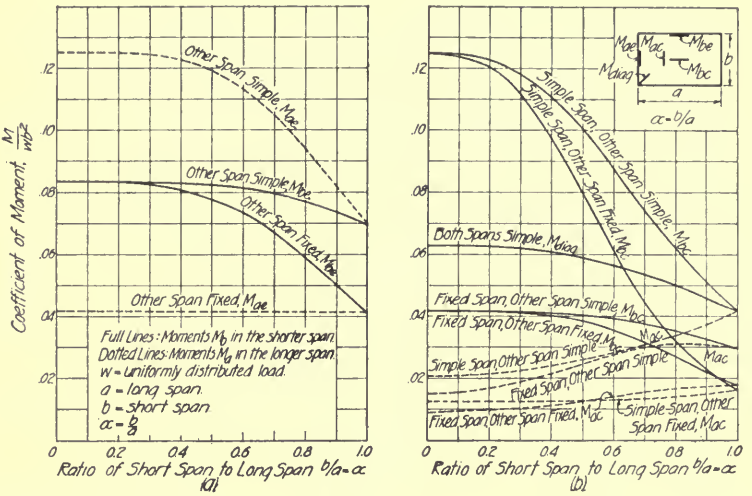
Coefficient of Moment, M/wb²
Other Span Simple, Mac
Other Span Simple, Mbc
Other Span Fixed, Mbc
Other Span Fixed, Mac
Full Lines: Moments Mb in the shorter span
Dotted Lines: Moments Ma in the longer span
w = uniformly distributed load
a = long span
b = short span
α = b/a
Ratio of Short Span to Long Span b/a = α
(a)
Both Spans Simple, Mdiag
Fixed Span, Other Span Simple, Mbc
Fixed Span, Other Span Fixed, Mbc
Simple Span, Other Span Simple, Mac
Simple Span, Other Span Fixed, Mac
Fixed Span, Other Span Fixed, Mac
Mac
Mbc
Mdiag
a
α = b/a
(b)

FIG. 9.—SUMMARY OF APPROXIMATE CURVES IN FIG. 3 TO FIG. 8; (*a*) NEGATIVE MOMENTS; (*b*) POSITIVE MOMENTS.

corner a positive moment across the diagonal is combined with an equally large negative moment along the diagonal. Though the stresses may be numerically larger at the center than at the corner, failure, nevertheless, may be nearer at the corner, because here the positive and negative moments are combined. Various theories concerning the tendency to failure have been advanced. One is represented in Fig. 10(b); it is the "shear and strain" theory, which was originated by A. J. Becker,* and which was indicated by him as applying to steel. Corresponding to a state of stress one may compute an "equivalent stress,"† which is a simple tension, in one direction only, which is as dangerous as the given compound state of stress.

* A. J. Becker. The Strength and Stiffness of Steel Under Biaxial Loading. University of Illinois Eng. Exp. Sta. Bull. 85, 1916.

† See, for example, Journal of the Franklin Institute, v. 189, 1920, p. 635.

If the shear and strain theory applies, the equivalent stress at a given point may be computed, as the larger of the following two quantities: one is the modulus of elasticity times the greatest unit-elongation or unit-shortening at the point in any direction; the other is the greatest shearing stress at the point, divided by a certain constant, which, according to Becker's results, is 0.6. An equivalent moment in a slab is a bending moment which would produce the equivalent stress. According to Becker's results, the equivalent moment at a point is computed, then, as the larger of the following two quantities: one is EI times the numerically largest curvature in any vertical section at the point; the other is the largest torsional moment

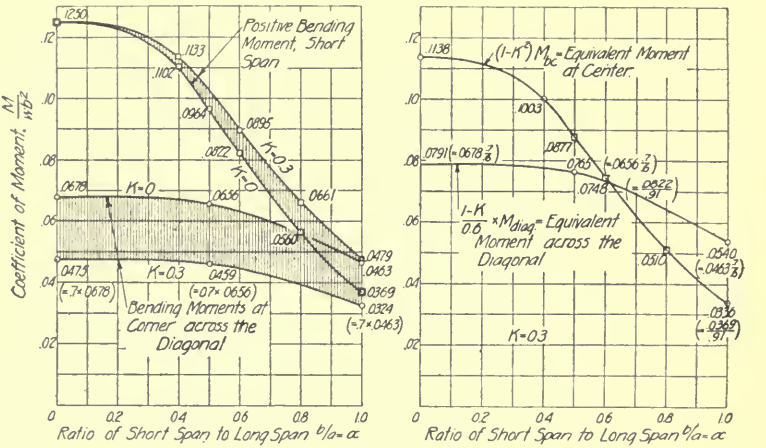
Positive Bending Moment, Short Span
K=0
K=0.3
Bending Moments at Corner across the Diagonal
Coefficient of Moment, M/wb²
Ratio of Short Span to Long Span b/a = α
(1-K²) M_bc = Equivalent Moment at Center
1-K/0.6 × M_diag. = Equivalent Moment across the Diagonal
K=0.3

(a) (b)

FIG. 10(a).—INFLUENCE OF VARIATION IN POISSON'S RATIO, K, ON THE MOMENTS IN RECTANGULAR SLABS WITH SIMPLY SUPPORTED EDGES.

FIG. 10(b).—"EQUIVALENT MOMENTS," BASED ON THE "SHEAR AND STRAIN" THEORY, IN RECTANGULAR SLABS WITH SIMPLY SUPPORTED EDGES.

in any section at the point, divided by 0.6. Such equivalent moments are indicated in Fig. 10(b). The slabs are the same as in Fig. 10(a), and the curves refer to the center and to the corner. The methods of computation are indicated in the figure. According to equations (15) and (20) in Art. 6, EI times the curvature may be computed as $(1 - K^2)$ times the moment corresponding to Poisson's ratio equal to zero. M_{bc} and M_{diag}, as used in the notes in Fig. 10(b), are the moments corresponding to Poisson's ratio equal to zero. The curves in Fig. 10(b) explain why a square slab with $K = 0.3$ may fail at the corners first, in spite of the fact that the stresses are smaller at the corner than at the center.

Fig. 10(a) and Fig. 10(b) and the discussion in connection with these figures show how the results derived for the case in which Poisson's ratio is

zero may be interpreted and used when Poisson's ratio has any other value, provided the law of failure of the material is known. Whether or not the curves and formulas indicated in Fig. 3 to Fig. 9, in Fig. 11, and in Table II may be applied as a basis for design of actual slabs, should be determined for the individual materials by comparison with experimental results.

8. MOMENTS IN SQUARE INTERIOR PANELS OF UNIFORMLY LOADED FLAT SLABS.

Notation:

l = span, measured from center to center of the columns.

c = diameter of the column capitals.

w = load per unit-area, uniformly distributed over all panels.

W = total panel load.

The slab under consideration is a girderless or "flat" slab, supported directly on the column capitals, which are assumed to be round. Lines connecting the centers of the columns divide the floor into square panels,

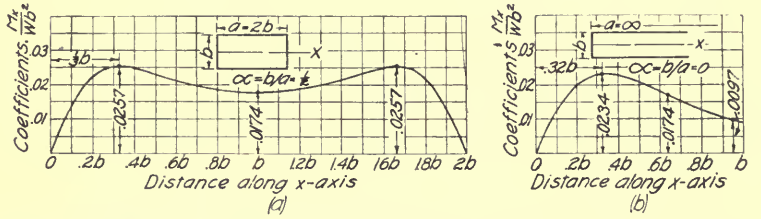

FIG. 11.—MOMENTS ALONG THE CENTER LINE OF THE LONG SPAN IN RECTANGULAR SLABS WITH SIMPLY SUPPORTED EDGES.

with a column at each point of intersection. An interior panel is considered. It is surrounded on all sides by similar panels, all carrying the same load. For the convenience of the analysis it may be assumed that there is an infinite number of equal, square panels, all carrying the same load. The slab is assumed to be fixed in the column capitals at the edge of each column capital. A panel of this description, loaded as indicated here, will be referred to as "a normal panel." On account of the symmetry, the column capitals supporting the normal panel will not tend to rotate about a horizontal axis, the tangents across the edges and center lines of the normal panel will remain horizontal, and the torsional moments along the center lines of the panel and along the parts of the edges between the column capitals will be zero.

Fig. 12 shows sections for which it has become customary to indicate the moments. The terms column-head sections, mid-section, outer sections, and inner section are in accordance with common practice. The moments in these sections are taken in a direction perpendicular to the straight parts of the sections. Moment coefficients for these sections will be stated pres-

ently, but first some remarks will be made concerning the processes of the analysis.

The present investigation is built, in part, on certain results which were found by N. J. Nielsen * in his analysis of plates by the method of difference equations. Nielsen analyzed various types of square interior panels of uniformly loaded flat slabs: first, point-supported slabs, in which the column capitals and the columns have been reduced to point supports; second, slabs in which the supporting forces are uniformly distributed within squares with side $0.2l$ and with the centers at the centers of the column; third and fourth, slabs supported on square column capitals with the sides $0.2l$ and $0.4l$, respectively; fifth, a slab with dropped panels (areas of increased thickness around the supports); and sixth, a slab in which there is no bending resistance across the central parts of the edges of the panels, that is, no bending resistance in parts of the mid-sections. Nielsen divided the panel into elementary squares with side $\lambda = 0.1l$. $1/6l$, $0.2l$, or $0.25l$. The

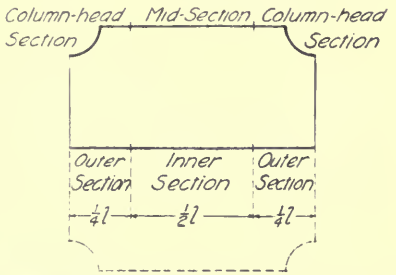

FIG. 12.—MOMENT SECTIONS FOR FLAT-SLAB PANELS.

variables in the equations are the deflections at the corners of these squares; one equation is indicated for each such corner. Since finite squares are used instead of infinitesimal rectangular elements the method is approximate, not exact, as applying to homogeneous slabs.† The smaller the value of λ the closer is the approximation. The value $\lambda = 0.1l$ gives, on the whole, rather satisfactory results. $\lambda = 1/6l$ to $0.25l$ gives results, use of which may be made in comparative studies of distributions of deflections and moments in different slabs; such use of some of Nielsen's results will be made later (in Art. 10). But the moment coefficients found with $\lambda = 1/6l$ or more, hardly seem to be sufficiently exact when considered as independent results applying to fundamental cases. For this reason the use of Nielsen's results was limited here to those obtained with $\lambda = 0.1l$. This value of λ was used by Nielsen only in the first two of the cases men-

* N. J. Nielsen, Bestemmelse af Spaendinger i Plader ved Anvendelse af Differensligninger, 1920 (referred to in Art. 4, footnote 27).

† The difference equations apply exactly to a certain rib-structure in which the bending deformations are concentrated at the points of intersection of the ribs, and in which the torsional resistance is supplied by special structural elements which connect one rib with another.

tioned, that is, in the analyses of the point-supported slab and of the slab with the supporting forces uniformly distributed within small squares; in the other cases he used $\lambda > 0.1l$. Those of Nielsen's results, with $\lambda = 0.1l$, which apply to the point-supported slab, were represented graph-

TABLE II.—APPROXIMATE FORMULAS FOR BENDING MOMENTS PER UNIT WIDTH IN RECTANGULAR SLABS AND ELLIPTIC SLABS SUPPORTED ON THE PERIPHERY.

The formulas are represented graphically in Fig. 3 to Fig. 9. a = longer span, b = shorter span, $\alpha = b/a$; Poisson's ratio = 0.

		Moments in span b		Moments in span a	
		At center of edge. $-M_{be}$	At center of slab. M_{bc}	At center of edge $-M_{ae}$	Along center line of slab. M_{ac}
Rectangular Slabs.	Four edges simply supported.	0	$\frac{1}{8}wb^2 \div (1+2\alpha^3)$	0	$\frac{wb^2}{48}(1+\alpha^2)$
	Span b fixed; Span a simple.	$\frac{1}{12}wb^2 \div (1+0.2\alpha^4)$	$\frac{1}{24}wb^2 \div (1+0.4\alpha^4)$	0	$\frac{wb^2}{80}(1+0.3\alpha^2)$
	Span a fixed; Span b simple.	0	$\frac{1}{8}wb^2 \div (1+0.8\alpha^2+0\alpha^4)$	$\frac{1}{8}wb^2 \div (1+0.8\alpha^4)$	$0.015wb^2 \frac{1+3\alpha^2}{1+\alpha^4}$
	All edges fixed.	$\frac{1}{12}wb^2 \div (1+\alpha^4)$	$\frac{1}{8}wb^2 \div (3+4\alpha^4)$	$\frac{1}{24}wb^2$	$0.009wb^2(1+2\alpha^2-\alpha^4)$
Elliptic slab with fixed edge; diameters 0 and b, $K=0$; $b/a=\alpha$.		$\frac{1}{12}wb^2 \div (1+\frac{2}{3}\alpha^2+\alpha^4)$	$\frac{1}{24}wb^2 \div (1+\frac{2}{3}\alpha^2+\alpha^4)$	$\frac{1}{12}wb^2\alpha^2 \div (1+\frac{2}{3}\alpha^2+\alpha^4)$	$\frac{1}{24}wb^2\alpha^2 \div (1+\frac{2}{3}\alpha^2+\alpha^4)$

ically for the purpose of the present investigation, and adjustments were made, similar to those by which a string polygon is modified into a string curve. By such adjustments of the curves for moments and deflections it was possible to improve the approximation slightly. It would be possible to analyze the point-supported slab by differential equations, and to obtain, thereby, an increased degree of exactness, but in this study it seemed desirable to make use of the available results. The degree of approximation obtained by this use may be judged by comparing the moment coefficients for square slabs supported on four sides, found by Nielsen with λ equal to one-tenth of the side, as quoted in the preceding article, with the corresponding moment coefficients found in other analyses.

The use of Nielsen's results in connection with results found in the present investigation by means of the differential equations will now be described. The point-supported slab is not important in itself, because actual slabs do not have point supports. But the results found for the point-supported slab may be used in the analysis of the normal panel, supported on round column capitals, in the same way as moment diagrams for simple beams are used in the study of continuous beams or beams with fixed ends. The diagrams for fixed beams can be found from the diagrams for simple beams by adding the effects of the end moments. The simple beam is considered in this connection as a "substitute structure" which temporarily replaces the given fixed beam, and which is made to act like the given beam by adding the end moments. In a similar way the point-supported slab may be used as a substitute structure which temporarily replaces the slab supported on column capitals, and which is made to act like the original slab, that is, have the same deflections and moments at all

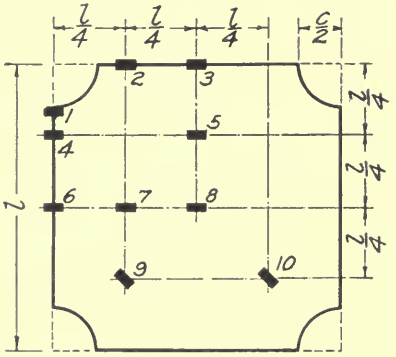

FIG. 13.—MOMENT SECTIONS REFERRED TO IN TABLE IV; THE HEAVY SHORT LINES INDICATE THE POSITIONS AND DIRECTIONS OF THE SECTIONS.

points outside the circles marked by the edges of the column capitals, by adding certain loads near the center of the column. The nature and intensity of these loads must be such that the resultant deflections and slopes at the circles marking the edges of the column capitals become zero. The essential part of the load of this kind, added at each column, may be termed a "ring load." It consists of a combination of an upward force uniformly distributed over the circumference of a small circle, drawn on the slab, with an equally large downward force at the center of this circle. The ring load may be considered as concentrated, just as a couple acting on a beam may be considered as concentrated at one point, for example, at the end point if the end is fixed. A ring load of the proper intensity at each point support, combined with a certain uniformly distributed bending moment applied at the edge of the whole slab (which includes many panels) and, combined with the original uniformly distributed load and the reac-

TABLE III.—PERCENTAGES OF SUM OF POSITIVE AND NEGATIVE MOMENTS RESISTED IN SECTIONS SHOWN IN FIG. 12.

Results of analysis of a square interior panel of a uniformly loaded homogeneous flat slab.
The sum of positive and negative moments is approximately equal to

$$M_o = \frac{1}{8} W l \left(1 - \frac{2}{3}\frac{c}{l}\right)^2.$$

c=diameter of column capital; l=span; W=total panel load; Poisson's ratio=0.

			c/l				Average.
			0.15	0.20	0.25	0.30	
Negative Moments	Column head section	Across edge of capital	31.8	37.1	40.2	42.7	$20+80\ c/l$
		Outside capital	16.5	11.3	8.1	5.7	$28-80\ c/l$
		Total	48.3	48.4	48.3	48.4	48
	Mid section		17.0	16.7	16.6	16.3	17
	Total negative moment		65.3	65.1	64.9	64.7	65
Positive Moments	Outer section		20.9	20.9	20.8	20.7	21
	Inner section		13.8	14.0	14.3	14.6	14
	Total positive moment		34.7	34.9	35.1	35.3	35

TABLE IV.—COEFFICIENTS OF MOMENT PER UNIT WIDTH, IN SECTIONS SHOWN IN FIG. 13.

Results of analysis of a square interior panel of a uniformly loaded homogeneous flat slab. Poisson's ratio=0.
The coefficients are values of the expression

$$\frac{M}{\frac{1}{8} w \left(l - \frac{2}{3} c\right)^2}$$

They are found by multiplying the coefficients in Fig. 14 to 16 by the factors 8, 9.52, 10.31, 11.39, and 12.46 for c/l=0, 0.15, 0.20, 0.25, and 0.30, respectively.

Section.	c/l=					Approximate Coefficients for c/l= 0.15 to 0.30
	0	0.15	0.20	0.25	0.30	
1	.....	−2.120	−1.854	−1.609	−1.424	$-\frac{1}{8}\left(\frac{l}{c}+4\right)$
2	−0.488	−0.461	−0.435	−0.409	−0.370	$-0.5-1.5\left(\frac{c}{l}\right)^2$
3	−0.255	−0.270	−0.275	−0.282	−0.289	−0.028
4	0.258	0.130	0.048	−0.046	−0.169	$0.23-4.5\left(\frac{c}{l}\right)^2$
5	0.015	0.015	0.015	0.016	0.015	+0.02
6	0.474	0.474	0.466	0.461	0.447	0.46
7	0.331	0.341	0.340	0.343	0.343	0.34
8	0.226	0.242	0.246	0.254	0.262	0.25
9	0.233	0.188	0.156	0.121	0.072	$0.23-1.8\left(\frac{c}{l}\right)^2$
10	−0.121	−0.110	−0.102	−0.093	−0.080	$\frac{1}{8}-\frac{1}{2}\left(\frac{c}{l}\right)^2$

tions at the point supports, will make the slab deflect in such a way that the circles marking the edges of the column capitals practically become a contour line along which the tangential planes are horizontal and coinciding. By introducing certain supplementary loads, beside the ring loads, the conditions of the edges of the column capitals may be satisfied with any desired degree of approximation. Corrections by means of such supplementary loads were omitted, because the degree of approximation obtained without these loads appeared to be acceptable; besides, since the degree of approximation is limited in one part of the problem by the use of the approximate results found by difference equations, the gain by a further increase of exactness in the part of the problem discussed here would be only slight.

It remained, then, to investigate the effects of the ring loads, to determine their intensity, and to make the proper additions to the moments in the point-supported slab. The method used was that of differential equations. Lagrange's equation ((11), (12), or (19), in Art. 6) was solved for the case of the ring loads by double-infinite series, and the moments at definite points, produced by the ring loads, were computed by corresponding double-infinite series. As in the preceding article, and for similar reasons, Poisson's ratio was taken as zero (compare, in particular, the discussion made in connection with Fig. 10 (a)). Details of this analysis will be presented in Appendix A.

The results will now be described. Reference is made again to Fig. 12, which shows the customary moment sections. Table III gives results found for these sections. The moments are stated in per cent of the sum of the numerical values of positive and negative moments in all the sections in Fig. 12. Values are given for four sizes of the column capital. The percentages resisted in the different sections in Fig. 12 are seen to change only slightly when c changes from $0.15l$ to $0.30l$, and to deviate only slightly from the constant values given in the last column: namely, 48 per cent in the column-head sections, 17 per cent in the mid-section, 21 per cent in the outer sections, and 14 per cent in the inner section.

The total moments in the various sections depend upon the moments per unit-width at the individual points of the slab. Fig. 13 indicates points and sections at which the moments per unit-width are of particular interest. Moment coefficients for these sections are stated in Table IV.

Fig. 14 shows diagrams of coefficients of moment per unit-width across the edge and the center line of the panel. The coefficients are values of M/wl^2.

Lavoinne,* in a paper published in 1872, derived the stresses in certain sections of a uniformly loaded point-supported slab. He stated coefficients of stresses; but moment coefficients M/wl^2, of the type used in Fig. 14, may be found by dividing his stress coefficients by six. Thus, Lavoinne's

* Lavoinne, Sur la résistance des parois planes des chaudières à vapeur, Annales des Ponts et Chaussées, 1872, pp. 276-295; the numerical coefficients are quoted from p. 286. See the historical summary in Art. 4, footnote 10.

analysis gives the following moment coefficients: at the center of the slab, $0.17/6 = 0.0283$, to be compared with 0.0283 in Fig. 14; at the center of the edge along the edge, $0.34/6 = 0.0567$, while Fig. 14 gives 0.0592; at the center of the edge across the edge, $-0.20/6 = -0.0333$, while Fig. 14 gives —0.0319. Since Lavoinne stated only two decimal places in each

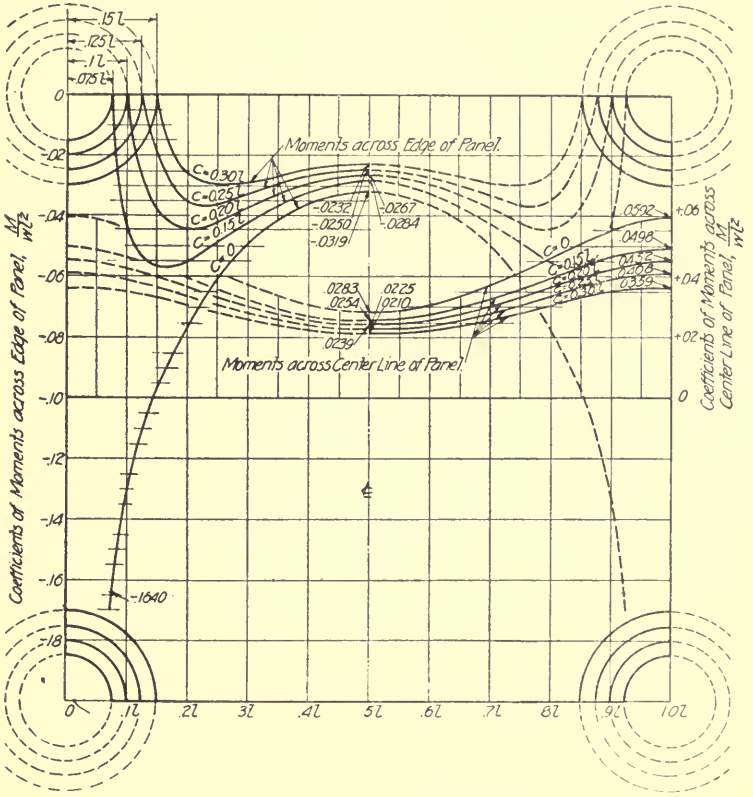

FIG. 14.—COEFFICIENTS OF BENDING MOMENTS PER UNIT WIDTH IN A SQUARE INTERIOR PANEL OF A UNIFORMLY LOADED FLAT SLAB WHEN POISSON'S RATIO IS ZERO; MOMENTS ACROSS THE EDGE AND THE CENTER LINE.

coefficient, the agreement may be considered as fairly satisfactory. Lavoinne's solution is by double-infinite trigonometric series.

Fig. 15 shows coefficients, M/wl^2, of moment per unit-width along the edge and the center line of the panel. Each of the curves must satisfy a certain condition, which applies also to beams with fixed ends: the positive and the negative area of each of the moment diagrams must be

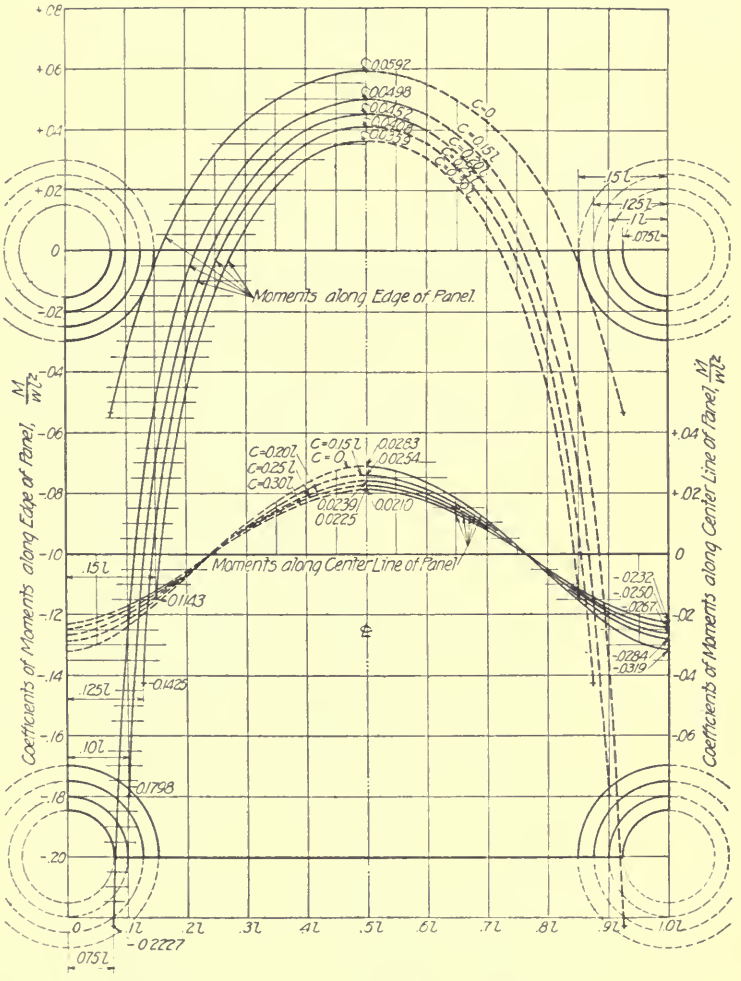

FIG. 15.—COEFFICIENTS OF BENDING MOMENTS PER UNIT WIDTH IN A SQUARE INTERIOR PANEL OF A UNIFORMLY LOADED FLAT SLAB WHEN POISSON'S RATIO IS ZERO; MOMENTS ALONG THE EDGE AND THE CENTER LINE.

numerically equal. This condition applies to the curves in Fig. 15 because the slope of the slab is zero at the edge of the column capital and at the center, that is, at the points where the curves in the diagram end; the application of the condition under these circumstances follows from equa-

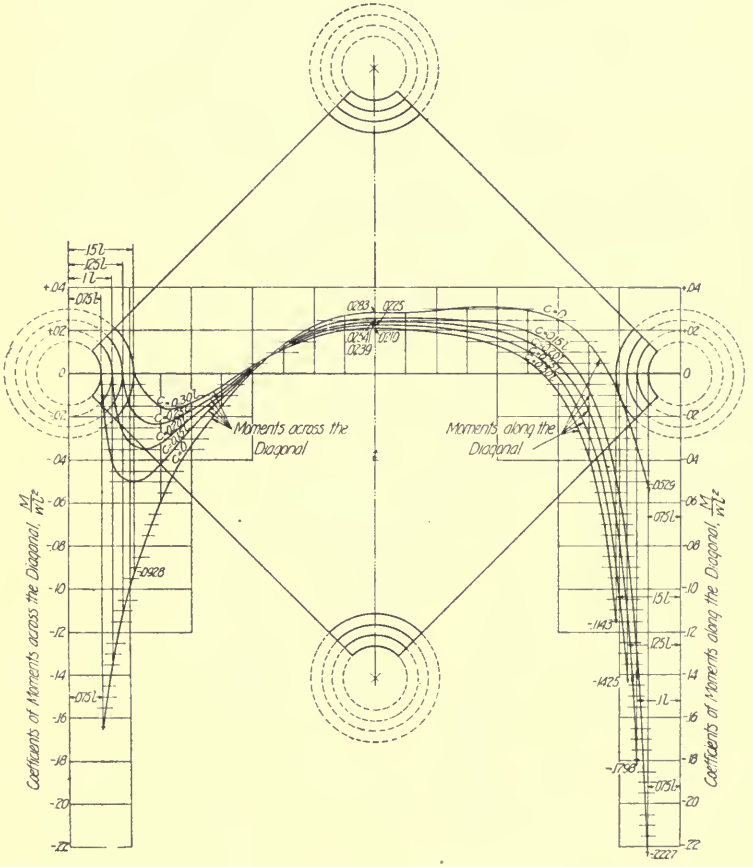
Moments across the Diagonal
Moments along the Diagonal
Coefficients of Moments across the Diagonal $\frac{M}{wl^2}$
Coefficients of Moments along the Diagonal $\frac{M}{wl^2}$

FIG. 16.—COEFFICIENTS OF BENDING MOMENTS PER UNIT WIDTH IN A SQUARE INTERIOR PANEL OF A UNIFORMLY LOADED FLAT SLAB WHEN POISSON'S RATIO IS ZERO; MOMENTS ACROSS AND ALONG THE DIAGONALS.

tions (20) in Art. 6. An examination of the curves in Fig. 15 showed equality of the positive and negative areas.

Fig. 16 shows coefficients of moment per unit-width across and along the diagonals. In drawing the curves for the moments along the diagonal, use was made of the condition that the positive and negative parts of each

moment diagram must be numerically equal. The diagonal moments at the edge of the column capital could not be determined with the degree of exactness obtained elsewhere, because the torsional moments at these points, in the point supported slab, in sections parallel to the panel edges, had not been determined by the difference equations with the same degree of exactness as other moments. The negative moment across the edge of the column capital is approximately the same along the diagonal, as along the panel edge, in fact, it is approximately constant all the way around the column capital. Accordingly, the coefficients of end-moment along the diagonal, stated in Fig. 16, were taken as equal to the corresponding negative moment coefficients in Fig. 15, which apply at the panel edge. Certain small discrepancies, which possibly may be explained by the deviations in the negative diagonal moments, will be discussed in connection with the next two figures.

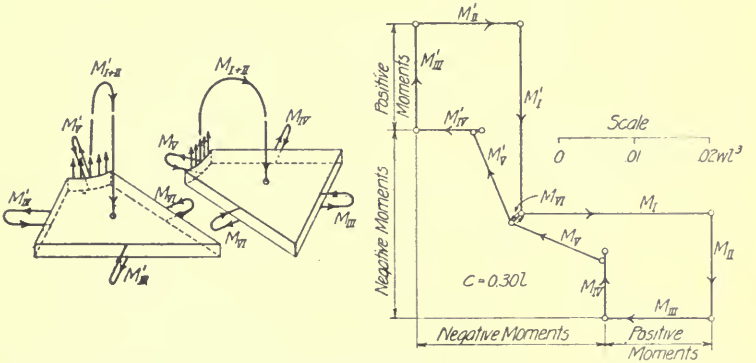

FIG. 17.—DIAGRAM SHOWING THE EQUILIBRIUM OF THE FORCES AND COUPLES ACTING ON AN OCTANT AND A QUADRANT OF A SQUARE PANEL ($c = 0.30$).

Fig. 17 shows forces and couples acting on two separate octants of a normal panel with $c = 0.30l$. For each octant the downward resultants of the applied loads acting at the centroids of the area, and the upward resultant of the vertical supporting forces or shears at the edge of the column capital form a couple; these couples are: M_{I+II} for one octant, M'_{I+II} for the other. In the plane vertical sections there are bending moments, M_{III} M_{IV}, and M_{VI} in one octant, M'_{III}, M'_{IV}, and M'_{VI} in the other, but on account of the symmetry there are no torsional moments and no vertical shears in these sections. The moment M_V and M'_V are the resultant moments in the curved sections at the edge of the column capital. In the diagram to the right, in the figure, the different couples are represented as vectors. Each vector is laid off parallel to the vertical plane of the couple which it represents; the direction is that of the upper one of two horizontal forces representing the couple. The couple vectors M_{I+II} and M'_{I+II}

are shown resolved into the components M_{I} and M_{II}, M'_{I} and M'_{II}. The couple vectors form two polygons, one for each octant, but with the side M_{VI} in common. Each octant is in equilibrium; therefore, if the couples are represented correctly, each polygon should close. Fig. 17 shows small gaps at the end points of the vectors M_{IV} and M'_{IV}. These gaps are a measure of the discrepancies which have entered, so far, into the calculations and into the particular graphical representation in the figure.

The method of obtaining the particular vectors represented in the vector diagram in Fig. 17 will now be described, and possible sources of the gaps will be discussed. The couple M_{I+II}, with the components M_{I} and M_{II}, is considered first. The two components could be computed exactly if the point of application of the resultant shear were known exactly. M_{I} and M_{II} were computed under the assumption that the vertical shear at the edge of the column capital is uniformly distributed, or, that the resultant passes through the centroid of the circular arc formed by the

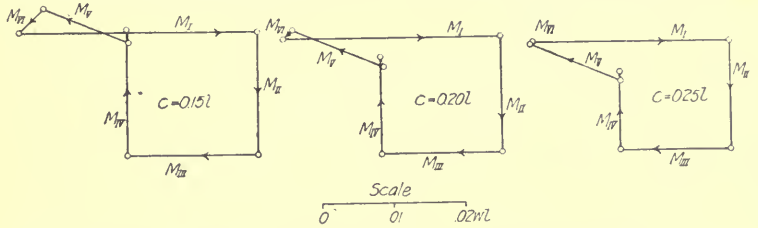

FIG. 18.—COUPLES ACTING ON AN OCTANT OF A SQUARE PANEL ($c = 0.15$; 0.20; 0.25).

section. The distribution of the shear at the edge of the column capital is known to be approximately uniform, but if it is not entirely uniform, the end point of M_{II} may have to be moved slightly. It is possible that a shifting of the end of M_{II} into its correct position would reduce the gap at the end of M_{IV}. The vectors M_{III} and M_{IV}, were determined by measuring areas in Fig. 14, of the diagrams of moments across the center line and the edge. M_{VI} was determined by a corresponding area in Fig. 16. M_{V} was computed under the assumption that the bending moment across the edge of the column capital is constant, and that the torsional moment along the edge of the column capital is zero. If these assumptions are correct, the direction of M_{V} will bisect the 45 deg. angle between the panel edge and the diagonal. But the assumption of even distribution is not more than approximately correct; as stated before, the diagonal moment across the edge is not known with the degree of exactness obtained elsewhere. By a slight change in the bending moments and by introducing small torsional moments, M_{V} may be changed so as to eliminate the gap between M_{IV} and M_{V}. In fact, the gap may be eliminated, practically, by changing the direction of the couple M_{V} slightly without changing the magnitude.

Fig. 18 shows vector polygons of the same kind as those shown in the preceding figures. The diagrams apply to slabs with $c/l = 0.15$, 0.20, and 0.25. As in the preceding figure, gaps are left open between M_{IV} and M_V.

The method used here in the study of the equilibrium of the resultant couples acting upon an octant of the slab is analogous to that used by J. R. Nichols * in his study of the moments in a quadrant of the slab. In fact, the analysis represented in Fig. 17 and Fig. 18 may be looked upon as Nichols's analysis applied to an octant of the slab. The sum of positive and negative moments indicated in Fig. 17 is the total moment indicated by Nichols's analysis. The approximate value which Nichols gave in the discussion of his paper †

$$M_0 = \frac{1}{8} Wl\left(1 - \frac{2}{3}\frac{c}{l}\right)^2 \qquad (23)$$

is so nearly equal to the value which he derived originally that it may be used instead; it is the value used in connection with Table 3 and stated at the head of this table.

The moment coefficients for the column-head sections, mid-section, outer sections, and inner section, as taken directly from the diagrams in Fig. 14, Fig. 15, and Fig. 16, led to the gaps in the polygons in Fig. 17 and Fig. 18. While a part of the discrepancy may be due to a slight error in the total moment, and while it is possible that the main part of the discrepancy is due to the unevenness in the distribution of moments at the edge of the column capital, it was considered feasible to make adjustments by correcting each bending moment in proportion to its size. That is, the percentages of total moment indicated in Table 3 were left unchanged; they are the original percentages based on areas measured in the diagrams in Fig. 14. Adjustments of the coefficients of moment per unit-width, stated in Table 4, were introduced by a correction of the factors which are stated at the head of the table, and which were used in transforming the coefficients M/wl^2, of the type used in the diagrams, into coefficients of the type used in Table IV.

9. UNBALANCED LOADS ON FLAT SLABS. The load on one panel of a flat-slab floor-structure has some influence on the stresses in the adjoining panels. If a load which is originally uniformly distributed over all panels is changed by removing or reducing the loads on some of the panels, the stresses in the remaining panels will be increased in some sections and decreased in others. The loads, by this change, become unbalanced. Unbalanced loads cause the tangents across the panel edges to rotate; they may produce bending moments in the columns or may cause the column capitals to rotate about horizontal axes. Unbalanced loads on continuous beams produce analogous effects; for example, the positive moments in one span increase when the downward loads in the two adjacent spans are removed. In the analysis of flat-slab structures the varying degree of

* See Art. 4, footnote 17.

† J. R. Nichols, Discussion on reinforced-concrete flat-slab floors. Am. Soc. C. E., v. 77, 1914, p. 1735.

stiffness of the columns must be taken into consideration; this stiffness of the columns affects the stresses under unbalanced loads.

Fig. 19 and Fig. 20 show certain results of the study of unbalanced loads. Further studies of the effects of these loads are made in connection with Fig. 21 to Fig. 24.

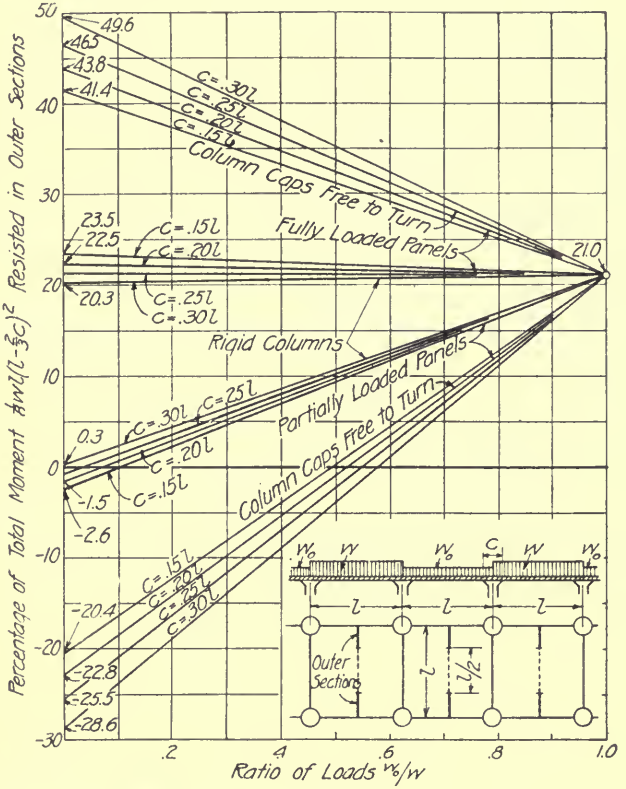

FIG. 19.—BENDING MOMENTS IN OUTER SECTIONS DUE TO UNBALANCED LOADS; DIFFERENT UNIFORM LOADS ON ALTERNATE ROWS OF PANELS.

A flat-slab structure is considered in which each floor consists of a large number of equal square panels. For the sake of convenience of analysis the number of panels may be assumed to be infinite in all directions, as in the preceding article. All the columns are assumed to be alike. Poisson's ratio is again assumed to be equal to zero. The small figures at the bottoms of Fig. 19 and Fig. 20 show the loading arrangement on one floor: each alternate row of panels carries the full uniform load, w per unit-area, the other rows carry the reduced uniform load, w_0 per unit-area.

The positive moments in the outer and inner sections shown in Fig. 19 and Fig. 20 reach extreme conditions when w is as large as possible, and when w_0 is as small as possible, for example, when w_0 is equal to the dead load only. The abscissas in Fig. 19 and Fig. 20 represent the ratio w_0/w of the loads. The left-hand edges correspond to $w_0 = 0$, that is, every other row

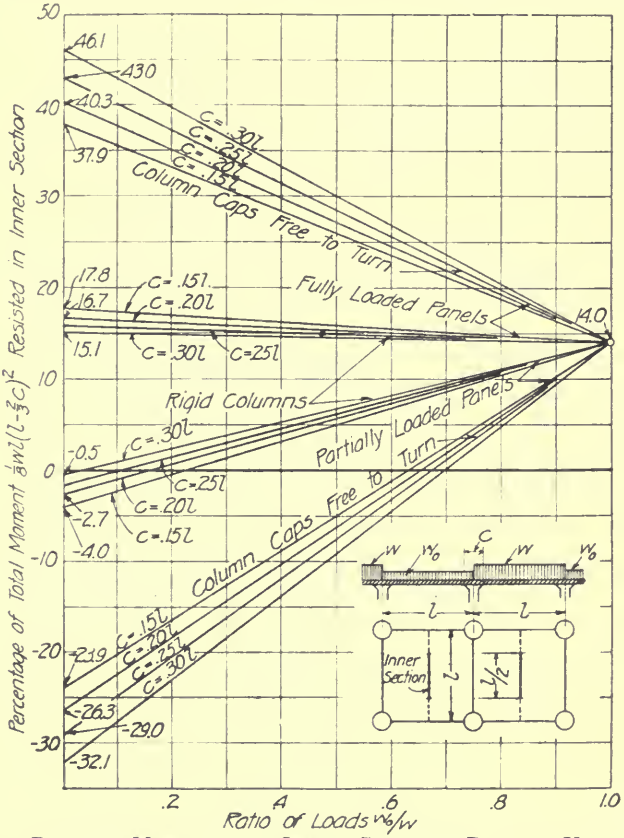

FIG. 20.—BENDING MOMENTS IN INNER SECTIONS DUE TO UNBALANCED LOADS; DIFFERENT UNIFORM LOADS ON ALTERNATE ROWS OF PANELS.

of panels is entirely unloaded. The right-hand edges correspond to $w_0 = w$, that is, uniform load w on all panels as in the preceding article. The ordinates in Fig. 19 and Fig. 20 represent percentages of the total moment $M_0 = \frac{1}{8} Wl(1 - \frac{2}{3}c)^2$; M_0 is the sum of the numerical values of the moments in the outer sections, inner section, column-head sections, and mid-section when the panel is loaded by w. The values indicated on the right-

hand edges, 21.0 in Fig. 19, and 14.0 in Fig. 20, are the percentages applying to the condition of uniform load over all panels. These two percentages are approximate values, taken from the last column in Table III in the preceding article; they are nearly equal to the exact values, which vary only slightly within the range of variation of c/l. The two upper pencils of lines in Fig. 19 refer to the fully loaded panels, the panels loaded by w; the two lower pencils refer to the panels which carry only the partial load w_0. Two extreme cases are represented, one by the two middle pencils, the other by the two outer pencils. In one extreme case the columns are perfectly rigid, and in the other the column capitals are perfectly free to rotate about horizontal lines. The latter condition may be established by introducing hinges in the columns directly below the column capitals and directly above the slab. Actual slab-structures fall between the two extreme conditions, which, therefore, are analyzed first. Methods by which one may interpolate between the extreme cases will be indicated later.

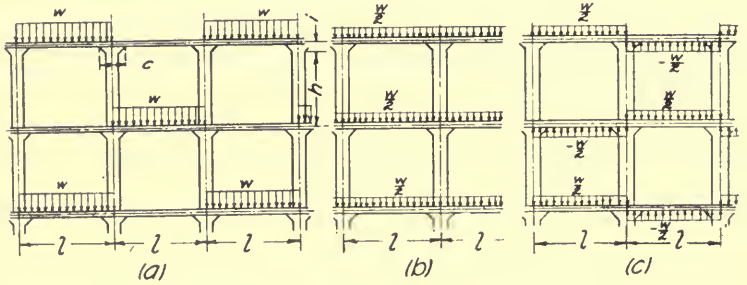

FIG. 21.—UNBALANCED LOADS PRODUCING MAXIMUM POSITIVE MOMENTS IN THE SLAB;

(a) total applied load;

(b) component, $+\frac{w}{2}$, of applied load.

(c) component, $\pm\frac{w}{2}$, of applied load;

According to Fig. 19, when w_0 is zero, and when the columns are rigid, the percentage of moment in the outer sections in the loaded panels ranges from 20.3 for $c = 0.3l$ to 23.5 for $c = 0.15l$. In the unloaded panels the corresponding percentage is small, ranging from + 0.3 to — 2.6, the latter figure indicating a small negative moment. When the columns are free to turn, the load on one panel has a marked influence on the moments in the other panels. According to Fig. 19, when w_0 is zero, the percentage for the outer section ranges from 41.4 to 49.6 for the loaded panels, and from — 20.4 to — 28.6 for the unloaded panels. The negative percentages represent fairly large negative moments. The use of the diagram may be illustrated by an example. Assume $w_0 = 0.4w$, $c = 0.2l$; then $M_0 = \frac{1}{8} wl\,(l - \frac{2}{3}c)^2 = \frac{1}{8} wl^3\,(1 - \frac{2}{3}.\ 0.2)^2 = 0.0939wl^3$. The diagram gives the following values of the moment in the outer sections: in the fully

loaded panels, $0.218M_0$ when the columns are rigid, $0.347M_0$ when the column capitals are free to turn; in the partially loaded panels, $0.075M_0$ when the columns are rigid, $-0.053M_0$ when the column capitals are free to turn.

Fig. 20, which refers to the inner section, is analogous to Fig. 19. The percentage of moment varies in the same general manner as in Fig. 19.

The procedure of the analysis will now be discussed. The load consisting of w and w_0 on alternate rows of panels is denoted by w,w_0. The moments produced by this load are linear functions of w_0; and when w is considered as a constant, they are linear functions of the ratio w_0/w. It follows that when the moments for the extreme values $w_0 = 0$ and $w_0 = w$ are known, that is, the moments represented at the left and right edges in Fig. 19 and Fig. 20 are known, then the moments for intermediate values may be determined by linear interpolation, as represented by the straight lines in the two figures. It remains, therefore, to make an analysis for the load $w,0$, (or w and zero in alternate rows of panels). This load, $w,0$, may be resolved into two components by the scheme indicated in Fig. 21 and Fig. 23.* The load $w,0$ on each floor in Fig. 21(a) is resolved into two components: $+\frac{w}{2}$, shown in Fig. 21(b), uniformly distributed over all panels; and $+\frac{w}{2},-\frac{w}{2}$, shown in Fig. 21(c), consisting of the upward and downward uniform loads $w/2$ on alternate rows of panels. The load $\frac{w}{2},-\frac{w}{2}$ is anti-symmetrical with respect to the dividing edges, that is, the edges at which the load changes from $+w/2$ to $-w/2$. The structure itself is symmetrical with respect to the vertical sections through these edges. Consequently, under the load $+\frac{w}{2},-\frac{w}{2}$, the deflections at points which are symmetrical with respect to the dividing edges are equal and opposite; the dividing edges remain straight and undeflected; the moments in sections which are symmetrical with respect to the dividing edges are equal and opposite; and the moments at the dividing edges are zero.

When the column capitals are free to turn, and when their diameter is small, the slab, under the load $+\frac{w}{2},-\frac{w}{2}$, will deflect within each row of panels as if that particular row were separated from the rest of the slab, and as if it were simply supported on girders at the two parallel edges of the row. The moment per unit-width across the center line of the row, accordingly, is $+\frac{1}{8}\frac{w}{2}l^2$ in the row loaded by $+\frac{w}{2}$, and $-\frac{1}{8}\frac{w}{2}l^2$ in the row loaded by $-\frac{w}{2}$. Since the column capitals are in the regions near the points of inflection, a change in the size of the diameter of the

* This scheme was used by Nielsen (Spaendinger i Plader, 1920, p. 192).

column capitals, even to the greatest size $c = 0.3l$, has only a slight influence on the state of flexure of the slab under the load $+\frac{w}{2}, -\frac{w}{2}$, as long as the column capitals are free to turn. Minor local redistributions of the moments occur near the edges of the column capitals as a result of this change in the diameter of the column capital, but in the inner and outer sections the influence of this change is negligible. That is, the values $\pm \frac{1}{8}\frac{w}{2}l^2$ may be used without reference to the size of the column capital. The method of calculation for the load $w,0$, when the column capitals are free to turn, may be shown by an example. Take $c = 0.2l$. The corresponding total moment is $M_0 = \frac{1}{8}wl^3\,(1 - \frac{2}{3}.\,0.2)^2 = 0.0939wl^3$. The moments in the outer sections due to the load $+\frac{w}{2}, -\frac{w}{2}$ are $\pm \frac{1}{8}\cdot\frac{w}{2}\cdot l^2\cdot\frac{l}{2}$ $= \pm \frac{w\,l^3}{32} = 0.333M_0$. The moment in the outer sections, due to the uniform load $\frac{w}{2}, \frac{w}{2}$, is $\frac{1}{2}\,.\,0.21M_0 = 0.105M_0$. The resultant moments in the outer sections are then: in the loaded panels, $0.333M_0 + 0.105M_0 = 0.438M_0$; in the unloaded panels $-0.333M_0 + 0.105M_0 = -0\,228M_0$. The percentages 43.8 and —22.8 are shown at the left-hand edge in Fig. 19. The other percentages represented at the left-hand edges in Fig. 19 and Fig. 20 were calculated in the same manner.

The slab-structure with rigid columns and immovable column capitals was analyzed as a statically indeterminate structure in which the turning couples transferred from the slab through the column capital to the column are introduced as statically indeterminate quantities. The structure with column capitals free to turn is used in the analysis as a substitute structure. In this substitute structure the column capitals turn under the influence of the load $+\frac{w}{2}, -\frac{w}{2}$, but the slope of the column capitals may be reduced to zero, and thus the substitute structure may be made to act like the original structure, by applying a turning couple of the proper magnitude and direction at each column capital. The resultant moments in the slab are found, then, by adding the moments produced by the turning couples to those already existing. In order to find the magnitude of the turning couples and the effects of them, a study was made of bending moments and slopes produced by turning couples $\pm 2l$ of constant magnitude, applied at the column capitals. Results of this study are stated in Table V(a). In order to derive these results the structure with column capitals free to turn was replaced by a second substitute structure in which the column capitals are removed altogether. This second substitute structure is the same point-supported slab that was used in the preceding article in the study of the slab with the same load in all panels. The second substitute structure is loaded at the points of support by concentrated couples

$\pm 2l$ and by certain additional concentrated loads which may be called ring couples. A ring couple may be obtained by applying two equal and two opposite ring loads, of the kind described in the preceding article, so close together that the whole system of forces may be considered as a concentrated load. The concentrated couples acting alone do not produce uniform slopes at the circles marking the edges of the column capitals; but uniformity of the slopes at these circles is restored by adding ring couples of the proper intensity. The second substitute structure is thus made to act like the first substitute structure, which is the slab with column capitals which are free to turn relative to the columns. The influence of the ring couples on the moments at the center line of the row is small; it is measured by the difference between the moments stated in the first column in

TABLE V (*a*).—BENDING MOMENTS AND SLOPES DUE TO TURNING COUPLES $+2l$ APPLIED AT THE COLUMN CAPITALS.

The turning couples are clockwise and counter-clockwise in alternate rows of columns.
x is perpendicular to the rows, y is in the direction of the rows. The couples are in planes parallel to xz.
l = span; c = diameter of column capital; I = moment of inertia per unit-width; Poisson's ratio = 0.

c/l		0	0.15	0.20	0.25	0.30
Moments in x-direction per unit-width.	Center of edge parallel to x	0.886	0.898	0.907	0.920	0.936
	Center of panel	1.081	1.073	1.066	1.057	1.046
	Average for width l	1.0	1.0	1.0	1.0	1.0
Moments in y-direction per unit-width.	Center of edge parallel to x	0.294	0.282	0.273	0.260	0.244
	Center of panel	—0.248	—0.240	—0.233	—0.224	—0.213
	Average for length l	0.	0.	0.	0.	0.
Total moments in x-direction.	Outer sections	0.469l	0.472l	0.475l	0.478l	0.482l
	Inner section	0.531l	0.528l	0.525l	0.522l	0.518l
Slope s of column capital, in x-direction		.....	$\frac{1.081l}{2EI}$	$\frac{0.975l}{2EI}$	....	$\frac{0.834l}{2EI}$
Approximate values of s, calculated by the formula $s=\frac{l-c}{2\cdot 0.82EI}$		.....	$\frac{1.037l}{2EI}$	$\frac{0.975l}{2EI}$	....	$\frac{0.854l}{2EI}$

Table V(a) and the moments in the remaining columns. The moments and slopes in Table V(a) were calculated by means of infinite series which are solutions of Lagrange's differential equation; details of this analysis will be given in the appendix.

The slope of the column capitals under the influence of the load $+\frac{w}{2}, -\frac{w}{2}$, or the load w, 0, is found to be, with close approximation,

$$s_0 = \frac{wl^3}{48EI}\left(1 - \frac{3}{8}\left(\frac{c}{l}\right)^2\right). \qquad (24)$$

The values of the slope s of the column capitals under the influence of the couples $\pm 2l$ are stated in Table V(a). The turning couples $\mp M_c$ which are necessary to make the resultant slope of the column capital

equal to zero is determined, then by the formula $M_c = 2\,l.\ \frac{s_0}{s}$ (25)

M_c is the resultant couple which is transferred through each column capital, from the columns to the slab in the original structure, which is the structure with rigid columns and immovable column capitals. An example will show the manner of computing M_c and the resultant bending moments which are shown at the left-hand edges in Fig. 19 and Fig. 20. Take $c = 0.2l$. Equation (24) gives $s_0 = \frac{w\,l^3}{48EI}\ .\ 0.985$. Table V(a) gives $s = \frac{0.975l}{2EI}$. The couple transferred through each column capital is, then, according to formula (25), $M_c = \frac{2l\,s_0}{s} = \frac{0.985}{0.975}\cdot\frac{wl^3}{12} = 0.0842wl^3 = 0.897M_0$. According to Table V(a) the moment in the inner section in the slab with column capitals free to turn, produced by the turning couples $\pm\ 2l$ is $\pm\ 0.525l$. The corresponding moment produced by the turning couples $\mp\ M_c$ is then $\mp\ \frac{0.525l\ .\ M_c}{2l} = \mp\ \frac{1}{2}\ .\ 0.525\ .\ 0.897M_0 = \mp\ 0.236M_0$.

The signs, minus and plus, refer to the loaded and unloaded row of panels, respectively. According to Fig. 20 the moments in the inner section in the slab with column capitals free to turn, produced by the load w,0, are $0.403M_0$ in the loaded row of panels and $-0.263M_0$ in the unloaded row. The resultant moments in the inner sections in the slab with rigid columns are then:

in the loaded row of panels: $0.403M_0 - 0.236M_0 = 0.167M_0$;
in the unloaded row of panels: $-\ 0.263M_0 + 0.236M_0 = -0.027M_0$.

The coefficients 0.167 and — 0.027 are expressed as percentages and are shown at the left-hand edge in Fig. 20. The remaining percentages belonging to the two middle pencils in Fig. 19 and Fig. 20 were computed in a similar manner.

Two extreme cases have been considered so far: one with perfectly stiff columns and fixed column capitals; the other with columns which are flexible or supplied with hinges at the ends, so as to allow the column capitals to turn freely with the slab. Actual slab-structures have an intermediate degree of rigidity of the column capitals. These structures can be dealt with if a method of interpolation between the extreme cases can be devised, so that one can say that a given case belongs, for example, 70 per cent or 0.7 to one extreme case, and 30 per cent or 0.3 to the other. For the purpose of the interpolation two definite ratios are introduced measuring the degree of fixity of the column capitals and the degree of freedom of the column capitals to rotate. These ratios are

k = fixity of the column capitals,
$k' = 1 - k$ = freedom of the column capitals to rotate.

These ratios are defined as follows: Let M denote the moment in a certain section, M_A and M_B the moments which would occur in the same section if the column capitals were fixed and free to turn, respectively. The ratios

k and k' are defined, then, as far as the particular section is concerned, by the equations:

$$M = kM_A + k'M_B, \tag{26}$$

$$k + k' = 1. \tag{27}$$

For example, $M = 130000$ in. lb, $M_A = 100000$ in. lb, and $M_B = 200000$ in. lb, gives $k = 0.7$, $k' = 3$; the column capitals may be said to be 70 per cent fixed and 30 per cent free to turn. M may be calculated by formula (26) when M_A, M_B, k and k' are known. The limiting values of k and k' are 0 and 1; the combination $k = 1$, $k' = 0$ represents the extreme case of fixed capitals; the combination $k = 0$, $k' = 1$ represents the case of column capitals which are free to turn.

The values of k and k' may be different at the different moment sec-

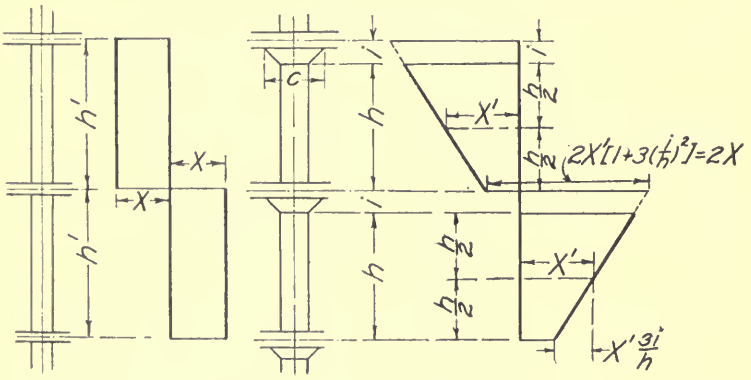

FIG. 22.—MOMENTS IN COLUMNS DUE TO UNBALANCED LOAD SHOWN IN FIG. 21;

(a) columns without capitals;
(b) columns with capitals;

tions. But in certain important cases, for example, in those shown in Fig. 21 and Fig. 23, k and k' are independent of the position of the moment section; k and k', then, are constants belonging to this structure as a whole. Let

M'_c = moment transferred from a column through the column capital to the slab in the structure with intermediate rigidity of the column capitals;

M_c = moment transferred from a column through the column capital to the slab in the structure with fixed column capitals.

Application of (26) to these moments gives

$$M'_c = k_c M_c \tag{28}$$

where k_c is the fixity k referring to the moments which are transferred through the column capitals. Assume that a calculation by (28) leads to

the same value of k_c for all the column capitals within an area which includes a large number of panels in both directions. It may be shown that k in (26), under this condition, is the same for all sections and is equal to the constant value k_c: the moment M in any section may be expressed as a linear function of the moments M'_c; by substituting $M'_c = k_c M_c$, the moment M becomes a linear function of k_c; according to (26) and (27) M is a linear function of k; the limits of k and k_c are the same, 0 and 1; consequently, $k = k_c$ as was to be proved. In Fig. 21 and Fig. 23 M'_c and M_c are the same in all columns, except for the direction clockwise or counter-clockwise; that is, in each slab, k is the same at all column capitals and in all moment sections. The loading arrangement in Fig. 21 produces the greatest possible moments in the outer and inner sections; the arrangement in Fig. 23 produces large moments in the columns.

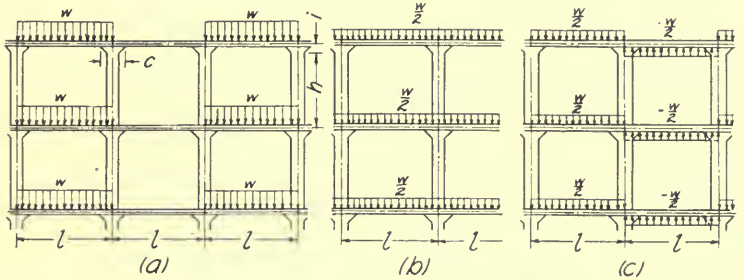

FIG. 23.—UNBALANCED LOADS PRODUCING LARGE MOMENTS IN COLUMNS;
(a) total applied load;
(b) component, $+\frac{w}{2}$, of applied load;
(c) component, $\pm\frac{w}{2}$, of applied load.

The analysis is facilitated by resolving the loads $w0$ shown in Fig. 21(a) and Fig. 23(a) in each case into two components: namely, $\frac{w}{2}$, $\frac{w}{2}$, shown in Fig. 21(b) and Fig. 23(b), and $\frac{w}{2}$, $-\frac{w}{2}$, shown in Fig. 21(c) and Fig. 23(c). To make the analysis simple, the dimensions, including the diameter of the columns, are assumed to be the same through several stories.

The dimensions and the loads are denoted as in Fig. 21 and Fig. 23. Fig. 22 and Fig. 24 show diagrams of the bending moments in the columns; they show also the notation for these bending moments. The moments of inertia of the sections are

I' = moment of inertia of the cross section of the slab for the whole panel width,

J = moment of inertia of the columns.

A simplified case is considered first, in which the slab-structure is replaced by a frame whose girders and columns have the same moments of inertia, I' and J, as the slab structure; at the joints there are no column

capitals, but the connections between the four adjoining members are rigid. The moment diagrams of the columns are shown in Fig. 22(a) and Fig. 24(a). Analysis, for example, by the method of least work, by the method of the substitute structure, or by the slope-deflection method, leads to the following values:

In Case I, Fig. 21 and Fig. 22 (a), with

$$K = \frac{J\,l}{I'\,h'}, \tag{29}$$

one finds

$$X = \frac{w\,l^3}{24}\left(1 - \frac{1}{1+K}\right), \tag{30}$$

that is,

$$k = 1 - \frac{1}{1+K}, \quad k' = \frac{1}{1+K}. \tag{31}$$

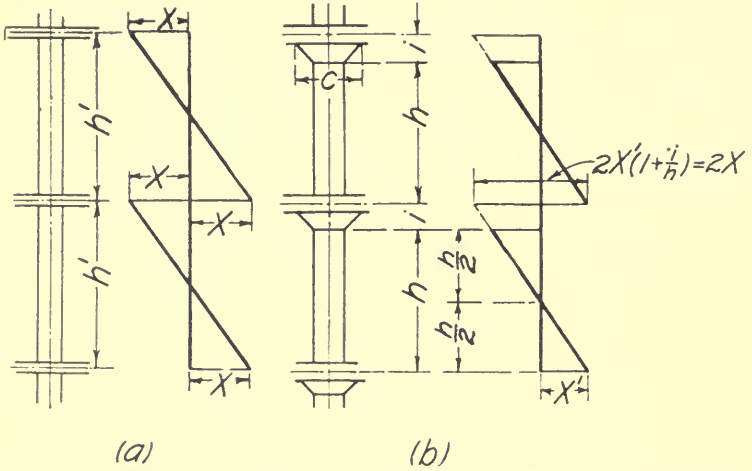

FIG. 24.—MOMENTS IN COLUMNS DUE TO UNBALANCED LOAD, SHOWN IN FIG. 23;

(a) columns without capitals;
(b) columns with capitals

In Case II, Fig. 23 and Fig. 24(a), again with

$$K = \frac{J\,l}{I'\,h'},$$

one finds

$$X = \frac{w\,l^3}{24}\left(1 - \frac{1}{1+3K}\right), \tag{32}$$

that is,

$$k = 1 - \frac{1}{1+3K}; \quad k' = \frac{1}{1+3K}. \tag{33}$$

In the slab-structure the bending moments are not uniformly distributed over the width of the sections. One may say, that the moment of inertia I' of the section is not fully effective. The presence of the column capitals, on the other hand, has the effect of reducing the clear spans and increasing the rigidity of the structure. The slopes or angles of rotation of the column capitals in Fig. 21 and Fig. 22(b) must be equal or equal and opposite. The moment diagram of the cylindrical part of the column between the top of the slab and the bottom of the column capital above, must have its centroid, therefore, at the center of the total distance measured between the centers of the slabs. In Fig. 24(b) the point of inflection is at the center of the cylindrical part of the column. The dimensions of the moment diagrams in Fig. 22(b) and Fig. 24(b) have been computed without considering the influence of the thickness of the slab upon the stiffness of the column. This influence may be taken into account by measuring h from the top of the slab to the bottom of the column capital above, i from the bottom of the column capital to the bottom of the slab; $h' = h + i$ is, accordingly, the clear distance from the top of one slab to the bottom of the slab above.

The slope of the column at the capital must be equal to the angle of rotation or slope of the capital. In terms of the moments in the columns, the slopes, θ, of the columns at the capitals are

$$\theta = \frac{X'h}{2\,EJ} \text{ in Fig. 22 (b)}, \quad \theta = \frac{X'h}{6\,EJ} \text{ in Fig. 24 (b)}. \tag{34}$$

In terms of the moments $\pm 2X$, transferred from the columns through the capitals to the slab, and in terms of the applied load w,0 or $+\frac{w}{2}$, $-\frac{w}{2}$, the angle of rotation, or slope, of the column capitals in Fig. 21 to Fig. 24 may be expressed approximately as follows, as may be seen by comparison with the last line in Table V(a) and with formula (24):

$$\theta' = -\frac{X\,(l-c)}{2 \cdot 0.80 \cdot 1.02 EI'} + \frac{w\,l^4}{48 \cdot 1.02 EI'}. \tag{35}$$

By equating θ to θ' and substituting the values of X given on the diagrams in Fig. 22(b) and Fig. 24(b), in terms of X', the following values are obtained:

In Case I, Fig. 21 and Fig. 22(b), one finds

$$X' = \frac{wl^2}{24} \frac{\dfrac{J\,l}{1.02 I'h}}{1 + \left(1+3\frac{i}{h}\right)^2 \left(1-\frac{c}{l}\right) \dfrac{J\,l}{0.80 \cdot 1.02 I'h}} \tag{36}$$

The fixity k of the column capitals is the ratio of this quantity to the value of the same quantity when $J = \infty$ that is,

$$k = 1 - \frac{1}{1+K}, \quad k' = \frac{1}{1+K}, \tag{37}$$

where

$$K = \frac{\left(1+3\left(\frac{i}{h}\right)^2\right)\left(1-\frac{c}{l}\right)}{0.80 \cdot 1.02} \cdot \frac{J\,l}{I'h}. \tag{38}$$

In case II, Fig. 23 and Fig. 24(b), one finds

$$X' = \frac{w\,l^3}{24} \frac{\frac{J\,l}{1.02I'h}}{\frac{1}{3} + \left(1+\frac{i}{h}\right)\left(1-\frac{c}{l}\right) \cdot \frac{J\,l}{0.80 \cdot 1.02I'h}}. \tag{39}$$

The fixity k of the column capitals is determined as in Case I by comparing X' with its value when $J = \infty$ one finds

$$k = 1 - \frac{1}{1+3K}, \qquad k' = \frac{1}{1+3K}, \tag{40}$$

where

$$K = \frac{\left(1+\frac{i}{h}\right)\left(1-\frac{c}{l}\right)}{0.80 \cdot 1.02} \cdot \frac{J\,l}{I'h} \tag{41}$$

When the fixity has been computed, the maximum moment X' in the cylindrical part of the column may be computed as

$$X' = \frac{w\,l^3}{24} \cdot \frac{0.80k}{\left(1+\frac{i}{h}\right)\left(1-\frac{c}{l}\right)} \tag{42}$$

Sample calculations of freedom of the column capitals to rotate, fixity of the capitals, and moments in the columns, according to formulas (26) to (42), are shown in Table V(b). In examples (1) the columns are rather slender, in examples (2) and (3) they are comparatively stiff. The material is assumed to be homogeneous. The dimensions i should be measured, as stated before, as the vertical distance between the bottom of the column capital and the bottom of the slab. In example (1), Case I, the column capitals are found to be about 28 per cent fixed, 72 per cent free to turn. Fig. 19 and Fig. 20 show that with these degrees of fixity and freedom to rotate, unbalanced loads will have a considerable influence on the bending moments. In examples (3), Case I, the fixity is 90 per cent; that is, the moments in the inner and outer sections of the loaded panels will not differ greatly from the moments under uniform load.

It should be noted that those approximate values of fixity, freedom to rotate, and moments in the column, which are computed by considering the structure as a frame, do not differ greatly from the corresponding values in the lower part of Table V(b), which are calculated more exactly. One may conclude that other flat-slab structures may be analyzed, in most cases with a satisfactory approximation, as far as the moments in the columns are concerned, by methods applying to frames. For example, the

TABLE V (b).—SAMPLE CALCULATIONS OF THE RIGIDITY OF COLUMN CAPITALS.

The material is assumed to be homogeneous. The dimensions and loads are indicated in Fig. 21(a) and Fig. 23(a). The moment diagrams of the columns are shown in Fig. 22 and Fig. 24.

I' = moment of inertia of slab per panel width;
J = moment of inertia of columns;
k = fixity of column capitals;
k' = freedom of column capitals to rotate.

EXAMPLE NO.		(1)		(2)		(3)	
Span between centers of Columns		l		l		l	
Total story height $h' = h + i$		l		$0.75\,l$		$0.50\,l$	
Thickness of slab, t		$l/24$		$l/32$		$l/32$	
Diameter of column, d		$l/12$		$l/8$		$l/8$	
A. Frame structure with $c = 0$, $i = 0$							
	$K = \frac{Jl}{Ih} = \frac{\pi \times 12 \times d^4}{64 t^3 h'}$	0.393		6.28		9.42	
Case I,	Freedom $k' = \frac{1}{1+K}$	0.718		0.137		0.096	
Fig. 21, 22(a)	Fixity $k = 1 - k'$	0.282		0.863		0.904	
Case II,	Freedom $k' = \frac{1}{1+3K}$	0.459		0.050		0.034	
Fig. 23, 24(a)	Fixity $k = 1 - k'$	0.541		0.950		0.966	
	Moment in column $X = K\frac{wl^2}{24}$	$0.0225\,wl^3$		$0.0396\,wl^3$		$0.0402\,wl^3$	
B. Flat-slab structure							
	c	$0.2\,l$	$0.3\,l$	$0.2\,l$	$0.3\,l$	$0.2\,l$	$0.3\,l$
	i	$0.05\,l$	$0.10\,l$	$0.04\,l$	$0.09\,l$	$0.04\,l$	$0.09\,l$
	h	$0.95\,l$	$0.90\,l$	$0.71\,l$	$0.66\,l$	$0.46\,l$	$0.41\,l$
Case I,	$K = \frac{(1+3(\frac{c}{h})^2)(1-\frac{c}{l})}{0.80 \cdot 1.02} \cdot \frac{Jl}{Ih}$	0.388	0.350	6.22	5.69	9.45	9.25
Fig. 21,	Freedom $k' = \frac{1}{1+K}$	0.720	0.741	0.138	0.149	0.096	0.098
Fig. 22(b)	Fixity $k = 1 - k'$	0.280	0.259	0.862	0.851	0.904	0.902
Case II,	$3K = \frac{3(1+\frac{c}{h})(1-\frac{c}{l})}{0.80 \cdot 1.02} \cdot \frac{Jl}{Ih}$	1.216	1.124	19.50	18.36	30.10	29.55
Fig. 23,	Freedom $k' = \frac{1}{1+3K}$	0.451	0.471	0.049	0.052	0.032	0.033
Fig. 24(b)	Fixity $k = 1 - k'$	0.549	0.529	0.951	0.948	0.968	0.967
	Coefficient $\frac{X}{wl^3} = \frac{1}{24}\frac{0.80K}{(1+\frac{c}{h})(1-\frac{c}{l})}$	0.0217	0.0227	0.0375	0.0397	0.0371	0.0378

slope-deflection method * may be used to advantage when the design is less uniform than assumed in Table V(b); for example, when the diameter of the columns is different in the different stories.

So far, attention has been given mainly to the moments due to unbalanced loads in the outer and inner sections. The negative moments in the column-head sections and mid-section are affected less by unbalanced loads than are the positive moments. In a frame structure the maximum negative moment in the second-floor girder between the third and fourth span occurs with the following combination of loaded and unloaded spans; W is the total load on one span:

	Loads on Span No.					
	1	2	3	4	5	6
4th floor		O	W	W	O	
3rd floor		W	O	O	W	
2nd floor	W	O	W	W	O	W
1st floor		W	O	O	W	

With span l, total story height h', and moments of inertia I' of the girders and J of the columns as before, the negative moment in the second-floor girder between the third and fourth span becomes, as may be verified by the slope-deflection method,

$$-M' = \frac{Wl}{24}\left(1 + \frac{1}{2}\frac{(K+2)^2 - 1}{K+1}\right), \tag{43}$$

where $K = \frac{Jl}{I'h'}$ as before (formula (29)). This moment is found to be approximately equal to

$$-M' = \frac{Wl}{24}\left(1 + \frac{0.4}{1+K}\right). \tag{44}$$

When $J = \infty$ the moment becomes $Wl/24$. Or, the ratio, Q, of increase of the negative moment by a change to columns of finite stiffness is approximately

$$Q = 1 + \frac{0.4}{1+K} = 1 + 0.4k', \tag{45}$$

where k' is the freedom of the column capitals to rotate under the loading arrangement in Fig. 21. The ratio Q may be assumed to apply approximately to the negative moments in flat slabs. For example, $k' = 0.72$, as given in the first column in Table 5(b), gives $Q = 1.29$, or 29 per cent increase, while $k' = 0.10$ gives an increase of 4 per cent.

The case in which only a single panel is loaded is of no particular importance as a condition for design; greater bending moments are produced by a uniform load on all panels or by loading in rows than by single-panel loading. A number of tests have been made, however, with a single panel loaded, and the case should be investigated for the purpose of the study of these tests.

---

* See Wilson, Richart, and Weiss, Analysis of Statically Indeterminate Structures, by the Slope Deflection Method, Univ. of Ill. Eng. Exp. Sta. Bull. 108, 1918; Hool and Johnson, Concrete Engineers' Handbook, 1918, p. 411, p. 629.

When the columns are stiff, the single-panel load produces approximately the same effects in the panel as a "checker-board load," by which the panels corresponding to the black and white fields of a checker-board are loaded and unloaded respectively.* The checker-board load leads to a simpler analysis than the single-panel load. The checker-board load W, O may be resolved into two components, one, $\frac{W}{2}, \frac{W}{2}$, uniformly distributed over all panels, the other, $+\frac{W}{2}, -\frac{W}{2}$, positive and negative in alternate panels. The first component produces one-half the moments derived in Art. 8. The second component, on account of the anti-symmetry leaves the panel edges straight; that is, if the column capitals are small, each panel deflects as a single square panel which is simply supported on four sides and loaded by $+W/2$ or $-W/2$.

A study is made of the equilibrium of one-half of a loaded panel. This half-panel is a rectangle with two sides of length l, containing the column-head sections, mid-section, outer sections, and inner section, and two sides of length $l/2$. The moments are taken about the edge containing the mid-section and column-head sections. The following results were found for the point-supported slab with checker-board loading W, O, the moments being expressed in terms of the total moment $M_o = \frac{1}{8} Wl$:

Moment in inner section:	$0.13M_o$;
outer sections:	$0.13M_o$;
mid-section:	$0.09M_o$;
column-head section:	$0.24M_o$.
Total for the moment sections:	$0.59M_o$
Moments of vertical shears plus torsional moments in the short sides of the rectangle:	$0.41M_o$
Total:	$1.00M_o$
Moment of applied load $W/2$:	$-1.00M_o$
Total moment about edge containing mid-section:	0.

According to these results 41 per cent of the total moment leaks out by shear and torsion in the short edges of the rectangle. In deriving the moments in the various sections use was made of the results, stated in Art. 8, Table 3, obtained for a flat slab with all panels loaded; of the value stated in Fig. 3(a), of the moment at the center of a square slab simply supported on four sides; and of the value of the moments and shears at other points of a square slab simply supported on four sides, stated by Leitz.† In slabs with column capitals the proportions of moments may be assumed to be approximately the same as in the slabs with point supports, provided the column capitals are not too large. Or, by substituting $M_o = \frac{1}{8} W l (1 - \frac{2}{3}\frac{c}{l})^2$, one may use the expressions just stated for the

* See Nielsen, p. 196, where this case is investigated.
† See Nielsen, p. 133.

point-supported slab, as approximate expressions for moments in the slab with column capitals.

10. MOMENTS IN WALL PANELS, CORNER PANELS, OBLONG INTERIOR PANELS, AND PANELS WITHOUT BENDING RESISTANCE IN THE MID-SECTION. Table VI contains approximate values of moments in panels of several different types. The results of the computations are found in the column next to the last in the table. The calculations are based on Nielsen's * work, and they are of an approximate character. In the analysis of these cases by difference equations Nielsen used a rather large value of the side λ of the elementary square, and he assumed point supports instead of supports on column capitals. It was his scheme that the values determined in this manner should be used as a basis of comparison between the different cases; this use has been made of his results in Table VI. The exterior panels dealt with in Table VI are assumed to be simply supported along the walls on rigid lintel beams.

An example will illustrate the method followed in computing Table VI. Take sections D and E in the third case in Table VI, that is, the case of two adjacent rows of wall panels with lintel beams. Nielsen† gives the following coefficients M/wl^2 of moment per unit width when Poisson's ratio is zero: at the center of D, $a_1 = 0.0861$; at the center of E, $c_1 = 0.0661$; midway between, $b_1 = 0.0725$. The spaces between these points are equal to the side $\lambda = l/4$ of the elementary square which was used in the difference equations. The three coefficients are to be interpreted as the altitude of three rectangles, placed together as in Fig. 25 at the left. The three rectangles constitute the moment diagram in approximate form. A more nearly correct diagram is obtained by drawing a smooth curve which has the altitudes of the rectangles as average ordinates in the three intervals covered by the rectangles. The curved diagram is now replaced, as shown at the right in Fig. 25, by two rectangles whose altitudes are average ordinates within the two intervals covered by the bases. The formulas stated in Fig. 25 for these altitudes apply approximately, and they were used in the calculation of the table. In this manner the following coefficients of moment per unit-width are found in sections D and E:
in the outer section D,

$$\frac{a_1 + b_1}{2} + \frac{a_1 - c_1}{15} = \frac{0.0861 + 0.0725}{2} + \frac{0.0861 - 0.0661}{15} = 0.0806,$$

and in the inner section E,

$$\frac{b_1 + c_1}{2} - \frac{a_1 - c_1}{15} = \frac{0.0725 + 0.0661}{2} - \frac{0.0861 - 0.0661}{15} = 0.0680.$$

The corresponding moments per unit width, $0.0806W$ and $0.0680W$, where $W = wl^2$, and the average value $0.0743W$ applying to section F, are stated in Table VI. By applying the same method, with the side of the elementary

* N. J. Nielsen, Spaendinger i Plader, 1920; the five cases represented in Table 6 are dealt with in his work on pages 210, 189, 212, 217, and 205, respectively.
† Nielsen, p. 214.

TABLE VI.—MOMENTS IN OBLONG PANELS, WALL PANELS, CORNER PANELS, AND PANELS WITHOUT BENDING RESISTANCE IN THE MID-SECTION.

W = load per panel (uniform over all panels). $M_o = \frac{1}{8} W l (1 - \frac{2}{3}\frac{c}{l})^2$. $M_o' = \frac{1}{8} W l (1 - \frac{2}{3}\frac{c}{l})^2$. $M_a = \frac{1}{8} W a (1 - \frac{2}{3}\frac{c}{a})^2$. $M_b = \frac{1}{8} W b (1 - \frac{2}{3}\frac{c}{b})^2$

Types of panels		Section		Length of section	Moment, M_n per unit width in Nielsen's analysis (point supports, $\lambda = \frac{1}{4}$ or $\frac{2}{5}$)	Ratio q_i of M_n to the M_n for normal panel	Deduced Moment M [$= M_o \cdot q_i$ (M_o = moment in normal panel)]	Location of sections
Square interior	Normal	Col-head	A	$\frac{1}{4}l$	-0.1067 W	1.00	-0.48 M_o	
		Mid	B	$\frac{1}{2}l$	-0.0495 W	1.00	-0.17 M_o	
		Total neg.	C	l	-0.0781 W	1.00	-0.65 M_o	
		Outer	D	$\frac{1}{2}l$	0.0579 W	1.00	0.21 M_o	
		Inner	E	$\frac{1}{2}l$	0.0359 W	1.00	0.14 M_o	
		Total pos.	F	l	0.0469 W	1.00	0.35 M_o	
	Without bending resistance across mid section	Col-head	A	$\frac{1}{2}l$		1.23	-0.59 M_o	
		Mid	B	$\frac{1}{2}l$		0.00	0.00	
		Outer	D	$\frac{1}{2}l$		1.10	0.23 M_o	
		Inner	E	$\frac{1}{2}l$		1.29	0.18 M_o	
Square exterior	Two adjacent rows of wall panels with lintel beams	Col-head	A	$\frac{1}{4}l$	-0.1380 W	1.29	-0.62 M_o'	
		Mid	B	$\frac{1}{2}l$	-0.0646 W	1.30	-0.22 M_o'	
		Total neg.	C	l	-0.1013 W	1.30	-0.84 M_o'	
		Outer	D	$\frac{1}{2}l$	0.0806 W	1.39	0.29 M_o'	
		Inner	E	$\frac{1}{2}l$	0.0680 W	1.89	0.26 M_o'	
		Total pos.	F	l	0.0743 W	1.58	0.55 M_o'	
		Lintel beams	L		-0.035 W		-0.035 Wl	
			M		0.0175 W		0.0175 Wl	
		Col-head	A'	$\frac{1}{4}l$	-0.1133 W	1.06	-0.51 M_o	
		Mid	B'	$\frac{1}{2}l$	-0.0327 W	0.66	-0.11 M_o	
			B$_1$'	$\frac{1}{4}l$	-0.0039 W		-0.01 M_o	
		Total neg.	C'	l	-0.0456 W	0.58	-0.38 M_o	
		Outer	D'	$\frac{1}{2}l$	0.0601 W	1.04	0.22 M_o	
		Inner	E'	$\frac{1}{2}l$	0.0222 W	0.62	0.09 M_o	
			E$_1$'	$\frac{1}{4}l$	0.0032 W		0.01 M_o	
		Total pos.	F'	l	0.0269 W	0.57	0.20 M_o	
	Four adjacent corner panels with lintel beams	Col-head	A	$\frac{1}{4}l$	-0.1264 W	1.18	-0.57 M_o'	
		Mid	B	$\frac{1}{2}l$	-0.0302 W	0.61	-0.10 M_o'	
			B$_1$	$\frac{1}{4}l$	-0.0008 W		-0.002 M_o'	
		Outer	D	$\frac{1}{2}l$	0.0740 W	1.28	0.27 M_o'	
		Inner	E	$\frac{1}{2}l$	0.0446 W	1.24	0.17 M_o'	
			E$_1$	$\frac{1}{4}l$	0.0121 W		0.04 M_o'	
			d	unit	0.0833 W		.0833 $w(l-\frac{1}{3}c)^2$	
			e	unit	0.0447 W		.0447 $w(l-\frac{1}{3}c)^2$	
			f	unit			.040 $w(l-\frac{1}{3}c)^2$	
			g	unit			.050 $w(l-\frac{1}{3}c)^2$	
			h	unit	0.066 W		.066 $w(l-\frac{1}{3}c)^2$	
			i	unit	-0.066 W		-.066 $w(l-\frac{1}{3}c)^2$	
	Oblong interior panels $\frac{a}{b} = 1.5$	Col-head	A	$\frac{1}{4}a$	-0.1248 wb^2	1.08*	-0.52 M_b	
		Mid	B	$\frac{1}{2}a$	-0.0314 wb^2	0.77*	-0.13 M_b	
		Total neg.	C	a	-0.0781 wb^2	1.00*	-0.65 M_b	
		Outer	D	$\frac{1}{2}a$	0.0696 wb^2	1.24*	0.26 M_b	
		Inner	E	$\frac{1}{2}a$	0.0242 wb^2	0.65*	0.09 M_b	
		Total pos.	F	a	0.0469 wb^2	1.00*	0.35 M_b	
		Col-head	A'	$\frac{1}{2}b$	-0.1012 wa^2	0.94*	-0.45 M_a	
		Mid	B'	$\frac{1}{2}b$	-0.0608 wa^2	1.20*	-0.20 M_a	
		Total neg.	C'	b	-0.0810 wa^2	1.00*	-0.65 M_a	
		Outer	D'	$\frac{1}{2}b$	0.0473 wa^2	0.90*	0.19 M_a	
		Inner	E'	$\frac{1}{2}b$	0.0407 wa^2	1.16*	0.16 M_a	
		Total pos.	F'	b	0.0440 wa^2	1.00*	0.35 M_a	

* Ratio of M to the M for normal panel with $l = a$ or $l = b$.

square again equal to $l/4$, to the normal interior panel, one finds the moment in the outer section D equal to $0.0579W$. The ratio of increase for the wall panel is calculated, then, as $q = 0.0806/0.0579 = 1.39$ (see fifth column for q). If this ratio is correct, the moment in section D in the wall panel, when the columns are replaced by point supports, may be computed as $M = qM_q$ where M_q is the moment in section D in the normal panel, that is, $M = 1.39 \cdot 0.21 \cdot \frac{Wl}{8} = 0.29 \cdot \frac{Wl}{8}$. When the point supports are replaced by columns with capitals, one may expect that the factor $\frac{Wl}{8}$ is to be replaced by $M'_0 = \frac{1}{8} Wl(1 - \frac{1}{3}\frac{c}{l})^2$; the coefficient $\frac{1}{3}$ occurs in this expression instead of the usual $\frac{2}{3}$ because the clear span in this case is $l - \frac{1}{2}c$ instead of the value $l - c$ found in the interior panels.

The moments in the lintel beam in sections L and M are computed under the assumption that the beam is continuous, with supports opposite the columns.

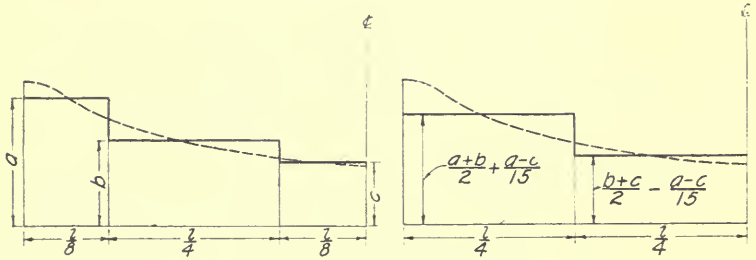

FIG. 25.—DIAGRAM INDICATING RELATIONS BETWEEN AVERAGE ORDINATES.

The values stated for panels without bending resistance across the mid-section were estimated on the basis of a similar case treated by Nielsen, in which there is no bending resistance in four-fifths of the mid-section. The proportions are nearly equal to those given by Nielsen. The side of the elementary square used in this case was $\lambda = l/5$.

The oblong interior panels have sides a and b, with $a = 1.5b$. The elementary squares used by Nielsen had the side $\lambda = b/4 = a/6$. The moments M_n in the short sections A', B', D', and E' were determined in the manner described in sections D and E in the wall panels. The average moment per unit-width in each of the sections A, B, D, and E was determined as the average of three values given by Nielsen, one for each elementary square adjacent to the section. The proportions of negative and positive moments M_n found in this way are approximately the same as in the normal panel. If they can be assumed to be exactly the same, the total moments in the sections C, C', F, and F' become $-0.65M_b$, $-0.65M_a$, $0.35M_b$, and $0.35M_a$, respectively, as stated in the column for M. These total moments are assumed to be distributed between the column-head sections and mid-sections, outer sections and inner sections according to the

proportions between the values of M_n. For example, one finds under this assumption in the column-head section:

$$M = \frac{-0.1248wb^2 \cdot \frac{1}{2}a}{-0.0781wb^2 \cdot a} \cdot (-0.65M_b) = -0.52M_b.$$

The remaining values of M were computed in the same manner. The ratios of M to the corresponding M in the normal panel were computed afterward.

The moments in the oblong panels are represented graphically in Fig. 26, where the abscissas are values of the ratio l_2/l_1 of the spans,; l_1 is the span in the direction in which the moment is taken. The points representing the moments in Table VI lie on or near the two straight lines and the

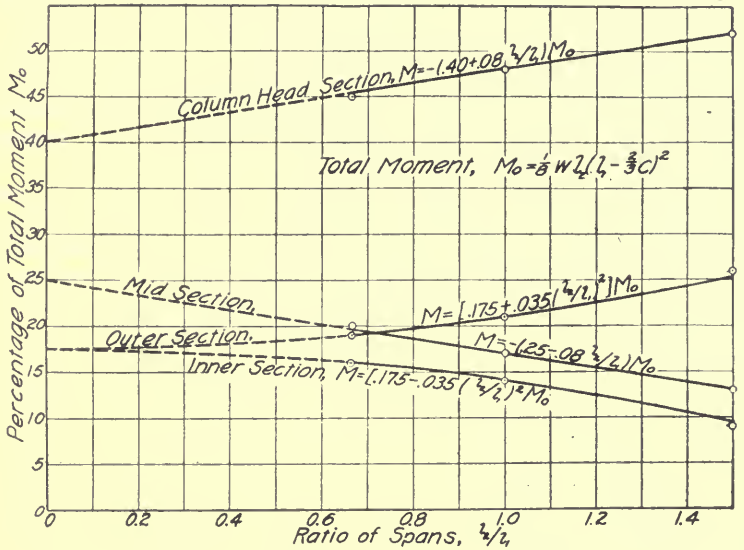

FIG. 26.—MOMENTS IN OBLONG PANELS.

two parabolas which are shown, with their equations, in Fig. 26. These equations may be used as formulas for the moments in the various moment sections in oblong panels. They show, as might be expected, that the moments are more nearly uniformly distributed over the short sections than over the long sections.

Nielsen derived the following values of the reactions of the columns: in the case of two adjacent rows of wall panels, $R = 1.203W$; in the case of four adjacent corner panels, $R = 1.313W$.

Nádai * derived the following values of the moments per unit width for a single square panel, which is simply supported on point supports at the four corners; he assumed Poisson's ratio equal to 0.3; at the center of the panel $M = 0.1115W$, at the center of the edge in the direction of the edge, $M = 0.151W$, the latter being the maximum moment in the panel.

* Nádai, p. 70.

III.—RELATION BETWEEN OBSERVED AND COMPUTED TENSILE STRESSES IN REINFORCED CONCRETE BEAMS.

By W. A. SLATER.

11. GENERAL CONSIDERATIONS. It has been generally recognized that in the tests which have been made on reinforced-concrete floors the measured tensile stresses in the reinforcement do not account for all of the moments which are applied to the slab. This has been especially apparent in the cases in which the measured stresses were low. In the tests of flat slabs the coefficient of the resisting moment of the measured steel stresses has been found to increase as the measured stresses increased. This increase in the coefficient indicates that, for the low loads at least, the tensile stress accounts for only a portion of the applied bending moment. Table VII quotes published results which show that for different loads, the difference in the proportion of the total moment which is accounted for by the measured tensile stresses is likely to be considerable. It is very desirable that a means be found for determining how great this difference is, but the slab tests cannot be used for this purpose since the coefficient of the bending moment is the main thing that is in question in the slab tests.

To show the relation between the bending moment and the resisting moment in beams a study of observed tensile stresses in 84 reinforced-concrete beams tested at an age of 13 weeks has been made. These beams were tested by the Technologic Branch of the United States Geological Survey at St. Louis about 1905 to 1908, and have been reported* in Technologic Paper No. 2 of the Bureau of Standards, by Humphrey and Losse. All the test data of those beams here presented may be found in that paper. The results of this study are shown in Fig. 31 and 32 as a relation between the observed and the computed stresses, but it is evident that the relation of the observed stress to the computed stress is the same as the relation of the computed moment of the observed tensile stresses to the applied moment. Test results from the same source and from other sources were used by Professor Hatt in a study of the relation of the computed moment of the measured tensile stresses in the reinforcement to the applied moment for beams and slabs. Professor Hatt found that beam tests from different sources gave different results, and the writer also has found this to be true. It is shown, however, in Professor Hatt's paper† that there is a certain degree of conformity between test results from a considerable variety of sources, and the writer feels justified in using the beams of Technologic Paper No. 2 for the purpose of determining a law which will serve as a basis for the comparative study of the moment in slabs.

12. LIMITATIONS TO GENERAL APPLICABILITY OF THE TEST RESULTS While it is recognized that there are limitations which must be observed in the application of these results to other conditions than those under which they were obtained, it is believed that, because of the wide range which the

* See also Bulletins 329 and 344, U. S. Geological Survey.

† W. K. Hatt, Moment Coefficients for Flat Slab Design with Results of a Test, Proceedings American Concrete Institute, Vol. 14, p. 165 (1918).

tests cover, the limitations are less serious than would be those of any other tests which might have been used for this purpose.

For the beam tests there are reasons for expecting a difference between the observed stresses and the computed stresses. In a cracked beam the stress at the cracks may approach the computed stress, but between the cracks the concrete assists so greatly in carrying the stresses that the average measured unit-deformation over the gage length is likely to be considerably less than the maximum unit-deformation, especially at the lower loads. It is possible also that even at the section where a crack occurs a portion of the moment may be resisted by the tensile stresses in the concrete. There probably are other reasons for the differences though it is believed that these are the most important.

By taking measurements of deformation over a short gage length within a longer gage length on the same reinforcing bar it has been shown* that higher stresses exist at certain places than are indicated by the average measured deformation. The fact that in the beams used as the basis of the present study failure occurred at observed stresses which were somewhat

TABLE VII.—UNCORRECTED MOMENT COEFFICIENTS FROM PUBLISHED REPORTS.

(Sum of coefficients for positive moment and negative moment.)

Test.	Load, lb. per sq. ft.	Coefficient.	Load, lb. per sq. ft.	Coefficient.	Load, lb. per sq. ft.	Coefficient.	Load, lb. per sq. ft.	Coefficient.	Reference.
Shredded Wheat Factory	56	0.0363	120	0.0356	191	0.0439	...	.....	Proc. A. C. I., 1914, p. 404.
Worcester Test Slab....	102	0.026	215	0.049	...	.....	...	.....	Univ. of Illinois Eng. Exp. Sta. Bull. 84, p. 103.
Purdue Test, "J" Slab..	150	0.0148	300	0.0246	450	0.0400	600	0.0539	Proc. A. C. I., 1918, p. 181.

lower than the known yield point of the steel is another indication that even at the high loads the real stresses were greater than the observed stresses.

There is another limitation to the interpretation of test results of slabs, which the results of the study of the beam tests does not help to remove. This limitation lies in the fact that in the measurement of the deformation in a slab at a position of rapidly changing stress the result represents the average unit deformation over the entire gage length and not at the end where the stress in the gage length is a maximum. In the beams tested the moment was constant over the entire gage length.

13. TEST SPECIMENS AND METHODS OF TESTING. Technologic Paper No. 2† of the Bureau of Standards describes the specimens and the methods of testing. Only the features which are of the most importance in connection with the present study are repeated here.

* F. R. McMillan, in unpublished data furnished to the writer.
† See also Bulletin 329, U. S. Geological Survey.

All the beams were 13 ft. long, 8 in. wide, and 11 in. deep. The amount of reinforcement varied in the different beams from two one-half-inch round to eight one-half-inch round bars. For the beams having four bars or less all were placed in one layer. For the beams having five bars or more the bars were placed in two layers. The vertical distance between the centers of the bars of the two layers was 1½ in. The distance from the top of the beam to the center of the lower layer of bars was 10 in. The ratio of reinforcement, based upon the depth to the center of gravity of the reinforcement, varied in the different beams from 0.0049 for the beams with two bars, to 0.0212 for the beams with eight bars. In Technologic Paper No. 2 the percentage of reinforcement was based upon the depth to the center of the lower layer of bars. On account of the difference in the method of computing the ratios of reinforcement the ratios given here are slightly greater for the beams having two layers of bars than the ratios given in Technologic Paper No. 2.

All the concrete used in the beams was of a 1:2:4 mixture. Four different aggregates were used. These were granite, gravel, limestone, and

TABLE VIII.—STRENGTH MODULUS OF ELASTICITY AND VALUES OF n.

	Compressive Strength lb. per sq. in.	Modulus of Elasticity, lb. per sq. in.	Values of n.
Granite Concrete	4,200	4,430,000	6.8
Gravel Concrete	4,000	4,620,000	6.5
Limestone Concrete	3,600	3,810,000	7.9
Cinder Concrete	2,200	1,820,000	16.6

NOTE.—The term n represents the ratio of the modulus of elasticity of the steel to that of the concrete. For this computation the modulus of elasticity of the steel is taken at 30,000,000 lb. per sq. in.

cinders. The strengths and moduli of elasticity of the concretes from these aggregates are given in Table VIII. It will be seen that while all of the concrete had a good strength there was considerable range in the strengths.

All the bars used as reinforcement in these beams were tested and they were classified according to the yield point. (In the earlier beams the elastic limit was used as the basis of classification.) This insured practically the same yield point for all the bars of any beam. The highest and the lowest yield points for the beams quoted in this paper were 43470 and 36110 lb. per sq. in. respectively. The unit used in the discussion in this paper is the average for three beams of a kind. On this basis the highest and lowest average yield points were 42900 and 36400 lb. per sq. in. respectively. The average yield point was 40200 lb. per sq. in. The yield points for all but two of the twenty-eight groups were within 5½ per cent of the average.

A span of 12 ft. was used in all the tests, and the loads were applied at the one-third points of the span. The deformations were measured over a gage length of 29.25 in. by means of extensometers which were attached to

the concrete and which did not measure directly the deformations in the steel. The arrangement of the extensometers gave the deformations in the steel at the level of the bottom layer of reinforcement. These are the deformations on which the studies in the Technologic Paper are based. Since in the present study the depth of the beam was taken as the depth to the center of gravity of the cross section of the reinforcement it became necessary to reduce the deformations reported in the Technologic Paper to the corresponding deformations at that depth. This modification affected only the beams having more than one layer of bars.

14. METHOD OF ANALYZING RESULTS OF BEAM TESTS. The analysis of the results of the beam tests consists in deriving an empirical equation for the observed stress in terms of the computed stress and the percentage of reinforcement. For the beams used in this study the load-strain diagrams (in which values of M/bd^2 were plotted as ordinates and the unit-deformations in the steel were plotted as abscissas) are made up of three parts, (1) the part in which little or no cracking of the concrete had taken place; (2) the part in which the concrete had cracked and the stress in the reinforcement was below the yield point; and (3) the part in which the stress in the steel was at or beyond the yield point. It was found that the first two parts were nearly straight lines which, if projected, intersected at a point which corresponds quite closely to the unit-deformation at which a breaking down of the concrete in tension may be expected to occur. In the study of the results of these beam tests empirical equations for these two straight lines were determined. In the diagrams representing these empirical equations the straight lines are connected by smooth curves, but no attempt has been made to state an equation for the curved portion. The part of the load-strain diagram for which the yield point of the steel has been reached or passed has not been included in the study.

Fig. 27 gives typical load-strain diagrams* for certain of the gravel concrete beams used in this study. In Fig. 29 there is a sketch of a load-strain diagram with notation which will assist in making clear the manner in which the analysis was carried out. The lines OA and BC represent the straight lines which may be fitted to the two portions of the diagrams below the yield point of the steel. The slopes of the line OA for all the beams used were plotted, and from these points an equation for the slope was derived. The plotted points and the equations of the lines which were fitted to them are given in Fig. 28. Likewise the slopes of the lines BC for all the beams used were plotted in Fig. 29 and the equation of the slope was derived. The intercept OB of the lines BC for all the beams were plotted in Fig. 30 and equations of the intercept were derived in like manner. The height of the intercept OB might be used as a measure of the load at which the breaking down of the concrete in tension occurred, but it is not entirely satisfactory as a measure of this action of the beams, and Fig. 30, showing these intercepts plotted as ordinates, is introduced only to indicate this

* The tabulated data used in this figure are given in Tech. Paper No. 2, U. S. Bureau of Standards, 1911.

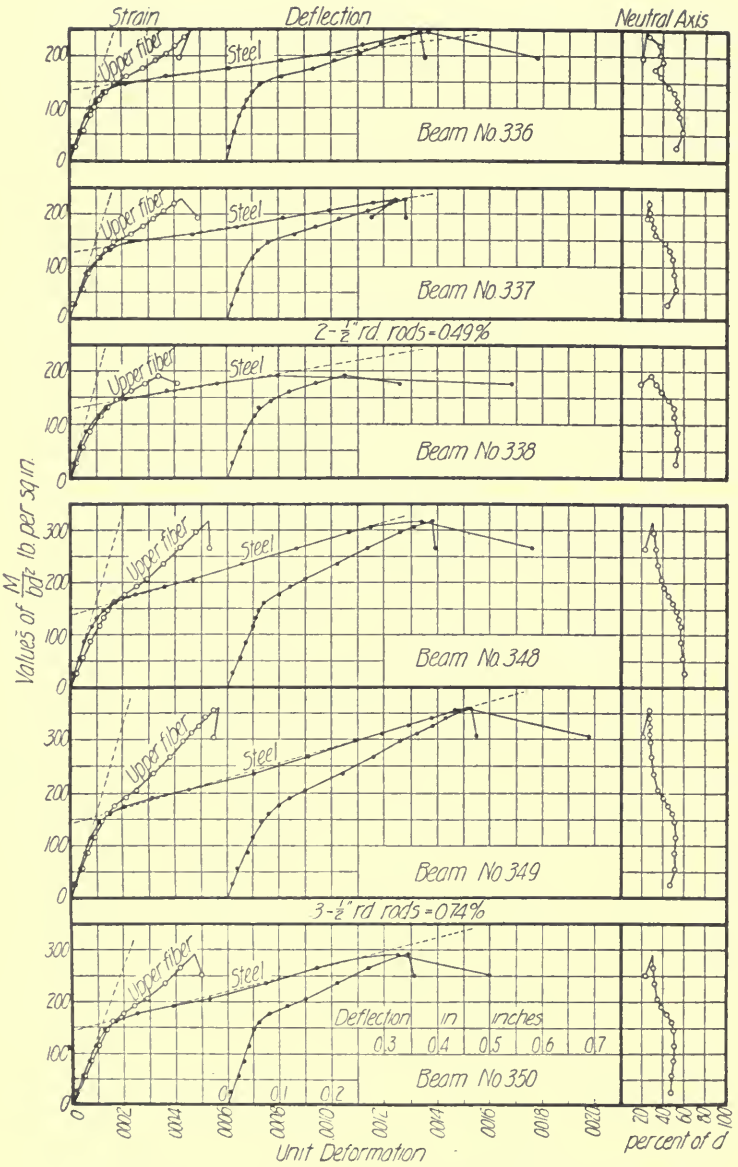

FIG. 27.—TYPICAL LOAD-STRAIN DIAGRAMS FOR BEAM TESTS.

step in the derivation of the equations of the relation between the observed and the computed stresses. The equation of the slopes of the lines OA, and the fact that the lines pass through the origin give sufficient information with which to determine the equation of the lines OA. The equation of the slope of the lines BC, and the equations of the intercept OB of these lines on the vertical axis, were stated in terms of observed and computed stresses, and were solved simultaneously for the equations of the lines BC. The graphical representation of the equations determined in this way for the granite, gravel, and limestone concretes is given in Fig. 31. The equations which apply to the beams of cinder concrete are somewhat different and are shown in Fig. 32. In all the computations the value of j (the ratio of the moment arm to the depth d) was taken as 0.866.

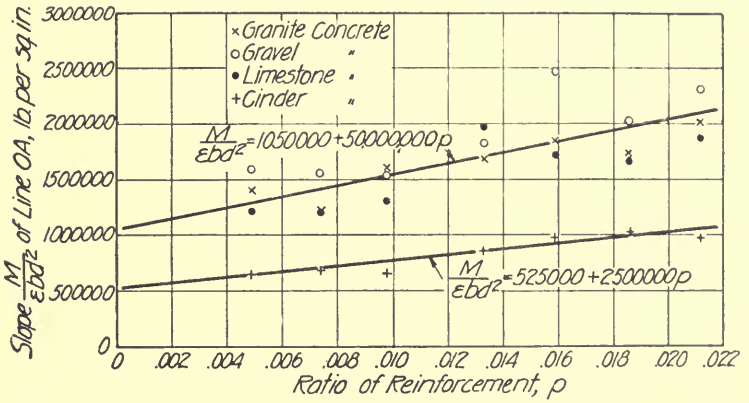

FIG. 28.—RELATION BETWEEN RATIO OF REINFORCEMENT AND SLOPE OF LOAD-STRAIN CURVE BELOW LOAD AT WHICH CONCRETE CRACKED.

15. EFFECT OF QUALITY OF CONCRETE AND AMOUNT OF REINFORCEMENT ON RATE OF INCREASE OF TENSILE DEFORMATION. Fig. 28 and 29 were prepared in order to study the action of the beam during the first two stages of the test which have been referred to in Art. 14. In each figure the ordinates of the plotted point represent slopes of a portion of the load-strain diagrams for all the beams used in this study. These slopes may be interpreted as the rate of increase of deformation with load. Fig. 28 represents the stage of the test below the cracking of the concrete. Fig. 29 represents the stage of the test between the cracking of the concrete and the reaching of the yield point of the reinforcement.

For stages of the test below the cracking of the concrete the rate of increase of tensile deformation was affected in an important degree by the quality of the concrete, while the effect of the amount of reinforcement on the rate of increase of deformation was almost negligible. For stages of the test above the cracking of the concrete the conditions were reversed;

the rate of increase of tensile deformation was affected in an important degree by the amount of reinforcement, while the effect of the quality of the concrete on the rate of increase in deformation was entirely negligible.

In Fig. 28 the magnitudes of the ordinates to the respective points are, in general, in the order of the values of the modulus of elasticity of the concretes represented. The ordinates representing the cinder concrete, which had a modulus of elasticity about half as great as that of the other concretes (see Table VIII), are uniformly about half of those for the other

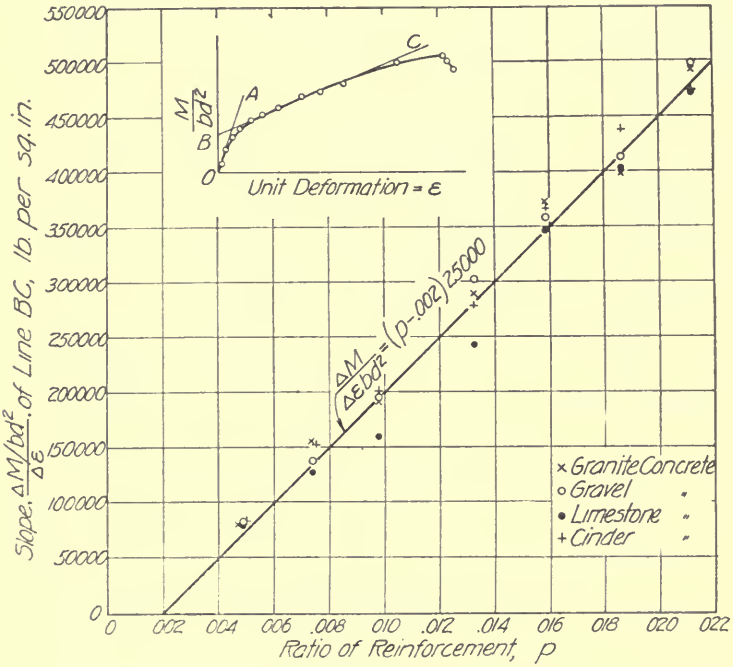

FIG. 29.—RELATION BETWEEN RATIO OF REINFORCEMENT AND SLOPE OF LOAD-STRAIN DIAGRAM ABOVE LOAD AT WHICH CONCRETE CRACKED.

concretes. Even for the granite, gravel, and limestone concretes, whose moduli of elasticity showed only slight differences, the magnitudes of the average ordinates to the points take the same order as the values of the modulus of elasticity. Although the compressive strengths occupy the same order of magnitude as the moduli, it seems logical to attribute the effect on the rate of deformation to the variation in the modulus of elasticity rather than to the variation in the compressive strength. Whether the important factor was the modulus of elasticity or the compressive strength, the facts here pointed out justify the statement that the rate of tensile

deformation was affected in an important degree by the quality of the concrete.

Since the abscissas in Fig. 28 are ratios of reinforcement the slopes of the curves fitted to the plotted points in this figure will be a measure of the effect of the amount of reinforcement on the rate of increase of tensile deformation. Both average lines (that for stone and gravel concretes and that for cinder concrete) have slopes which are very small in proportion to the slope of the line in Fig. 29, which represents the conditions for the stage of the test after the formation of cracks. This comparison justifies the statement that the effect of the amount of reinforcement on the rate of deformation was almost negligible for the stage of the test in which the concrete was not generally cracked.

The greatly increased slope of the average line in Fig. 29 over the slopes shown in Fig. 28 forms the basis of the statement that for stages

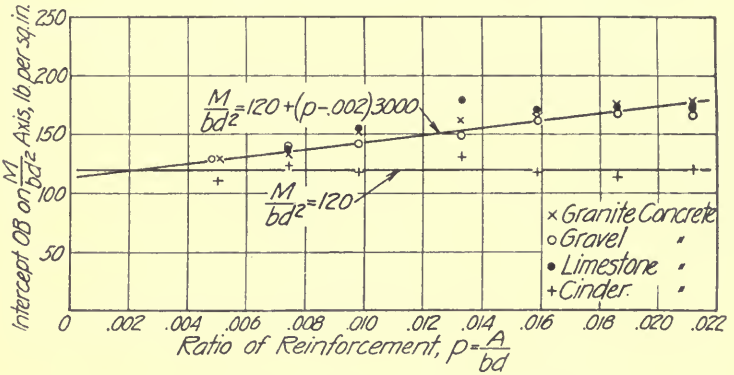

FIG. 30.—RELATION BETWEEN RATIO OF REINFORCEMENT AND INTERCEPT OB OF FIG. 29 ON LOAD AXIS.

of the test above the cracking of the concrete the rate of tensile deformation was affected in an important degree by the amount of reinforcement. To appreciate fully the relative importance of this factor account must be taken of the fact that in Fig. 29 the scale of ordinates is only one-tenth of that used in Fig. 28.

In the arrangement of the points in Fig. 29 there is no regularity which is dependent upon the strength or modulus of elasticity of the concrete. The points representing the cinder concrete are intermingled with the points representing the other grades of concrete in such a way that one average line represents all the results with as great accuracy as would be possible with an independent line for each kind of concrete. This clearly warrants the previous statement that for the stages of the test above which cracks occurred the effect of the quality of the concrete on the rate of tensile deformation was entirely negligible.

16. RELATION BETWEEN OBSERVED AND COMPUTED TENSILE STRESSES. The significance and scope of the results of the study of the relation between the observed and the computed stresses in the reinforcement may best be visualized by reference to Fig. 31 and 32, which show graphically the derived equations of the observed stress in terms of the computed stress and the percentage of reinforcement. For the part of the test below which the concrete is cracked these equations are,

$$f = \frac{0.52 f_s}{1 + \frac{.021}{p}} \quad \text{for the stone and gravel concretes and} \tag{1}$$

$$f = \frac{1.04 f_s}{1 + \frac{.021}{p}} \quad \text{for the cinder concrete.} \tag{2}$$

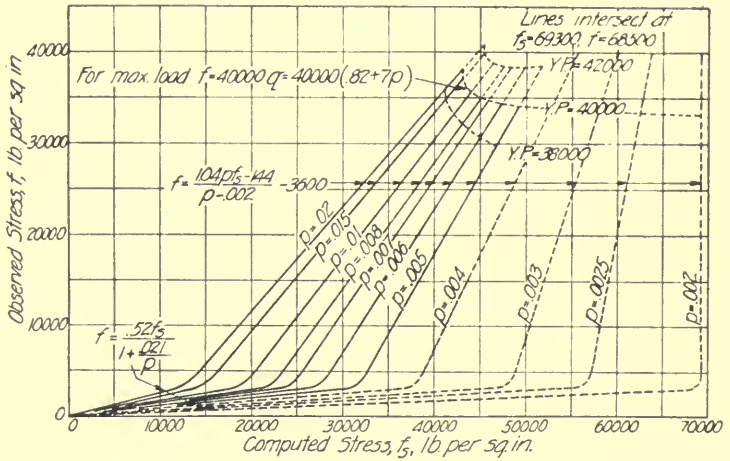

FIG. 31.—RELATION BETWEEN OBSERVED AND COMPUTED TENSILE STRESSES IN REINFORCEMENT OF BEAMS TESTED AT ST. LOUIS.

Diagrams from derived equations for beams of stone concrete and of gravel concretes.

For the part of the test above which the concrete is generally cracked the equations are,

$$f = \frac{1.04 p f_s - 144}{p - .002} - 3600 \quad \text{for stone and gravel concretes and,} \tag{3}$$

$$f = \frac{1.04 p f_s - 144}{p - .002} \quad \text{for cinder concrete.} \tag{4}$$

In these equations, f is the observed stress, f_s is the computed stress, and p is the ratio of longitudinal reinforcement based upon the depth from the

compression surface of the beam to the center of gravity of the tension reinforcement.

In Fig. 31 and 32 the lines representing the stresses in beams having less than 0.5 per cent of reinforcement are dotted because these lines represent extrapolation below the lowest percentage of reinforcement used in any of the beams tested. Since most of the slabs to whose study the results of these beam tests may be applied have not more than 0.5 per cent of reinforcement it is important to consider whether the extrapolation is justifiable. The average lines fitted to the points in Fig. 28, 29 and 30 were projected from 0.0049, the lowest ratio of reinforcement for any of the beams tested, to the lower value of 0.002. This extrapolation covers a small portion of the total range in the percentages of reinforcement repre-

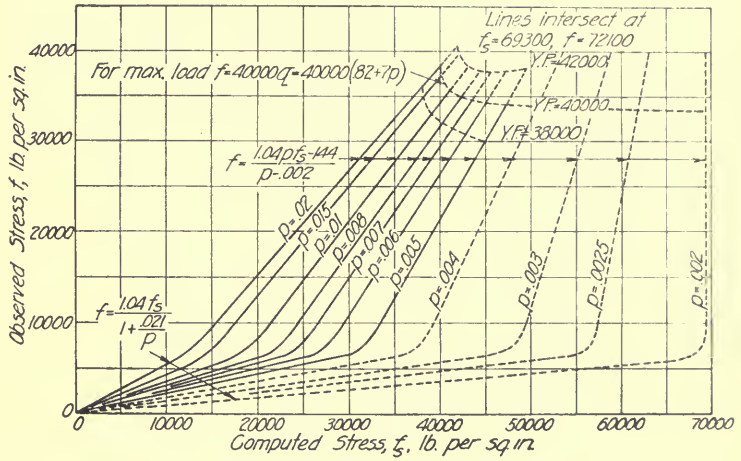

FIG. 32.—RELATION BETWEEN OBSERVED AND COMPUTED TENSILE STRESSES IN REINFORCEMENT OF BEAMS TESTED AT ST. LOUIS.

Diagrams prepared from derived equations for beams of cinder concrete.

sented by the beams which were tested, and the curves which were projected are well defined by the experimental points. It seems, therefore, that there is justification for this extrapolation. An inspection of Fig. 28, 29 and 30, on which the curves of Fig. 31 and 32 are based, will assist in forming an opinion as to whether the extension of the scope of the diagrams of Fig. 31 and 32 below 0.49 per cent of reinforcement is warranted by the test data.

Fig. 29, 31, and 32 indicate that for beams having only 0.2 per cent of reinforcement when the concrete breaks down in tension the reinforcement immediately would be stressed to failure. That is, when the concrete breaks down in tension the slope of the load strain diagram becomes zero for a beam with only 0.2 per cent of reinforcement. That this condition is approached as the amount of reinforcement becomes small is shown by

inspection of Fig. 29. The same thing is shown directly in the flatness of the slope of the load stress diagrams for beams 336, 337 and 338 of Fig. 27, which have the smallest amount of reinforcement of any of the beams studied. That there should appear to be no difference in the amount of reinforcement required to bring about this condition for the beams of cinder concrete from that which was required for the beams of stone concrete, may be due to a break in the mean line of Fig. 29 between 0.5 and 0.2 per cent of reinforcement. Whether such a break occurs is not

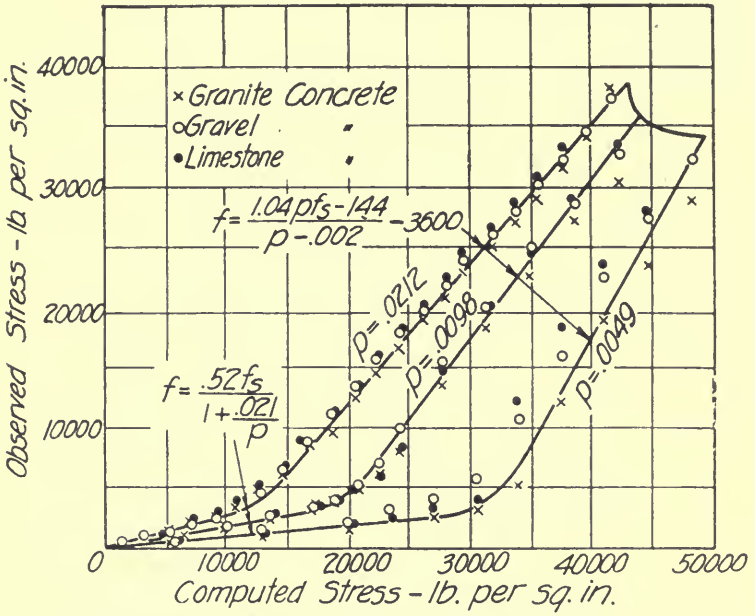

FIG. 33.—RELATION BETWEEN OBSERVED AND COMPUTED TENSILE STRESSES IN REINFORCEMENT OF BEAMS TESTED AT ST. LOUIS.

Test results for beams of stone concrete and of gravel concrete compared with results from derived equations.

known because no beams with less reinforcement than 0.49 per cent were tested.

In order to make certain by a direct comparison, that equations (1) to (4) represent the relation between the observed and the computed tensile stresses, Fig. 33 and 34 have been prepared. Points showing the observed and the computed unit deformations throughout the tests of representative beams have been plotted, and for comparison with them the graphs of the equations which represent the relation between the observed and the computed stresses for the same beams are shown in the same figures. Each point plotted in these figures represents the average load and the average deformation for the three beams of its kind. Considering the

range of concretes and the range in the amounts of reinforcement used in the beams represented, the agreement between the test results and the empirical equations seems good.

In Fig. 31 and 32 the slopes of the lines which represent the stages of the test in which the concrete had not cracked were approximately inversely proportional to the values of the modulus of elasticity of the concrete. The slopes ($1.04 f_s$) of all the lines for the cinder concrete beams were just twice as great as the slopes ($0.52 f_s$) for the corresponding beams of stone or gravel concrete. The values of n (the ratio of the modulus of

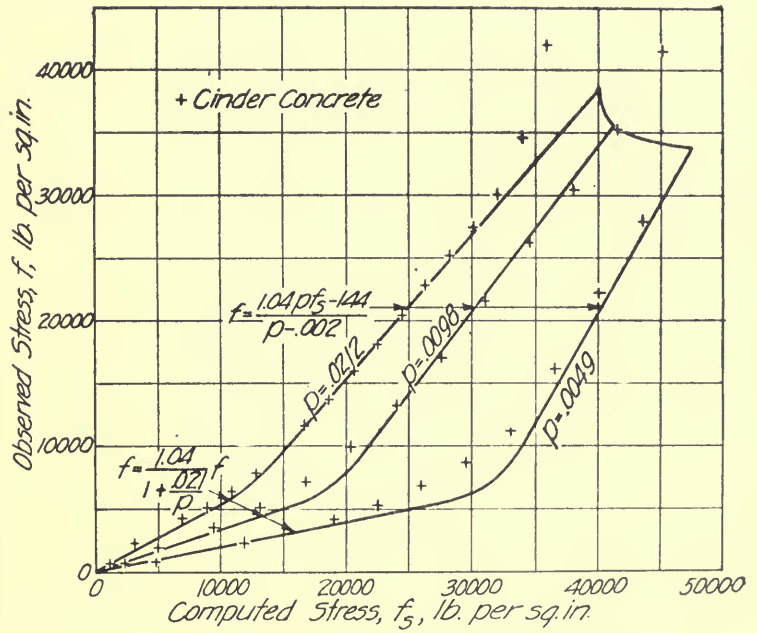

FIG. 34.—RELATION BETWEEN OBSERVED AND COMPUTED TENSILE STRESSES IN REINFORCEMENT OF BEAMS TESTED AT ST. LOUIS.

Test results for beams of cinder concrete compared with results from derived equation.

elasticity of the steel to that of the concrete) were, on the average, 2.33 times as great for the cinder concrete as for the stone and the gravel concretes. Assuming that the value of the slope may be taken as proportional to the value of n an equation is found which gives values closely approximating the test results when the proper values of n are used in the equation. The equation is

$$f = \frac{.07\, nf_s}{1 + \frac{.021}{p}} \qquad (5)$$

For all the beams of stone or gravel concrete reported in Technologic Paper No. 2 the average of the unit-deformations in the reinforcement at the time that the first crack was observed is 0.000113 and this corresponds to a stress of 3390 lb. per sq. in. For all the cinder concrete beams reported in that paper, the average unit-deformation at the occurrence of the first crack was 0.000179. This deformation corresponds to a stress of 5370 lb. per sq. in. The intersections of the two straight portions of the diagrams of Fig. 31 for the stone and gravel concretes, lie at an observed tensile stress of about 3200 lb. per sq. in. In Fig. 32 the intersections for the cinder concrete lie at a tensile stress of 6260 lb. per sq. in. These values are seen to correspond quite closely to the stresses at which the first cracks were discovered.

For the stage of the test above the cracking of the concrete the only difference between the equation which represents the relation between the observed and the computed stresses for the stone and gravel concrete (equation (3)) and the corresponding equation for the cinder concrete beams (equation (4)) is that in the former there is an additive term (— 3600 lb. per sq. in.) which is lacking in the equation for the cinder concrete beams. It may seem unexpected that such a term as this should be present, but that the difference expressed by the term is present is made entirely clear by attempting to fit the equation for the cinder concrete to the results for the stone and the gravel concretes.

The intensity of the bond stresses between cracks will be affected by variations in the modulus of elasticity of the concrete, and it may be permissible to assume that the variation in the additive term in equation (3) is proportional to the variation in the value of n (the ratio of the modulus of elasticity of the steel to that of the concrete). With this as an assumption a more general equation which, for the beams under consideration, represents quite accurately the relation between the observed tensile stress and the computed stress after the concrete had cracked is

$$f = \frac{1.04\,pf_s - 144}{p - .002} - 400\,(16 - n) \qquad (6)$$

17. OBSERVED TENSILE STRESS AT MAXIMUM LOAD. It is desirable to determine the relation between the maximum loads which the beams carried and the stress in the steel which corresponds to the observed deformation (here termed observed stress) at those loads. On account of the possibility that the steel had been stressed beyond the proportional limit before reaching the maximum load it is not feasible to determine the stress at the maximum load directly from the measured deformation. In order to determine the desired relation, the straight lines BC of Fig. 29 were produced to the maximum load, and the unit-deformation given by this line at the maximum load was used to determine the stress at that load. In this way the ratios, q, of the stress at maximum load to the yield point were determined and are given in Fig. 35. The equation which expresses the average relation between q and the ratio of reinforcement, p, is

$$q = 0.82 + 7p. \qquad (7)$$

The yield-point stress used in these computations was 40,000 lb. per sq. in.

The observed tensile stress at the maximum load was generally slightly less than the yield point. It is possible that the stress at a crack was enough greater than the stress found from the deformations over the entire gage length to bring the stress at the maximum load up to the yield point. This possibility is further indicated by the fact, which is brought out in equation (7), that the observed stress approached the yield point more closely for the beams with a large percentage of reinforcement than for the beams with a small percentage. The result expressed in equation (7) should not be unexpected since the bond stresses between cracks would have more influence in reducing the total deformations in beams in which the amount of reinforcement is small than in those in which it is large.

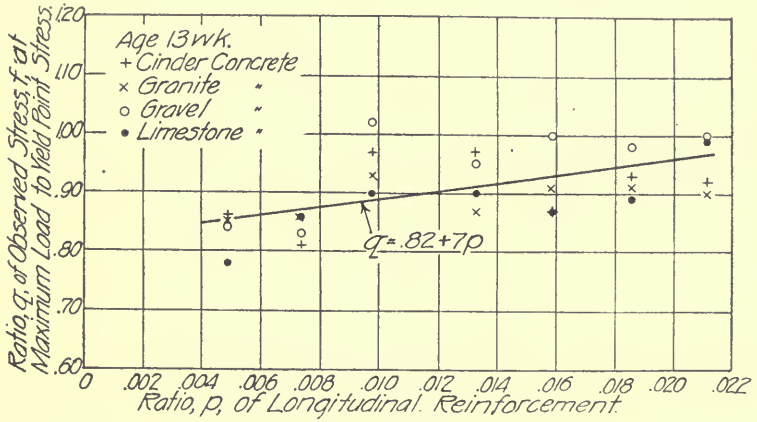

FIG. 35.—RELATION BETWEEN RATIO OF REINFORCEMENT AND RATIO OF OBSERVED STRESS AT MAXIMUM LOAD TO YIELD-POINT STRESS.

Equation (7) has been introduced into the diagrams of Fig. 31 and 32 to show the observed and the computed stresses at which tension failure in the reinforcement is likely to occur. In making this application of the equation the yield point was assumed to be 40,000 lb. per sq. in., approximately the average value found in the tests of the coupons taken from the beams. No test data were available from which to show the relation between the stress at maximum load and the yield-point stress for higher or lower yield points. However, by assuming that for small differences in yield point the loads carried would be proportional to the yield-point stress, the dotted curves for yield points of 38,000 and 42,000 lb. per sq. in. were obtained. The error of these estimates becomes large for the beams with small amounts of reinforcement, hence these additional curves were not carried beyond the values for one-half per cent of reinforcement.

18. FACTOR OF SAFETY AGAINST TENSION FAILURE. The factor of safety for a structure may be defined as the ratio found by dividing the working

load for the structure into the load which will cause failure of the structure. There may be differences of opinion as to how the load which is to be used for determining the factor of safety should be applied. For these tests there was only one possible load which could be considered, the load which was built up by uniform increments until failure was brought about, the whole test requiring not more than a few hours. For the purpose of eliminating from the study of the factor of safety the effect of slight variations in the yield point of the steel, the maximum loads given in Technologic Paper No. 2 were corrected to give a load which presumably would have caused failure if the yield point of the steel had been 40,000 lb. per sq. in. The maximum loads reported were increased or decreased by an amount which was proportional to the difference between the yield-point stress and 40,000 lb. per sq. in. To these corrected maximum loads were added the weights of the beams, and the resulting loads were used in the computation of the factor of safety. The working load was taken as the load which gives a computed tensile stress of 16,000 lb. per sq. in. In these computa-

TABLE IX.—FACTORS OF SAFETY AGAINST TENSION FAILURE.

Kind of Concrete.	Ratio of Reinforcement.							Average Factor of Safety.
	0.0049	0.0074	0.0098	0.0133	0.0159	0.0186	0.0212	
Granite	3.09	2.83	2.75	2.69	2.67	2.52	2.53	2.72
Gravel	3.25	2.92	2.88	2.95	2.88	2.77	2.78	2.92
Limestone	2.96	2.62	2.65	2.64	2.48	2.51	2.70	2.65
Cinder	2.96	2.85	2.74	2.68	2.56	2.63	2.36	2.68
Average	3.06	2.80	2.76	2.74	2.65	2.61	2.59	2.74

tions the value of j (the ratio of the moment arm to the depth d) was taken as 0.875. The factors of safety found in this way are shown as plotted points in Fig. 36. Each point represents the average for three beams. The values from which these points were plotted are given in Table IX.

From the definition of the factor of safety it will be seen that the ratio of the computed stress at the maximum load to the computed stress at the working load will be the factor of safety. From this relation another method of determining the factor of safety is afforded, since Fig. 31 and 32 show, more or less exactly, the values of the computed stress in tension at the maximum load. These stresses divided by 16,000 lb. per sq. in. give the values of factor of safety shown by the smooth curves in Fig. 36. The irregularities have been smoothed out by the fact that the values shown by these curves represent the intersections of mathematical curves. The dotted portions of the two curves express the indications of Fig. 31 and 32 as to what the factor of safety would be for beams which have smaller percentages of reinforcement than any of the beams which form the basis of this study.

The agreement between the plotted points and the smooth curves is as good as will generally be found from methods which are as nearly independent as were these. Both sets of results are based upon the same reasoning, but they are reached by different methods of using the test data.

The indication of the smooth curves is that the factor of safety for the cinder concrete was less than that of the other concretes, but the plotted values do not bear out this conclusion. It cannot be said, however, that the arrangement of the points is independent of the kind of concrete. If an attempt were made to draw a curve which fits the values shown for each kind of concrete the curve for the gravel and that for the limestone concrete would be the highest and the lowest respectively, while the curves for the granite concrete and the cinder concrete would be intermediate and would practically coincide. This is somewhat surprising since both the

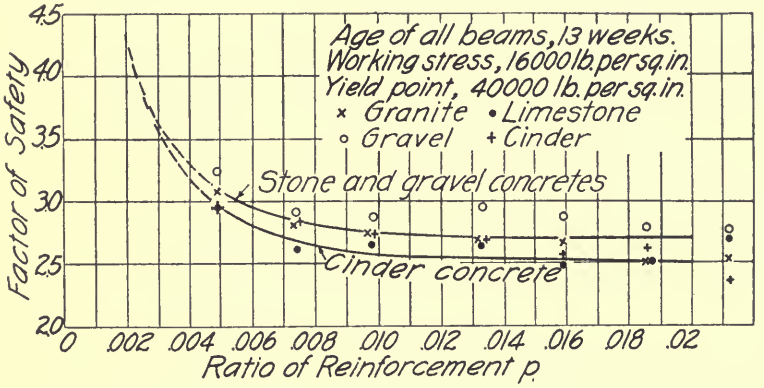

FIG. 36.—FACTOR OF SAFETY AGAINST TENSION FAILURE OF BEAMS TESTED AT ST. LOUIS.

compressive strength and the modulus of elasticity were highest for the granite concrete and lowest for the cinder concrete. This would indicate that it is some other property of the beams than the strength of the concrete which determined the differences in the factor of safety developed.

It is of interest that a tendency toward a higher factor of safety for the beams with a small amount of reinforcement than for the beams with large amounts of reinforcement appears in this figure. Apparently, as a criterion of the load-carrying capacity of the beams throughout the range of the tests the yield point of the steel is much more nearly correct than is the ultimate strength of the steel. It is quite clear that this figure gives no basis for claiming a factor of safety of four for a beam having the usual amount (say 0.7 per cent) of reinforcement of structural grade, if the working stress in tension is 16,000 lb. per sq. in. An estimate of the factor of safety of these beams, based upon the ultimate strength of the steel, would give from 3.25 to 4.0. These and many other tests have made

it clear that such a basis of estimating the factor of safety is wrong, and yet occasionally a claim of such a factor of safety, arrived at in this manner, is made.

19. SUMMARY. (a) It was found that the load-strain diagrams for the beams could be represented quite closely by two straight lines which intersect at a point which corresponds to the strain, in the tension side of the beam, at which the concrete cracked in tension. Through a study of the average slopes, and average intercepts of these lines, it was found to be possible to state equations which give, with a considerable degree of accuracy, the relation between the observed and the computed stresses in the reinforcement of the beams.

(b) The relation between the observed and the computed stresses in the reinforcement for the beams studied was found to be affected by the variation in the quality of the concrete, the amount of reinforcement, and the intensity of the computed stress.

(c) For stages of the test below the cracking of the concrete the rate of increase of the tensile deformation was affected in an important degree by the quality of the concrete, while the effect of the amount of reinforcement on the rate of increase of tensile deformation was almost negligible.

The rate of increase in the tensile deformation in the reinforcement at this stage of the test was found to be approximately proportional to the reciprocal of the modulus of elasticity of the concrete in compression as determined by tests of control cylinders.

(d) For stages of the test above the cracking of the concrete the rate of increase of the tensile deformation was affected in an important degree by the amount of reinforcement, while the effect of the quality of the concrete on the rate of increase in deformation was entirely negligible.

The total amount of deformation, however, was found to be greater for the beams of cinder concrete than for the beams having a greater compressive strength and modulus of elasticity. The difference in amount of the deformation for the different concretes was constant for all percentages of reinforcement and for all stages of the test between the cracking of the concrete and the reaching of the maximum load, as far as the data of the tests give a basis for judgment on this subject.

(e) The observed tensile stress in the reinforcement was less than the computed stress for all loads up to and including the maximum load. The difference was greater both proportionally and quantitatively for the beams with small percentages of reinforcement than for beams with large percentages. This was true for all loads. Correspondingly for all percentages of reinforcement the difference was greater for low loads than it was for high loads.

(f) The indications were that with a reinforcement of not less than 0.2 per cent the strength of the reinforced beam would be the same as the strength of an unreinforced beam. This holds for the cinder concrete beams as well as for those made with concrete of a higher compressive

strength and higher modulus of elasticity. Since no beams with less than 0.49 per cent of reinforcement were tested this observation must be taken as an indication and not as a fact established for the beams studied.

(g) The observed stress in the reinforcement at the maximum load was found to be less than the yield point for all the beams studied. It was found, however, that the ratio of the stress at maximum load to the yield point was greater for the beams with large percentages of reinforcement than for the beams with small percentages.

(h) The average factor of safety (see Art. 18 for definition) was found to be 10 per cent greater than the ratio of the yield point of the reinforcement to the working stress in tension which was used in determining the working load. When averages for all the concretes are considered a consistent decrease in the factor of safety with increase in percentage of reinforcement was found. The factor of safety was 18 per cent greater for beams with 0.49 per cent of reinforcement than for beams with 2.12 per cent of reinforcement.

IV.—TESTS OF SLABS SUPPORTED ON FOUR SIDES.

By H. M. WESTERGAARD.

20. TESTS OF SLABS SUPPORTED ON FOUR SIDES. Information as to the strength of slabs supported on four sides was obtained by a series of tests made during the years 1911 to 1914 in Stuttgart in Germany under the direction of Bach and Graf,* and by a test made in 1920 at Waynesburg, Ohio, for J. J. Whitacre, under the direction of W. A. Slater.

In Bach's and Graf's test 52 slabs, simply supported along the edges, and 35 control strips, supported as beams, were loaded to failure. The strength of the slabs was to be compared with the strength of the strips. A record of the progress of the test was obtained by measuring the deflections at a number of points and the slopes at the centers of the edges, and by observing the development of cracks. Fig. 37 and Fig. 38 show typical examples of the record made of the cracks; the numbers indicate the loads in metric tons at which the particular cracks appeared.

Two mixtures of concrete were used, with the following properties:

Type	A	B
Mixture	1:2:3	1:3:4
Per cent of water	9.2	9.7
Prism strength in compression after 44-48 days, lb. per sq. in.	2,290	1,835
Initial modulus of elasticity in compression, lb. per sq. in.	4,050,000	3,400,000

The 1:3:4 mixture was used in three slabs, which were designed to fail

* Reported by Bach and Graf in Deutscher Ausschuss für Eisenbeton, v. 30, 1915. See the Bibliography in Appendix C.

in compression (slabs g in Table II) and in the corresponding six control strips (26 and 27 in Table X). The 1: 2: 3 mixture was used in all the other slabs and strips. At the time of the test the age of the specimens was from 40 to 54 days. The yield point of the steel was from 49,600 lb. per sq. in. to 75,200 lb. per sq. in. The slabs were two-way reinforced, with the bars parallel either to the sides or to the diagonals.

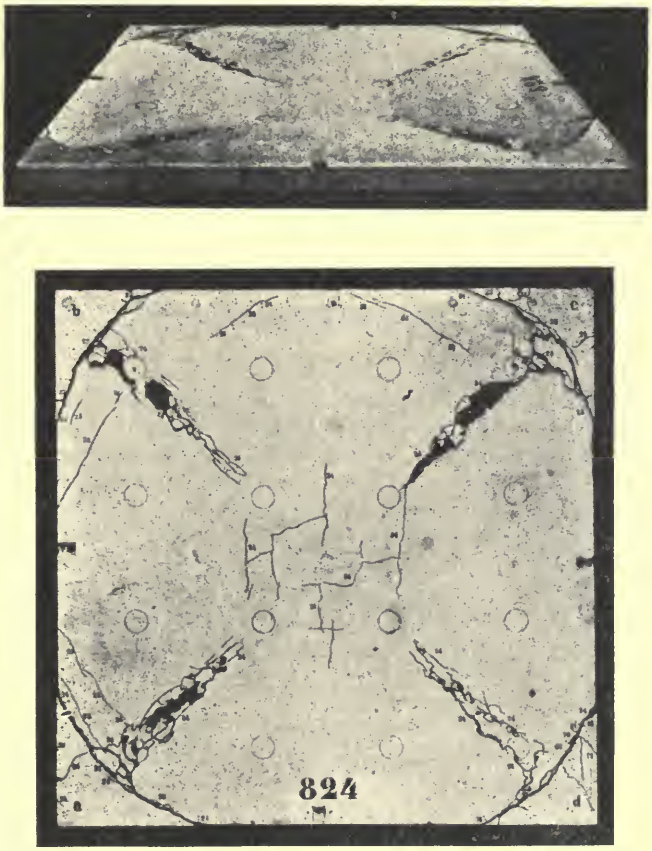

FIG. 37.—TOP OF SQUARE SLAB OF 200 CM. SPAN, TESTED BY BACH AND GRAF.

Table X and Fig. 39 show certain results of the tests of the control strips. In order to imitate the conditions of the two-way reinforced slabs most of the strips were built with transverse bars either above or below the longitudinal reinforcement (as indicated in one of the columns in Table X). The transverse bars were found to hasten the development of

the first crack, but the table shows that these bars have only little influence on the ultimate strength of the strips. The strips of types 18 to 25 failed by tension in the steel. The table gives the modulus of rupture of the steel, that is, the steel stress computed by the ordinary theory of reinforced-concrete with $n = 15$, for the observed maximum load (with the dead

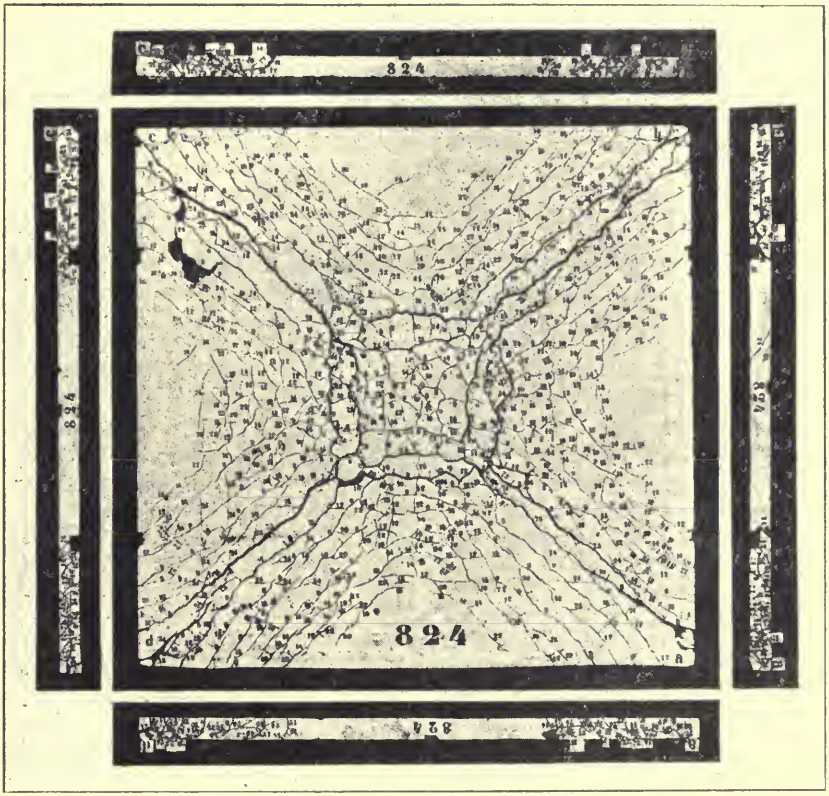

FIG. 38.—BOTTOM OF SQUARE SLAB OF 200 CM. SPAN, TESTED BY BACH AND GRAF.

weight taken into consideration). In the strips that failed in tension the ratio of the modulus of rupture of the steel to the yield point of the steel was found to be approximately $f_{bs}/f_y = 1.26\ (1 - 10p)$, where p is the ratio of steel. The strips of types 26 and 27 failed in compression at an average modulus of rupture of the concrete of 3490 lb. per sq. in. (computed with $n = 15$), that is, 1.90 times the prism strength.

Table XI* and Fig. 40 show some of the results obtained from the tests of 40 slabs out of the 52 which were tested. The surface of each of the square slabs, *a* to *g* of the rectangular slabs *h*, and of the rectangular slabs *i*, was divided into 50 cm. squares; that is, into 16, 24, and 32 squares, respectively; equal loads were applied at the centers of these squares, each load

TABLE X.—MODULI OF RUPTURE (COMPUTED ULTIMATE STRESSES) IN CONTROL STRIPS TESTED BY BACH AND GRAF.

The strips were tested as beams with 200 cm span. Computed stresses for n = 15. Graphical representation in Fig. 39.

Type No.	Number of strips	Dimensions: Width of strip cm	Dimensions: Total depth cm	Dimensions: Effective depth cm	Reinforcement: Number of bars	Reinforcement: Diam. of bars mm	Reinforcement: Area cm²	Reinforcement: Percentage 100p	Reinforcement: Transverse bars	Modulus of rupture: Yield point, steel, f_y lb/in²	Modulus of rupture: steel, f_{bs} lb/in²	Modulus of rupture: concr. f_{bc} lb/in²	Ratio f_{bs}/f_y: Computed value	Ratio f_{bs}/f_y: Approx formula $1.26(1-10p)$
18	4	50.1	12.08	10.82	5	7	2.06	0.380	none	58000	69700		1.202	
19	4	50.2	12.12	10.76	5	7	2.06	0.381	above	58000	71200		1.228	
20	4	50.0	12.15	10.19	5	7	2.07	0.406	below	58000	69200		1.194	
						Average:	0.389						1.208	1.210
21	3	50.2	8.07	6.81	5	7	2.09	0.511	none	58000	69400		1.197	
22	4	50.1	8.07	6.71	5	7	2.06	0.613	above	58000	69300		1.195	
23	4	49.9	8.10	6.14	5	7	2.06	0.672	below	58000	68200		1.176	
						Average:	0.632						1.189	1.180
24	3	50.4	12.10	10.60	5	10	3.96	0.741	above	49600	57200		1.154	
25	3	44.4	12.17	9.67	5	10	3.22	0.913	below	49600	56500		1.140	
						Average:	0.827						1.147	1.155
26	3	48.1	8.00	6.49	8	10	6.50	2.082	above	49600	47750	3475		
27	3	50.2	8.07	5.56	10	10	8.07	2.892	below	49600	35920	3505		
						Average:	2.487					3490		

Total: 35

* Table XI is modeled after similar tables used by E. Suenson (Ingenioeren, 1916, p. 541) and by N. J. Nielsen (Ingenioeren, 1920, p. 724), in the studies of the same experimental material. Table XI was computed from the original data reported by Bach and Graf; the results computed here agree approximately with those found by Suenson and by Nielsen. Suenson compared the experimental coefficients of moment in rectangular slabs with those found by an approximate theory. Nielsen computed the stresses by using coefficients which he derived by the method of difference equations.

distributed within a circle 9 cm. in diameter. Thus, the loads on each of these slabs were nearly uniformly distributed. Of the remaining twelve slabs, not included in Table XI, two were loaded by a concentrated load at the center, seven by eight concentrated loads near the center, while three slabs were double panels, continuous over a transverse beam, and carrying nearly uniformly distributed loads.

If a square slab, simply supported on four sides, is loaded uniformly by the total load W, the average moment across the diagonal becomes $1/24\ W = 0.0417W$. If the total load W is divided into 16 concentrated equal loads applied at the centers of 16 squares into which the slab is divided, the average moment across the diagonal becomes $3/64\ W = 0.0469\ W$. When these 16 loads, instead of being concentrated, are distrib-

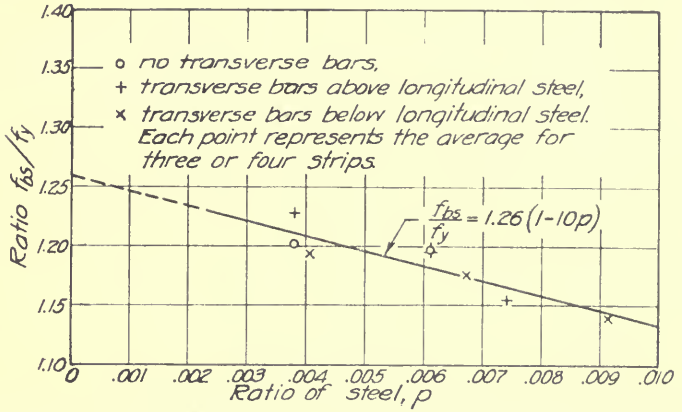

FIG. 39.—RATIOS OF MODULUS OF RUPTURE (COMPUTED ULTIMATE STEEL STRESS, f_{bs}) TO YIELD POINT, f_y, IN CONTROL STRIPS TESTED BY BACH AND GRAF.

uted uniformly within small circles, drawn at the centers of the squares, with a diameter equal to 9/200 of the span, then the average moment per unit-width across the diagonal, as may be verified by a simple statical computation, becomes $0.0460W$,* that is, 1.104 times the moment due to a uniform load. An equivalent uniform load was derived, therefore, in Table XI, for the square slabs, by multiplying the load applied at 16 points by 1.104 and by adding the dead loads, 1200 kg and 800 kg for the 12 cm and 8 cm slabs, respectively (that is, the dead weights within the supporting edges). In the rectangular slabs the section of maximum stress is not along the diagonal; for these slabs the equivalent uniform load was computed as the sum of the applied load and the dead load. The following coefficients of moments were used in Table XI: 0.0417, the coefficient of the average moment across the diagonal, was used for all the square slabs; in

* E. Suenson, in Ingenioeren, 1916. p. 538, states this moment as $\frac{1}{21.3}\ W = 0.0459\ W$.

addition, the coefficients 0.0369 and 0.0463, applying to the center and to the corner, respectively,—see Fig. 3(a) in Art. 7,—were used for the square slabs with non-uniform spacing of the steel (slabs d_1 and d_2); finally, 0.0733 and 0.0964, coefficients of moment per unit-width, in the short span at the center, taken from Fig. 3(a) in Art. 7, were used for the rectangular slabs h and i. Since the bending moments computed for the square slabs are moments across the diagonal, the section modulus pjd^2 per unit-width may be taken as the average for the two layers of steel if the steel is parallel to the sides; in the slabs, f_1, f_2, and g, with reinforcement parallel to

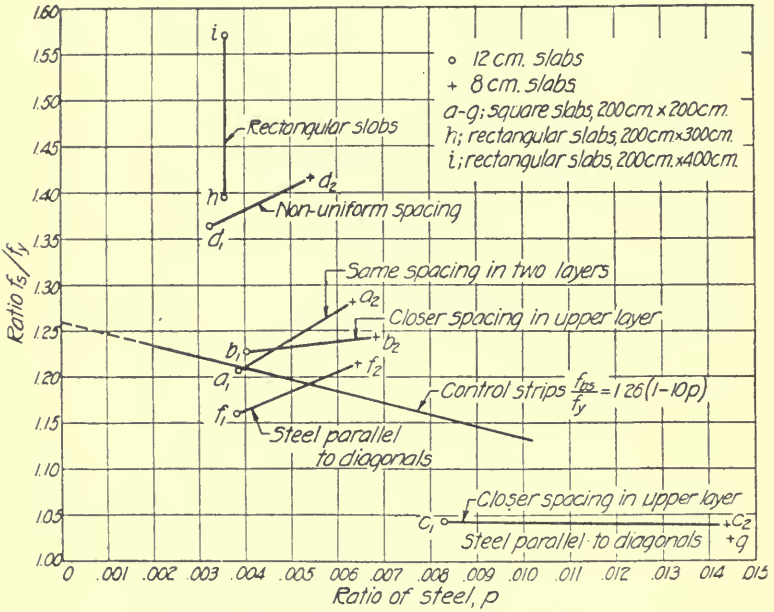

FIG. 40.—RATIOS OF MODULUS OF RUPTURE, f_s, TO YIELD POINT, f_y, IN SLABS SUPPORTED ON FOUR SIDES, TESTED BY BACH AND GRAF. POINTS d_1 AND d_2 REPRESENT AVERAGES OF TWO TESTS EACH, OTHER POINTS AVERAGES OF THREE TESTS EACH.

the diagonal, the section moduli in the two directions are practically equal and the average value may be used again. In the rectangular slabs, h and i, the section modulus by which the stresses are computed may be taken as that defined by the bottom layer, which is in the direction of the short span.

As an example of the computations in Table XI the derivation of the stress f_s in the slabs a_1 may be shown:

$$f_s = \frac{M}{pjd^2} = \frac{0.0417 \cdot 45700\text{kg}}{0.387\text{cm}^2} \cdot 14.22 \frac{\text{lb.cm}^2}{\text{kg.in}^2} = 70000 \frac{\text{lb}}{\text{in}^2}.$$

The stress f_s is the steel stress, computed by the ordinary theory of

reinforced-concrete with $n = 15$, developed under the observed maximum load; that is, f_s is the modulus of rupture in bending.

The stresses f_s developed in the slab may be judged by comparison with the yield point f_y of the steel and the modulus of rupture f_{bs} devel-

TABLE XI.—MODULI OF RUPTURE (COMPUTED ULTIMATE STRESSES) IN SLABS, SIMPLY SUPPORTED ON FOUR SIDES, WITH LOADS NEARLY UNIFORM, TESTED BY BACH AND GRAF.

The slabs extended 5 cm beyond the supporting edges. Two-way reinforcement at bottom, diagonally in types f_1, f_2, and g, parallel to the sides in all other types; 1 cm concrete below bottom layer. $n=15$; f_{bs} = stress in corresponding central strip; $f_{bs}/f_y = 1.26(1-10\rho)$; in square slabs ρ = average of ratios for two layers.

Type	Slabs No.	Thickness	Reinforcement Diam.	Spacing Upper layer	Spacing Lower layer	Percentage of steel Upper layer	Percentage of steel Lower layer	Section modulus jbd^2 per unit width Upper layer	Section modulus jbd^2 per unit width Lower layer	Max. loads Appl. load	Max. loads Equiv. uniform load	Coeff. of moment	Yield point steel	Computed stress, f_s	Ratios (f_{bs} = stress in strips) $\frac{f_{bs}}{f_y}$	Ratios $\frac{f_s}{f_y}$	Ratios $\frac{f_s}{f_{bs}}$
		cm	mm	cm	cm			cm^2	cm^2	kg	kg	M/wb^2	lb./in²	lb./in²			
Square slabs, span 200 cm.																	
a_1	825, 826, 827	12.2	7.2	10.0	10.0	0.401	0.375	0.373	0.400	0.387	40133	45700	0.0417	58000	70000	1.210	1.207	0.997
a_2	819, 822, 824	8.13	7.2	10.0	10.0	0.669	0.600	0.218	0.244	0.231	25517	29000	0.0417	58000	74400	1.180	1.282	1.087
b_1	831, 837, 840	12.13	7.2	9.3	10.0	0.434	0.377	0.397	0.397	0.397	42167	47100	0.0417	58000	71200	1.209	1.228	1.016
b_2	828, 830, 841	8.1	7.2	8.8	10.0	0.765	0.603	0.245	0.243	0.244	26167	29700	0.0417	58000	72100	1.174	1.243	1.058
c_1	884, 892, 899	12.1	10.0	8.9	10.0	0.919	0.741	0.732	0.729	0.730	56667	63700	0.0417	49600	51700	1.155	1.043	0.903
c_2	869, 872, 877	8.1	10.0	8.3	10.0	1.689	1.189	0.441	0.441	0.441	34000	38300	0.0417	49600	51500	1.079	1.038	0.962
d_1	846, 847, ave.	12.1	7.0	9.3	10.0	0.412	0.358	0.375	0.376	0.376			0.0369		59400		1.023	
	center			11.11	11.76	0.345	0.305	0.317	0.322	0.319	37500	42600	0.0417	58000	79100	1.220	1.364	1.118
	edge			14.0	14.3	0.274	0.250	0.254	0.267	0.260			0.0463		107800		1.860	
d_2	842, 843, ave.	8.1	7.1	8.8	10.0	0.744	0.587	0.239	0.237	0.238			0.0369		60200		1.038	
	center			11.11	11.76	0.589	0.499	0.191	0.203	0.197	24000	27300	0.0417	58000	82100	1.192	1.416	1.188
	edge			14.5	14.3	0.451	0.410	0.148	0.169	0.159			0.0463		113100		1.951	
e	924, 946, 951	8.1	10.1	5.0	6.0	2.860	2.023	0.721	0.725	0.723	43000	48300	0.0417	75200	39600			
f_1	853, 858, 859	12.17	7.0	9.3	10.0	0.409	0.356	0.378	0.378	0.378	41333	46800	0.0417	63200	73300	1.212	1.160	0.957
f_2	848, 849, 850	8.13	7.0	8.8	10.0	0.720	0.568	0.233	0.232	0.233	26667	30200	0.0417	63200	76800	1.179	1.215	1.031
g	910, 913, 916	8.07	10.0	8.3	10.0	1.699	1.195	0.439	0.439	0.439	33333	37600	0.0417	49600	50700	1.077	1.023	0.950
Rectangular slabs, short span 200 cm, long spans 300 cm (h) and 400 cm (i); bottom steel in short span																		
h	863, 866, 868	12.13	7.0	10.0	10.0	0.382	0.357		0.377		44333	46100	0.0733	60800	84900	1.214	1.396	1.150
i	860, 861, 862	12.13	7.0	10.0	10.0	0.382	0.357		0.377		50667	52700	0.0941	60800	95500	1.214	1.571	1.294

oped in the strips. Such comparisons are made in the last three columns in Table XI. The ratios f_s/f_y are represented graphically in Fig. 40.

The slabs e were designed to fail in compression. The stresses developed were: tension, 39,600 lb. per sq. in.; compression, 3430 lb. per sq. in..

which is 0.983 times the corresponding stress developed in the strips, and 1.87 times the prism strength of the concrete in compression.

Certain conclusions may be drawn from Table XI and from Fig. 40:

(a) The slabs show, on the whole, the same decrease of modulus of rupture with an increasing ratio of steel as did the strips which were tested as beams.

(b) The thinner slabs develop, on the whole, greater moduli of rupture than the thicker slabs with the same span and reinforcement. This result may be explained by the dish action which occurs when the deflections have become appreciable compared with the thickness of the slab. The slabs a_1 and a_2, for example, which were 12 cm and 8 cm thick, respectively, deflected about 6 cm at the center at the maximum load. By the double curvature of a slab the vertical sections resisting the bending moments assume an arc-shape instead of the original rectangular shape, and thus the section modulus is increased. At a given deflection, this effect is comparatively greater in a thin slab than in a thick slab. The dish action of the thin slab may be interpreted as a reversed dome action, in which the central area is essentially in tension, while the outer area is essentially in compression. The additional tensions and compressions explain the added carrying capacity, beyond what may be expected on the basis of the coefficients of moment which were derived for the medium-thick stiff homogeneous elastic plates.

(c) The design with closer spacing of the bars in the upper than in the lower layer of steel, so as to make the section moduli equal for the two layers, does not appear to be advantageous.

(d) Reinforcement parallel to the diagonals appears to be less effective than reinforcement parallel to the sides. If the corners had been prevented from bending up by anchoring,—the corners were observed to deflect slightly upward,—and if the steel along the diagonal had been bent up so as to reinforce against negative moments at the corner, greater strength might possibly have been developed with the same amount of steel.

(e) The slab has an ability to redistribute the stresses as the deflections increase, as the steel stresses approach or reach the yield point, and as cracks develop. By the redistribution the large stresses become smaller and the small stresses larger than would be predicted according to the distribution in the homogeneous elastic slabs for which the theory in Part II was derived. The phenomenon of redistribution is well known from other fields. For example, in a flat steel tension bar with a circular hole there is, at small stresses, a relative concentration of stress at the edge of the hole, but when the yield point has been reached the stresses may be practically uniformly distributed. Redistribution of stresses is a typical general feature in statically indeterminate structures of ductile materials. Thus, the property of the slab as a highly statically indeterminate structure becomes important; it explains additional strength beyond what might otherwise be expected. In the homogeneous elastic square slab with simple supports on four sides and with Poisson's ratio equal to zero the coefficients of moment per unit-width across the diagonal are, according to Art.

7: at the corner, 0.0463; at the center, 0.0369; average for the whole diagonal, 0.0417. The stresses across the diagonal may be redistributed so as to become nearly uniform; accordingly the average coefficient, 0.0417, was applied to all the square slabs in Table XI. The maximum coefficient 0.0463 would have made the corresponding stresses and ratios of stresses in Table XI and in Fig. 40, 1.11 times greater than the values shown. The coefficients 0.0463 would have led to a less close agreement between the slab strength and the strip strength than is found in Table XI and in Fig. 40. The redistribution of stresses across the diagonal may explain the rather large stresses computed for the corners of the slabs d_1 and d_2. These stresses were computed by using the largest coefficient of moment in connection with the smallest percentage of steel. Evidently the stresses have transferred toward the center, where the spacing of the steel is closer, and as a result of this redistribution the steel at the center appears to be more effective, per pound weight, in resisting the utlimate loads, than the steel near the edges. In the rectangular slabs the rather large moduli of rupture, 84,900 and 95,500 lb. per sq. in., computed by the coefficients of moment for the short span at the center, may be explained partly by a redistribution of the stresses across the long center line, whereby the actual stresses at the center are reduced, and partly by a transfer of stresses from the short span into the long span. N. J. Nielsen,* by using moment coefficients found by the method of difference equations, with Poisson's ratio equal to zero, determined ratios of slab strength to strip strength for the square slabs loaded nearly uniformly, for the square slabs loaded by eight forces near the center, for the square slabs loaded by one force at the center, and for the rectangular plates. He found the ratio of slab strength to strip strength to be fairly uniform for all the slabs, including the rectangular slabs, by assuming different values of the moment of inertia for the two spans, namely, such values that the maximum computed stresses become equal in the two spans, with the steel in the two directions utilized fully.

A comparative study of computed and observed deflections of one of the double panels (two square panels, continuous over a transverse beam), under a load equal to about one-fourth of the ultimate load, was made by N. J. Nielsen,† who used the method of difference equations. By considering the plate as made of homogeneous material with a modulus of elasticity of 4,110,000 lb. per sq. in., and by taking the deflections of the transverse beam as observed, he found the computed and the observed deflections at the centers of the panels to be equal, and he found the deflection curves and contour lines shown in Fig. 41. Near the transverse beam the observed deflections are seen to be smaller than the computed deflections. This difference may be due to the rather heavy reinforcement across the transverse beam.

The test made in 1920 at Waynesburg, Ohio, for Mr. J. J. Whitacre, throws further light on the question of the redistribution of stresses, as compared with the stresses in homogeneous elastic slabs, and on the ques-

* Ingenioeren, 1920, p. 724.
† N. J. Nielsen, Spaendinger i Plader, 1920, p. 74.

tion of the ultimate strength of the slabs.* The test was made with a two-way reinforced-concrete and hollow tile floor slab, 6 in. thick, with 18 panels. Fig. 42 shows the plan of the floor. The tiles are 6 in. by 12 in. by 12 in., open at the ends so as to allow the concrete to flow in, filling up a part of the tile. The tiles are separated by 4-in. concrete ribs in both directions. Each rib is reinforced by a ½-in. round bar at the bottom, and, in addition, in the part of the rib near the panel edges, by a ½-in. round bar at the top. The yield point of the steel was 54,000 lb. per sq. in.

Large negative moments were produced at the edges by loading all the panels and the cantilevers adjacent to B, C, and E, at the same time. Results of this part of the test are shown in Table XII. The applied load on each panel was a nearly uniformly distributed load, consisting of four piles of bricks with 18-in. aisles. Equivalent entirely uniformly distributed applied loads were derived by multiplying the average applied loads (within the areas defined by the clear spans) by the factors 0.91, 0.92, and 0.93 for the square, medium long, and longest panels, respectively; these

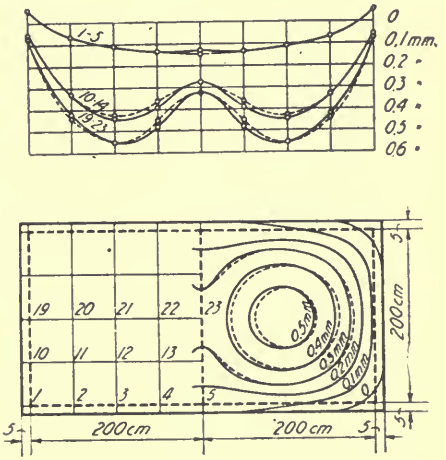

FIG. 41.—COMPARATIVE STUDY BY N. J. NIELSEN OF OBSERVED DEFLECTIONS (SHOWN BY DOTTED LINES) AND COMPUTED DEFLECTIONS (SHOWN BY FULL LINES) IN A DOUBLE PANEL TESTED BY BACH AND GRAF.

factors were determined by an approximate theory. The equivalent loads stated at the head of Table XII are found by adding the dead load, 50 lb. per sq. ft., to the equivalent uniform applied load. The observed stress, f, at the center of the edges, was considered to be made up of an estimated dead-load stress of 500 lb. per sq. in., plus the increase of stress due to the live load; this increase was found as the maximum ordinate of a smooth curve plotted from strain-gage readings on several gage lines across the

* A detailed report on this test has not yet been published. Only certain aspects which have a general bearing on the question of the moments and stresses in slabs are discussed here.

particular edge. In Table XII the ratio of the corrected steel stress, f_s, corresponding to the computed stress in a beam, to be observed stress, f, has been determined by means of formulas (1) and (3) in Part III, as though the material were solid stone or gravel concrete instead of concrete and hollow tiles. Since the reinforcing bars are 16 in. apart, the ratio of reinforcement at the center of the edge is, $p = 0.00260$. Formula (1), which applies at small stresses, before the concrete has cracked, gives then,

$$\frac{f_s}{f} = \frac{0.52}{1 + \frac{0.021}{p}} = \frac{1}{17.5},$$

and formula (2), which applies after the cracking has begun, gives the relation

$$\frac{f_s}{f} = \frac{54000}{f} + 0.222,$$

by which the values were computed in Table XII. The computation of the

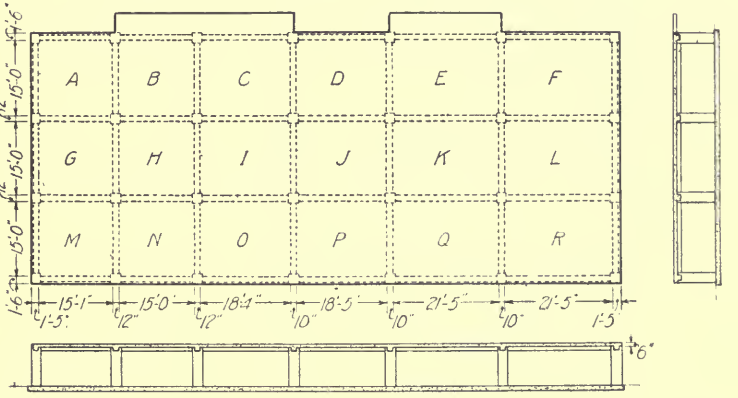

FIG. 42.—PLAN OF FLOOR SLAB TESTED AT WAYNESBURG, OHIO; THICKNESS, 6 IN.

coefficients of moment in Table XII may be shown by an example. For the edge AB (in the first line of the table) the observed moment coefficient, based on the observed stress, 45,000 lb. per sq. in., is found to be

$$\frac{M}{wb^2} = \frac{pjd^2f}{wb^2} = \frac{0.00260 \cdot 0.920 \cdot 4.71^2\text{in}^2 \cdot 45000\frac{\text{lb}}{\text{in}^2}}{388\frac{\text{lb}}{\text{ft}^2} \cdot 15^2\ \text{ft}^2} = 0.02735.$$

Since the corrected stress is 1.422 times the observed stress, the corresponding corrected moment coefficient becomes

$$1.422 \cdot 0.02735 = 0.0389.$$

TABLE XII.—COEFFICIENTS OF NEGATIVE MOMENTS IN WAYNESBURG TEST.

Test of reinforced concrete and hollow tile floor slab; 18 panels supported on girders as shown in Fig.—42Stresses and moments at centers of edges. All panels loaded. Equivalent uniform loads (incl dead load) in lb. per sq ft. 388 on panels A.M; 411 on B.G.H.N; 308 on C.D.I.J.O.P; 264 on E.F.K.L.Q.R.

	Panel	Edge	Observed stress f lb/in²	Ratio $\frac{f_s}{f}$	Coefficients of max neg. moment M/wb^2 Observed	Corrected	Theory, Fig. 8(b)	Edge	Observed stress f lb/in²	Ratio $\frac{f_s}{f}$	Coefficients of max neg. moment, M/wb^2 Observed	Corrected	Theory, Fig 8(b)
Square panels, span 15 ft.	A	AB	45000	1.422	.0274	.0389		AG	51500	1.270	.0313	.0398	
	B	BA	38000	1.693	.0218	.0358							
	B	BC	17000	3.397	.0098	.0331		BH	36500	1.701	.0210	.0357	
	G							GA	50000	1.302	.0287	.0374	
	G	GH	39500	1.589	.0227	.0360		GM	41000	1.539	.0235	.0362	
	H	HG	39500	1.589	.0227	.0360		HB	48500	1.336	.0278	.0372	
	H	HI	38000	1.643	.0218	.0358		HN	48500	1.336	.0278	.0372	
	M	MN	44000	1.449	.0268	.0388		MG	53000	1.240	.0322	.0400	
	N	NM	41000	1539	.0235	.0362		NH	51500	1.270	0296	.0376	
	N	NO	42500	1.493	.0244	.0364							
		Average coefficient:			.0363	.0417		Average coefficient:			.0376	.0417	
Oblong panels, 15ft X 18.25 ft.	C	CB	29000	2.084	.0222	.0463							
	C	CD	24500	2.425	.0188	.0455		CI	26000	2.300	.0199	.0458	
	D	DC	33500	1.834	.0257	.0471							
	D	DE	35500	1.744	.0272	.0474		DJ	42500	1.493	.0325	.0486	
	I	IH	38000	1.643	.0291	.0478		IC	50000	1.302	.0383	.0499	
	I	IJ	39500	1.589	.0303	.0481		IO	51500	1.270	.0395	.0501	
	J	JI	38000	1.643	.0291	.0478		JD	51500	1.270	.0395	.0501	
	J	JK	47000	1.371	.0360	.0494		JP	51500	1.270	.0395	.0501	
	O	ON	38000	1.643	.0291	.0478		OI	50000	1.302	.0383	.0499	
	O	OP	48500	1.336	.0371	.0496							
	P	PO	38000	1.643	.0291	.0478		PJ	42500	1.493	.0325	.0486	
	P	PQ	44500	1.436	.0341	.0490							
		Average, long span:			.0478	.0417		Average, short span:			.0491	.0572	
Panels, 15 ft X 21.5 ft	E	ED	20000	2.922	.0179	.0522							
	E	EF	33500	1.834	.0300	.0549		EK	41000	1.539	.0367	.0564	
	F	FE	24500	2.425	.0219	.0531		FL	51500	1.270	.0460	.0585	
	K	KJ	42500	1.493	.0380	.0567		KE	54000	1.222	.0483	.0590	
	K	KL	42500	1.493	.0380	.0567		KQ	54000	1.222	.0483	.0590	
	L	LK	39500	1.589	.0353	.0561		LF	51500	1.270	.0460	.0585	
	L							LR	54000	1.222	.0483	.0590	
	Q	QP	33500	1.834	.0300	.0549		QK	54000	1.222	.0483	.0590	
	Q	QR	48500	1.336	.0433	.0579							
	R	RQ	54000	1.222	.0483	.0590		RL	54000	1.222	.0483	.0590	
		Average, long span:			.0537	.0417		Average, short span:			.0585	.0674	

The theoretical values of the coefficients were taken from the approximate curves in Fig. 8(b) in Art. 7. These values are somewhat smaller than the corresponding directly determined coefficients in Fig. 8(a), but they may be assumed to apply after the stresses across the edges have been redistributed to some extent. That a further shifting of the stresses from the short span to the long span takes place at increasing deformations, is indicated by the fact that the oblong panels in Table XII have corrected coefficients, based on observations, which are greater than the theoretical values for the long span, and are smaller than the theoretical values for the short span; but the sum of the corrected coefficients for the long span and the short span is approximately equal to the sum of the corresponding theoretical coefficients. It is probable that at increasing loads there is also a transfer of stress from the edges to the central portion of each panel; and that this transfer may partly explain the rather small values found for some of the coefficients in Table XII.

In a later part of the test large loads were applied in panels H, J, and K, while the loads on the surrounding panels were reduced. In the square interior panel H, for example, the average applied load was increased to 1413 lb. per sq. ft., giving, by the computation used in Table XII, an equivalent uniform load of $50 + 0.91 \cdot 1413 = 1336$ lb. per sq. ft. This value is probably somewhat too large because of the unavoidable arch action in the piles of brick; the four piles were joined together 12 ft. above the slab and were continued as one pile up to the total height of almost 22 ft. When the deflections increase the resultant pressure transmitted through each of the four piles is thrown toward the corners of the panel, and the equivalent uniform load becomes correspondingly smaller. Since the amount of the reduction is not known, the value just stated, 1336 lb. per sq. in., will be used without reduction in the computation of stresses. Since the adjacent panels were unloaded, the panel H may be considered in this computation as a single square panel with the edges half fixed and half simply supported. Accordingly, the average of the numerical values of the moment coefficients at the center and at the edge in slabs with simply supported and with fixed edges is used, that is (see Fig. 3(a), Fig. 7(a), and Fig. 8(a)).

$$\frac{1}{4}\,(0.0369 + 0 + 0.0177 + 0.0487) = 0.0258.$$

By assuming this moment coefficient, and by assuming the same effective depth and ratio of steel as in the calculation of Table XII, one finds the "computed stress" in panel *H* under the maximum load equal to

$$f_s = \frac{0.0258\ wb^2}{pjd^2} = \frac{0.0258 \cdot 1336 \cdot 15^2}{0.00260 \cdot 0.92 \cdot 4.71^2} = 146000 \text{ lb. per sq. in.}$$

This stress is 2.71 times the yield point stress of the steel, $f_y = 54{,}000$ lb. per sq. in., and 2.21 times the strip strength, $f_{bs} = 66.200$ lb. per sq. in., as determined from Bach's and Graf's tests by the line in Fig. 39. In estimating the significance of this result it should be noted that some arch action in the piles of brick probably made the applied load not fully effective; that the material is different from ordinary reinforced-concrete; that

the moment coefficients may have been reduced by redistribution of the stresses across the center line, across the diagonal and across the edge; that this redistribution may have been aided by the deflections of the supporting girders; and that the deflection at the center was so large, 1.4 in., that the dish action or reversed dome action which is characteristic of thin slabs, may have aided in carrying the load. It is not known what load would have produced failure.

The average loads, determined by dividing the total applied load by the panel area, applied in panels J and K at the same time and under similar conditions without producing failure, were 1184 lb. per sq. ft. and 920 lb. per sq. ft., respectively.

V.—TESTS OF FLAT SLABS.

By W. A. SLATER.

21. GENERAL DESCRIPTION. In the following pages are given the results of tests of certain flat slabs. It has been necessary to make the discussion of the results very brief and only sufficient statement on each subject has been made to enable the reader to interpret the data given in the diagrams and tables.

The study of the tests is based almost entirely upon tensile stresses since it is impossible to know with sufficient accuracy for this purpose what compressive stresses are indicated by the compressive deformations and because the amount of reinforcement in flat slabs is generally so small that the tensile stresses will almost always be critical rather than the compressive stresses.

The results for most of the tests have been published previously. Those for the two Purdue tests, the Sanitary Can Building test, and the Shonk Building test have not been published, and those of the International Hall test* were published only in part. Because of the fact that the results of the Purdue test had not been published, the reinforcing plans, the location of gage lines, the measured deformations and the deflections are given in Appendix B. Further data are given in Table XIII.

It had been expected to give the results for the Sanitary Can Building test and the Shonk Building test as fully as for the Purdue tests, but this has not been possible. The following statement, together with the data given in Table XIII, will be sufficient to give significance to the moment coefficients given in Fig. 45 for these tests. It is expected that in a later publication of the Bureau of Standards the full data of these tests will be included.

The tests of the Sanitary Can Building and the Shonk Building were made by A. R. Lord, of the Lord Engineering Company, Chicago, Ill. Prof. W. K. Hatt, of Purdue University, Lafayette, Ind., was in touch with these tests at the request of the Corrugated Bar Company. The report by Mr.

* Trans. A. S. C. E., Vol. LXXVII, p. 1433 (1914).

Lord and that by Professor Hatt have been drawn upon for the data used in preparing this paper.

Both buildings are located at Maywood, Ill., a suburb of Chicago. The floors of both are flat slabs, having column capitals 5 ft. in diameter and dropped panels 8 ft. square. In each building four panels were loaded and in each case two of the loaded panels were wall panels and the other two were the adjacent interior panels. The panel length in the direction parallel to the wall and also perpendicular to the wall for the two interior panels is 22 ft. for both buildings. For the wall panel, the panel length perpendicular to the wall is 21 ft. 3 in. for the Sanitary Can Building and 20 ft. 7 in. for the Shonk Building. The Sanitary Can Building has 24-in. octagonal interior columns and wall columns 20 by 45 in. rectangular in cross section. The Shonk Building has 22-in. octagonal interior columns and wall columns 21¾ in. rectangular in cross section. The Sanitary Can Building has two-way reinforcement and the Shonk Building has four-way reinforcement. There was some difference in distribution of reinforcement, but in the two slabs the total area provided for negative moment was about the same, and the total area for positive moment was about the same. The area of reinforcement at the principal design sections and the measured depth d to the reinforcement are shown in Table XIII.

Each floor was designed for a live-load of 150 lb. per sq. ft. The maximum superimposed test load was about 400 lb. per sq. ft. The dead load brought the total test load up to about 535 lb. per sq. ft. in each test. The highest observed stresses in the reinforcement were about 24,000 lb. per sq. in. in both floors, and this high stress occurred in only a few places.

The misplacement of the reinforcement in the Bell St. Warehouse* probably had an influence on the distribution of resisting moments between positive and negative, which would not be expected in slabs of that type. At least, this feature should be considered in studying the results of the test.

The original data of the test of the Western Newspaper Union Building were not available, therefore, in determining the moment coefficients for this test, it was assumed that the moment of the observed tensile stresses at any load less than the maximum bore the same ratio to the resisting moment reported for the test load of 913 per sq. ft.† that the sum of the observed stress and the estimated dead load stress for the load under consideration bore to the sum of the observed stress for the maximum test load and the estimated dead load stress.

22. CORRECTION OF MOMENT COEFFICIENTS. In reporting results of flat slab tests it has been customary to state the moment of the observed stresses in the reinforcement as a proportion of the product of the total panel load and the span. It has been known from beam tests that the

* Pacific N. W. Soc. Civ. Eng., Vol. 15 (Jan. and Feb., 1916); Eng. Record, Vol. 73, p. 647; Eng. News-Record, April 19, 1917.

† Bulletin 106, Univ. of Ill. Eng. Exper. Sta., p. 36. Also Proc. A. C. I., Vol. XIV, p. 192 (1918).

total moment of the observed stresses is less than the applied moment. The ratio of the applied moment to the moment of the observed stress is equal to the ratio of the computed stress to the observed stress. This may be shown as follows:

$$M = KWl = Af_s jd$$
$$M_1 = K_1 Wl = Af_1 jd$$

from which $$\frac{M}{M_1} = \frac{K}{K_1} = \frac{f_s}{f_1}$$

and $$K = \frac{f_s}{f_1} K_1$$

where K and K_1 are coefficients
KWl = applied moment
$K_1 Wl$ = moment of observed stress
f_s = computed stress
f_1 = observed stress

Other terms have their usual significance.

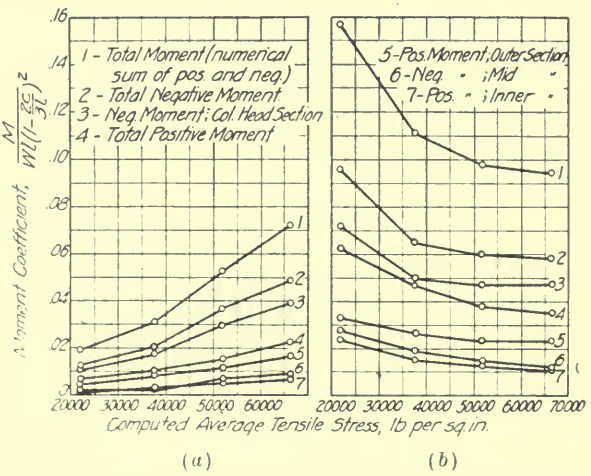
1 - Total Moment (numerical sum of pos. and neg.)
2 - Total Negative Moment
3 - Neg. Moment; Col. Head Section
4 - Total Positive Moment
5 - Pos. Moment; Outer Section
6 - Neg. " ; Mid "
7 - Pos. " ; Inner "
Moment Coefficient, M/Wl(1-2c/3l)
Computed Average Tensile Stress, lb per sq. in.
20000 30000 40000 50000 60000
20000 30000 40000 50000 60000 70000
(a)
(b)

FIG. 43.—MOMENT COEFFICIENT FOR SLAB J; (*a*) UNCORRECTED; (*b*) CORRECTED.

These equations show that for a beam the true moment coefficient K_1 may be determined by multiplying the moment coefficient of the observed stress by the ratio of the computed stress to the observed stress. This ratio is here termed the moment correction. Although it is recognized that the behavior of a slab differs from that of a beam it seems reasonable to assume that the relation between applied moments and the moment of the observed tensile stresses in the reinforcement should be the same for a slab as for a beam if the percentage of reinforcement, the modulus of elasticity of the concrete, the depth d and the depth of covering of the reinforcement are the same for the slab as for the beam.

The beams tested by the U. S. Geological Survey, and reported in Part III, afford a basis for determining the moment correction for a wide range in the percentage of reinforcement and the modulus of elasticity of the concrete, and to this extent the moment corrections found for these beams will be useful for estimating from the observed stress in the slabs the moment applied to the slabs. The fact that in this investigation only one depth, *d*, and only a slight variation in the covering of the tension reinforcement were used, limits the usefulness of this investigation as applied to interpreting test results of flat slabs, but no other series of tests is known which covers so wide a range of conditions, and, notwithstanding these limitations, it seems reasonable to expect that, on the whole, the application of the moment corrections from Fig. 31 and Fig. 32 to the

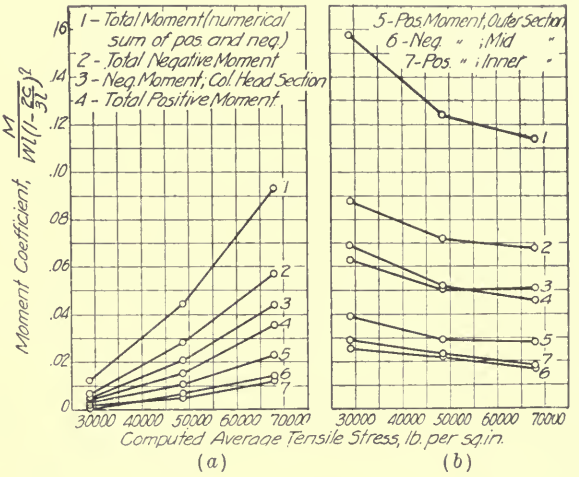
1 - Total Moment (numerical sum of pos. and neg.)
2 - Total Negative Moment
3 - Neg. Moment, Col. Head Section
4 - Total Positive Moment
5 - Pos. Moment, Outer Section
6 - Neg. " ; Mid "
7 - Pos. " ; Inner "
Moment Coefficient, M / Wl(1 - 2c/3l)²
Computed Average Tensile Stress, lb. per sq. in.
(a)
(b)

FIG. 44.—MOMENT COEFFICIENTS FOR SLAB S; (*a*) UNCORRECTED; (*b*) CORRECTED.

moment coefficient, determined by means of the observed stress in the flat slab, should give a fair idea of the true moment coefficients for these slabs.

23. MOMENT COEFFICIENTS. The moment coefficients have been stated as values of the expression $\frac{M}{Wl\left(1-\frac{2}{3}\frac{c}{l}\right)^2}$ in which M is the sum of the positive and negative moments in the direction of either side of the panel, W is the total panel load, c is the diameter of the column capital and l is the span in the direction in which moments are considered. This is a convenient form of expression and it has been found possible to state the moments found by the analysis in terms of it with a satisfactory degree of accuracy.*

*See Art. 8, p. 30.

The use of the same form of expression in stating the test results simplifies the comparison with the analytical result. In determining the value of M from the tests for use in calculating these moment coefficients the equation $M = Af_s jd$ was evaluated. Wherever it was possible the moments were determined separately for the sections of positive and of negative moment shown in Fig. 12, using the values A, f, and d, shown by observation for these sections. In some cases it was necessary to use an average value of f_s for both sections of positive moment and another average value for both sections of negative moment. In some cases measured values

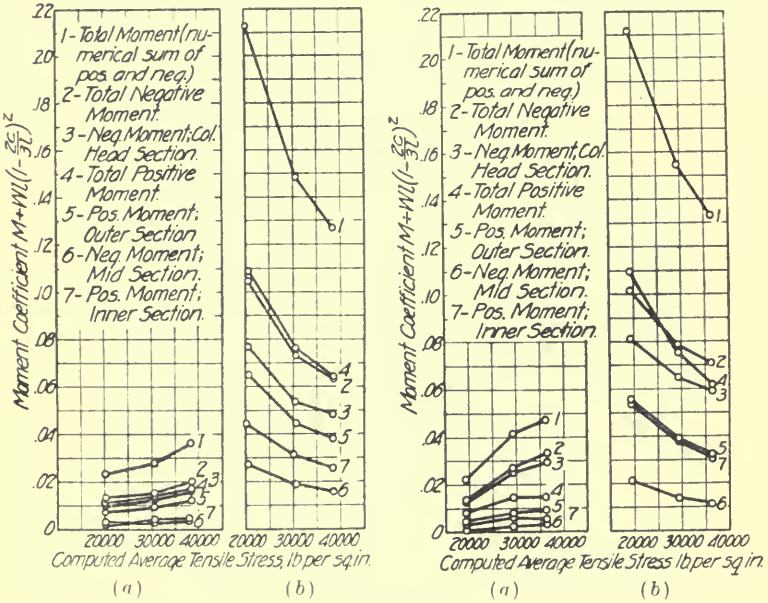

FIG. 45.—MOMENT COEFFICIENTS FOR SANITARY CAN BUILDING; (*a*) UNCORRECTED; (*b*) CORRECTED.

FIG. 46.—MOMENT COEFFICIENTS FOR SHONK BUILDING; (*a*) UNCORRECTED (*b*) CORRECTED.

of d were not available and it was necessary to use what appeared to be the most probable values, taking into account the total thickness of the slab, the size of reinforcing bars and the number of layers of reinforcement. It is apparent that these uncertainties will introduce corresponding uncertainties into the moment coefficients, but the errors are believed to be no greater than the errors which are inevitably involved in other experimental work of an equal degree of complexity.

Generally the computations were made separately for the moments in the directions of the two sides of the panel, and were combined for presentation in Fig. 43 to 48. In all the slabs for which the moment coefficients

are shown the panel lengths in the two directions were so nearly the same that it did not seem desirable to show separately the coefficients for the two directions. The deficiencies in the test data available, and the unknown factors which affect the behavior of the slab, would introduce errors which are larger than the difference between the moments in the two directions. In order to determine experimentally the difference in moments in the two directions, when the spans are so nearly equal, a large number of tests would be required, and the deficiencies in the test data would have to be

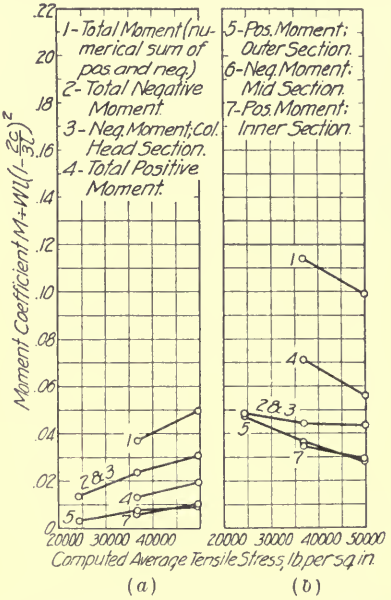

FIG. 47.—MOMENT COEFFICIENTS FOR BELL STREET WAREHOUSE; (*a*) UNCORRECTED; (*b*) CORRECTED.

supplied. One test, that of the Larkin Building, was available, in which the differences in the size of the panels was considerable; but in this test, except in the lower loads, the number of panels loaded was not sufficient to give corresponding conditions in the two directions, and the coefficients for that slab are not presented.

The computed average tensile stress, shown as abscissas in Fig. 43 to 48, were determined from the equation

$$f_s = \frac{\frac{1}{8} Wl \left(1 - \frac{2}{3}\frac{c}{l}\right)^2}{\Sigma Ajd} \quad \text{in which}$$

W is the total panel load, live and dead, and ΣAjd is the sum of the

values of Ajd for the sections shown in Fig. 12. The values of Ajd for these sections are given in Table XIII.

It was shown in Art. 16 that the relation between the observed stress and the computed stress in the reinforcement is affected by variations in the value of n (that is, of the modulus of elasticity of the concrete, since that of the steel is practically constant). Equations (5) and (6), Art. 16, show this effect below and above the load at which the concrete cracked. Correspondingly the value of the corrected moment coefficient will be affected by these variations in n.

Fig. 49 has been prepared to show the effect of a variation in the value of n on the coefficients. Small circles indicate the coefficients for the value of n, which was used in obtaining the corrected moment coefficients shown in Fig. 43 to 48. This is the average value of n for the stone and the

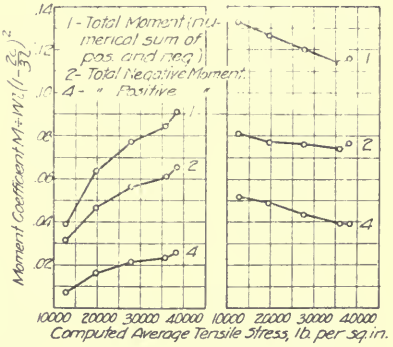

FIG. 48.—MOMENT COEFFICIENTS FOR WESTERN NEWSPAPER UNION BUILDING; (*a*) UNCORRECTED; (*b*) CORRECTED.

gravel concretes of the beams used in the tests by the U. S. Geological Survey. (See Table VIII, Part III). The smooth curves show the corrected coefficients which have been found by using a range of values of n in the determination of the corrections.

It will be seen that in order to bring the coefficients to the theoretical value of ⅛ the value of n for the Purdue tests would be about 9 and that for the Sanitary Can Building and the Shonk Building would be about 11.5. While it cannot be stated that these are the correct values of n for the concrete in these slabs, it seems reasonable to believe that they are more nearly correct than the value of 7, which was used in computing all corrected moment coefficients. The available data from the slab tests strengthen this belief, but the reliability of the test data which bear on this subject was not sufficient to justify introducing into the computation of the corrected moment coefficients the experimental values of n, determined in the tests of these structures.

It will be seen in Figs. 43 to 48 that the uncorrected moment coefficients are all less than the theoretical value, ⅛. For the lower computed stresses the corrected coefficients are generally in excess of ⅛, but for the highest computed stress, that is, for the highest load applied, the average coefficient, 0.111, is less than the theoretical coefficient.

The fact that for the lower computed stresses the corrected moment coefficients generally were higher than the theoretical value, indicates that too large a correction factor was used. No means of knowing how much the factor used was in error is evident, but the fact that as the computed stress increases the uncorrected and the corrected moment coefficients approach each other in value seems to reduce the uncertainties as to the correct values of the moment coefficients to a narrower margin than that which has limited the usefulness of practically all the field tests that have ever been made on reinforced-concrete slabs. On the average, the agreement

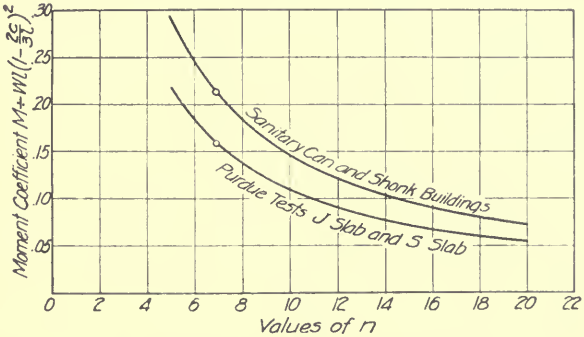

FIG. 49.—EFFECT OF VARIATION IN MODULUS OF ELASTICITY ON VALUE OF MOMENT COEFFICIENTS AT LOW LOADS.

of the corrected coefficients for the higher computed stresses with the result found by analysis in Part II is sufficiently close to warrant the belief that, if all the sources of error in the measurement of deformations and in the interpretation of test results could be removed, the analysis and the tests would be in substantial agreement. It is pointed out in Art. 20, in discussing the results of the test of a slab in which there were beams on the boundary lines of the panels, that although, for the lower loads, the test results were in fair agreement with the analysis of that type of slab, there was, for the higher loads, an accommodation of the slab to the conditions imposed upon it, which made the slab capable of carrying a much greater ultimate load than is accounted for by equating the applied bending moment and the apparent resisting moment. On account of the lack of tests of flat slabs carried to the point of failure, and in which the design was such as to preclude failure from some other cause than bending, it cannot be stated that, to the same extent, a similar source of additional strength is present in flat slabs as was present in the Waynesburg slab, which was supported on

four sides. There are some indications, however, that there was greater strength in the flat slabs than appears from the conclusion that the test results and the analysis of moments are in fair agreement. Some indication of this greater strength is seen in the description of the Purdue tests, Appendix B.

24. FACTOR OF SAFETY. Table XIII gives summarized data of all the tests studied. The purpose of this table is to give the best estimate of what the factor of safety against failure of the structure would have been if sufficient load had been applied in each case to produce failure. For all the tests reported, except the Purdue tests, the factor of safety is an estimated quantity which gives the ratio of the estimated maximum load which the slab would carry to the design load (sum of dead and live load), computed as indicated in the table. Although the factor of safety is shown for three moment coefficients, the design load is shown for only one coefficient. The design load will be inversely proportional to the coefficient used in the design. For the Purdue test slabs the factors of safety given are the ratios of the load actually applied to the slab to the design load shown in the table. The "average observed stress, f_1," of the table, therefore, has no significance for those slabs, but they are given because of their value as matters of general information concerning the tests. The stresses for the maximum load of 872 lb. per sq. ft., on slab J, were not reported, and the average observed stress given for that slab is, therefore, that for the load of 664 lb. per sq. ft. (live and dead), the highest load for which the measured stresses were reported. For all other tests the average observed stress given in the table is that for the "maximum test load" given in the table. The average observed stresses, as reported, were roughly weighted to take account of the distribution of the gage lines over the sections of maximum stress due to negative moment and positive moment. For the Purdue tests this weighting was not necessary, since the stresses were measured in all the bars crossing these sections.

The "estimated dead load stress" of Table XIII is given by equation (1) or equation (3) of Part III, in which f_s is the value of

$$f_s = \frac{\frac{1}{8} W l \left(1 - \frac{2}{3}\frac{c}{l}\right)^2}{\Sigma A j d}$$

In this equation W is taken as the total dead load of the panel. Since the value of f_s was generally below the points in the curves of Fig. 31, which represent the cracking of the concrete, equation (1) was generally used in estimating the dead load stress rather than equation (2).

In estimating the maximum load for slabs it was assumed that the yield point of the steel was 40,000 lb. per sq. in., and that failure would have occurred at a computed average stress, which is the same as the computed stress given in Fig. 31 at the intersections of the straight lines, of equation (3), part III, with the locus representing the equation $f = 40{,}000\ (0.82 + 7p)$ given in Fig. 31. The assumption of 40,000 lb. per sq. in. as

TABLE XIII.—ESTIMATED FACTOR OF SAFETY AGAINST TENSION FAILURE

Name of Structure		Shredded Wheat Factory		Jersey City Dairy Co. Building	Purdue Test Slabs "S"	Purdue Test Slabs "J"	Sanitary Can Factory	Shonk Building	Larkin Building		Franks Building		Shulze Baking Company Building		Western Newspaper Union Building	Northwestern Glass Company Building.		Bell Street Warehouse	Channon Building	International Hall
Type of reinforcement		2-way		2-way	2-way	2-way	2-way	4-way	4-way		4-way		4-way		4-way	4-way		4-way	†	4-way
Panel dimensions, l_1 and l_2		20'-0" × 22'-0"		17'-11½" × 19'-8½"	16'-0"	16'-0"	22'-0" × 22'-0"	22'-0" × 22'-0"	20'-0" × 24'-2"		20'-3" × 19'-4"		20'-0" × 17'-6"		17'-4½" × 19'-4½"	16'-0" × 17'-0"		20'-0" × 20'-9"	20'-0"	18'-0"
Col. head diam. c, inches		42"		62"	45"	45"	60"	60"	60"		44"		54"		54"	56"		57"	54"	40"
Slab thickness, inches		7.29"		8"	5.77"	5.47"	10.57	10.8	9"		9.25"		8.87		8.5"	8.08"		10.86"	8"	7.1"
Drop thickness, inches		9.13"		10"	7.74"	7.61"	14.07"	13.8	15.75		13.25"		14.28		No drop	No drop		No drop	12½"	No drop
No. panels loaded		9		1	4	‡ 4	4	4	5		4		4		4	4		4	4	2
Max. test load, w_t (live+dead) lb/ft²		282		508	522	‡872	532	535	730		428		722		1019	349		834	750	483
Shearing stress (v) at max test load, lb/in² ¶		118			132	233	115	118	106		81.5		122		300	67.5		233	207	
Depth (d) to c.g. reinf. in.	Col-head section, d_1	6.82		5.87	6.385	6.10	10.1	10.0	13.75		11.21		10.15		6.25	7.23		7.49	9.8	5.31
	Mid- " d_2	4.95		5.75	4.66	3.98	6.5	7.1	7.5				6.9		6.25	7.23		7.49	6.15	
	Outer " d_3	4.95		6.75	4.97	4.58	9.6	9.4	7.5		8.13		7.45		7.50	6.89		10.10	6.90	6.55
	Inner " d_4	4.95		6.42	4.86	4.61	8.8	9.2	7.5		7.89		7.45		7.50	6.70		9.54	6.94	6.55
Sectional area (A) of reinforcement sq. in.	Col-head "	6.16	6.77	5.80	2.69	4.244	8.59	11.59	8.94	13.27	13.75	12.91	12.02	10.22	15.85	3.93	4.07	12.65	8.16	6.20
	Mid- "	1.96	2.35	1.89	1.10	1.104	3.00	1.3	0	0	0	0	1.43	1.21		0	0	0	2.38	0
	Outer "	4.63	4.63	3.43	1.98	3.067	5.48	3.73	2.65	4.52	3.53	3.14	3.45	2.55	13.37	1.66	1.66	3.34	5.16	1.52
	Inner "	1.96	2.35	2.26	1.10	1.100	2.67	3.61	5.02	6.02	5.11	4.89	4.63	4.06		2.27	2.41	4.72	2.21	2.03
Per cent reinf. p; av. for all sections		.0055		.0048	.0033	.0047	.0041	.0040	.0052		.0064		.0051		.01	.0038		.0068	.0048	.0052
Ajd $j=.875$	Col-head section	36.80	40.80	29.80	15.05	22.67	75.9	101.3	107.3	159.5	134.90	126.70	106.70	90.8	86.70	28.45	29.40	83.05	70.00	26.6
	Mid- "	8.49	10.17	9.51	4.48	3.85	17.1	8.08	0	0	0	0	8.64	7.31		0	0	0	12.81	0
	Outer "	20.05	20.05	20.26	8.62	11.97	46.02	30.65	17.4	29.7	25.15	22.32	22.5	16.63	87.71	11.44	11.44	29.52	31.20	8.7
	Inner "	8.49	10.17	12.70	4.69	4.33	20.58	29.05	33.0	39.5	35.20	33.80	30.24	26.46		15.23	16.17	39.40	13.40	11.6
ΣAjd for all sections		73.83	81.19	72.27	32.84	42.82	159.60	169.08	157.7	228.7	195.25	182.82	168.08	141.2	174.41	55.12	57.01	151.97	127.41	49.1
$c \div l$ (l = span c. to c. cols)		.175	.159	.275	.234	.234	.227	.227	.250	.208	.181	.190	.225	.257	.244	.292	.275	.233	.225	.185
$125 l (1-\frac{2}{3}c/l)^2$	*See footnote	234	264	*111.8	17.11	17.11	23.8	23.8	20.9	26.8	23.5	22.1	21.69	18.05	19.40	15.53	16.97	21.81	21.75	20.53
Design live & dead load	Total; $W=6000 \Sigma Ajd - 125 l (1-\frac{2}{3}c/l)^2$ lb	50400	49200	102500	30700	40100	107300	114000	121000	136500	133000	132300	124000	125200	143800	56700	53800	111,500	93100	38300
	Unit; $w_t = W \div l_1 \times l_2$ lb/ft²	114	112	294	120	156.5	221	235	250	284	340	338	354	357	425	209	198	269	232	118
Ratio max test load to design load w_t		2.47	2.52	1.73	4.26	4.24	2.41	2.27	2.92	2.57	1.26	1.27	2.04	2.02	2.4	2.15	2.27	3.10	3.23	4.09
Av. observed stress f_s lb/in²		9450	13750	5000	‡50000	‡50000	10975	14390	11900	14300	3450		4942		25390	10375		18747	18000	19300
Estimated dead load stress f_2 lb/in²		1400	1400	1050	‡	‡	850	800	800	800	685	685	514	514	671	646	646	1000	800	800
$f_1 + f_2$		10850	15150	6050	‡	‡	11825	15190	12700	15100	4135	4135	5456	5456	26061	11021	11021	19747	18800	20100
$f_{ult} - (f_1 + f_2) = w_{ult} \div w$		1.42	1.26	1.72	‡	‡	1.27	1.22	1.36	1.31	2.75	2.75	1.98	1.98	1.69	1.24	1.24	1.30	1.25	1.19
Factor of safety ($\frac{w_{ult}}{w_t} \times \frac{w}{w_t}$) based on moment of	$125 W l (1-\frac{2}{3}c/l)^2$	3.54	3.19	2.96	4.26	5.57	3.06	2.77	3.97	3.36	3.47	3.49	4.04	4.00	4.06	2.67	2.82	4.03	4.04	4.89
	$1067 W l (1-\frac{2}{3}c/l)^2$ J.C.	3.02	2.72	2.54	3.63	4.75	2.61	2.36	3.39	2.86	2.96	2.98	3.45	3.41	3.46	2.28	2.41	3.44	3.45	4.17
	$.09 W l (1-\frac{2}{3}c/l)^2$ A.C.I.	2.55	2.30	2.15	3.07	4.00	2.21	2.00	2.86	2.42	2.50	2.51	2.91	2.88	2.92	1.92	2.03	2.90	2.91	3.52

NOTE: l_1 = short span c. to c. cols, l_2 = long span c. to c. cols; $v = (w l_1 l_2) \div (\pi c d_1)$; w_{ult} = ultimate load, lb/ft², f_{ult} = computed tensile stress at ultimate load, lb/in²

* $.0745 l (1-\frac{2}{3}c/l)^2$ for Jersey City Dairy † Principally circumferential reinforcement. ‡ See discussion of "Factor of Safety", Art. 24, p. 508.

¶ Shear on section of depth jd and distant d from capital.

the yield point was made in order to bring all the tests to a common basis for the purpose of comparison and in order to obtain a factor of safety not higher than might be expected if reinforcement having that yield point were used. Obviously reinforcement having a yield point of 55,000 lb. per sq. in. should be expected to give a higher factor of safety than that having a yield point of 40,000 lb. per sq. in., when the working stress in tension is 16,000 lb. per sq. in. in both cases.

The considerations in the two preceding paragraphs indicate that the true factor of safety was probably higher than the values given in Table XIII. On the other hand it must be recognized that the design load found with the use of the measured depth d would be smaller and the factor of safety somewhat larger if the depth d assumed in the design of the slabs were used for the computations of factor of safety. This is due to the fact that, on account of misplacement of the reinforcement, the measured depth to the reinforcement is usually somewhat less than the depth used in design.

The average factor of safety for the structures reported in Table XIII, estimated on the basis of a moment coefficient of $0.1067\ Wl\left(1-\frac{2}{3}\frac{c}{l}\right)^{2*}$ is 3.23 and that for the moment coefficient of $0.09\ Wl\left(1-\frac{2}{3}\frac{c}{l}\right)^{2*}$ is 2.72.

It is to be noted that for the tests which were carried to destruction of the slab, or nearly so (the two Purdue tests and Western Newspaper Union Building test) the values were above these average values.

It has been established by tests that the maximum load on a simple beam occurs at a tensile stress only slightly greater, say 10 per cent, for steel of structural grade, than the yield point of the steel in tension and not at the ultimate strength of the steel. This is true not only for reinforced concrete beams† but also for steel beams.‡

Recognizing this fact, and at the same time using a working stress of 16,000 lb. per sq. in. in steel of structural grade, whose yield point is 33,000 lb. per sq. in.,§ is, in fact, recognizing the sufficiency of a factor of safety of about 2.25. Based upon the use of a moment of $0.09\ Wl\left(1-\frac{2}{3}\frac{c}{l}\right)^{2}$ for design, the slabs reported in Table XIII would, on the average, develop this factor of safety of 2.25 even though they were to have failed at loads approximately 15 per cent greater than the loads which were applied. To one familiar with the behavior of the structures listed in Table XIII, or with similar structures during and after the tests, it is obvious that they would have carried at least that much additional load.

---

* These are the total moments recommended by, respectively, the Joint Committee on Concrete and Reinforced Concrete and the American Concrete Institute Committee on Reinforced Concrete and Building Laws.

† Art. 18 and Fig. 36; also A. N. Talbot Bull. 1, Univ. of Ill. Eng. Exp. Sta. (1904), p. 27; Turneaure and Maurer "Principles of Reinforced Concrete Construction," 2nd ed. (1909), p. 142.

‡ H. F. Moore Bull. 68, Univ. of Ill. Eng. Exp. Sta. (1913), p. 14.

§ Standard Specifications for billet steel concrete reinforcement bars A 15-14, A. S. T. M. Standards, 1918, p. 148.

It seems certain, therefore, that for the flat slabs under discussion the factor of safety against failure in bending, based on a total moment of $0.09\ Wl\left(1-\frac{2}{3}\frac{c}{l}\right)^2$, is at least as great as that which can be counted upon in the most elementary flexural unit, the simple beam built of, or reinforced with, steel of structural grade and designed with the usual working stresses. Based upon a total moment of $0.125\ Wl\left(1-\frac{2}{3}\frac{c}{l}\right)^2$ the factor of safety is correspondingly greater.

An effort was made to obtain, from failures of flat slabs in service, information as to what were the serious weaknesses in the design. A study of a letter from Edward Godfrey* citing 29 failures of reinforced-concrete buildings brings out the fact that all of the building floors there discussed, including flat slabs among others, failed during construction or as a result of a severe fire. While some of the failures during construction may have been partly due to deficiencies in the design the lack of proper safeguards in construction were so evident and so important that with the meager data available any effort to analyze the failures would be long drawn out and largely speculative. The fact that the majority of the failures referred to occurred during winter weather or in structures which had no opportunity to cure properly in warm weather is in itself sufficient indication that poor construction conditions contributed largely to the failure. To attempt to guard against abusive lack of safeguards in construction by severe requirements for design would be ineffective and prohibitively extravagant and would itself encourage the omission of these safeguards. There probably are cases in which deficiencies of design have caused trouble in flat slab structures, but cases of this kind, with data of the design and loading sufficient to be of value in the study of the factor of safety, have not been found in the preparation of this paper.

25. SHEARING STRESSES. In Table XIII the maximum shearing stresses on a vertical section at a distance d, from the edge of the column capital for the tests summarized in that table are given. Those shearing stresses were computed on the basis of a depth jd. The highest shearing stress developed was in the case of the Western Newspaper Union Building. The report† does not indicate that the test developed any weakness in shear. In order to develop a factor of safety as high in shear as the estimated factor of safety in bending based upon the total moment, $0.1067\ Wl\left(1-\frac{2}{3}\frac{c}{l}\right)^2$, the shearing stress in the section under question could have been at least 87 lb. per sq. in. at the design load. Using the factor of safety in bending for the total moment of $0.09\ Wl\left(1-\frac{2}{3}\frac{c}{l}\right)^2$ the shearing stress for the design load could have been at least 102 lb. per sq. in. There were some indications that the failure of slab J may have been due to shear.

---

* Edward Godfrey, "An open letter to W. A. Slater," Concrete, February, 1921.
† Univ. of Ill. Eng. Exp. Sta. Bulletin 106.

The allowable shearing stresses at the design load which would give the same factors of safety as those shown for the moments would have been 49 lb. per sq. in. and 58 lb. per sq. in. respectively.

The shearing stresses are not given for the Jersey City Dairy building nor for the International Hall. This is because the loads reported in this table were not such as to give uniform shear around the perimeter of the column capital, and it is not known what the maximum shear was.

VI.—SUMMARY.

The theoretical analysis deals with slabs of homogeneous perfectly elastic material and of uniform thickness. Two types are considered in particular: slabs supported on four sides and flat slabs supported on columns with round capitals. Moment coefficients derived by principles of equilibrium and continuity are shown in the diagrams and tables.

The close agreement between the moment coefficients, determined by several investigators, in slabs supported on four sides, is an indication that dependable methods are now available by which homogeneous elastic slabs may be analyzed.

In the analysis of flat slabs the moment sections used in the Joint Committee report of 1916 were found suitable for the purpose of stating the resultant moments. In a square interior panel of a uniformly loaded floor slab, with a large number of panels in all directions, the percentages of the total moment (or sum of positive and negative moments) which are resisted in the column-head sections, mid-section, outer sections, and inner section are found to be nearly independent of the size of the column capital.

A study is made of unbalanced loads, for example, loads in rows; unbalanced loads are found to produce large moments in the slabs if the columns are slender, and large moments in the columns if the columns are rigid. Moment coefficients are stated also for various cases of oblong panels, wall panels, and corner panels.

The tests of slabs supported on four sides indicate that when the deformations increase, certain redistributions of moments and stresses take place, with the result, in general, that the larger coefficients of moments are reduced. The ultimate load is found to be, in general, larger, and in some cases much larger, than would be estimated on the basis of the theoretical moment coefficients and the known strength of beams with the same ratio of steel.

When the moments of resistance of the observed stresses in the reinforcement in flat slabs were multiplied by the ratio of the applied moment in simple beams to the resisting moment of the observed stress, corrected moments for the slabs were obtained which, in comparison with the results of the analysis of flat slabs presented in Part II, were (a) much greater for the lower loads than for the higher loads, (b) greater for the lower loads than the theoretical moments and (c) slightly less for the higher loads than the theoretical moments.

If the effect of the difference in the modulus of elasticity for the slabs from that for the beams on which the comparison is based could be eliminated it seems that the agreement between the analysis and the tests would be fair. Such information as is available on the effect of the modulus of elasticity on the results points in the direction stated.

The average value of the estimated factor of safety for the slabs studied was 3.23 for the working loads based upon the moment coefficients recommended by the Joint Committee on Concrete and Reinforced Concrete and 2.72 for the working loads based on the coefficients recommended by the American Concrete Institute.

APPENDIX A.

DETAILS OF THE ANALYSIS OF HOMOGENEOUS PLATES.

BY H. M. WESTERGAARD.

A1. *Notes referring to Art. 7. Solutions of the Differential Equation of Flexure for Slabs Supported on Four Sides.* (a) *Rectangular slabs with simply supported edges.**

The analysis of the rectangular slab with simply supported edges is simplified by assuming certain special values of the dimensions, of the elastic constants, and of the load: namely,

$a = \pi$ = long span, in the direction of x;

$b = \propto \pi = \dfrac{\pi}{\beta}$ = short span, in the direction of y;

$w = \dfrac{\beta^2}{\pi^2}$ = load per unit-area;

$EI = 1$; Poisson's ratio $K = 0$.

The origin of the coördinates x, y is at the center of the slab.

With these special values, one finds $wb^2 = 1$; that is, the moments become equal to the coefficients of moment, $\dfrac{M}{wb^2}$. Since $EI = 1$ and $K = 0$, the moments or coefficients of moment become numerically equal to the curvatures. The expediency of analyzing with a Poisson's ratio equal to zero was discussed in Articles 6 and 8, where also methods of modifying the results when Poisson's ratio has some other value were indicated. (See equations (15) to (18) in Art. 6 and Fig. 10(b)).

In order to solve Lagrange's equation of flexure ((11), (12), or (19) in Art. 6),

$$\Delta\Delta Z = \frac{(1-K^2)w}{EI} = w = \frac{\beta^2}{\pi^2} \qquad (46)$$

where

$$\Delta\Delta = \frac{\delta^4}{\delta x^4} + 2\frac{\delta^4}{\delta x^2 \delta y^2} + \frac{\delta^4}{\delta y^4}$$

---

* Navier's solution is used here (see, for example, A. E. H. Love, Mathematical Theory of Elasticity, ed. 1906, p. 468). Lévy's solution (Love, p. 469) was used by Nádai in dealing with the same problem (see the historical summary in Art. 4, footnote 36).

the term $\frac{\beta^2}{\pi^2}$ is expressed by a double-infinite Fourier series, as follows:

$$\frac{\beta^2}{\pi^2} = \frac{16\beta^2}{\pi^4} \sum_{1,3\cdots}^{m} \sum_{1,3\cdots}^{n} \frac{-(-1)^{\frac{m+n}{2}}}{mn} \cos mx \cos \beta ny$$
$$(m, n = 1, 3, 5, 7 \cdots\cdots) \qquad (47)$$

This expression applies at all points of the slab except at the edges. If the load w had consisted of only one of the terms in (47), the solution of Lagrange's equation would be: z equal to a similar term, which is equal to a constant times the load at the particular point. With w equal to the complete series (47), the solution of (46) becomes:

$$z = \frac{16\beta^2}{\pi^4} \sum_{1,3\cdots}^{m} \sum_{1,3\cdots}^{n} \frac{-(-1)^{\frac{m+n}{2}}}{mn(m^2+\beta^2n^2)^2} \cos mx \cos \beta ny \qquad (48)$$

This solution satisfies equation (46), as may be verified by substitution, and it satisfies also the boundary conditions, that at the edges $z = 0$, $\frac{\delta^2 z}{\delta x^2} = 0$, and $\frac{\delta^2 z}{\delta y^2} = 0$. The deflections, therefore, are expressed correctly by equation (48).

By double differentiations of (48), one finds the bending moments (according to (20) in Art. 6) to be:

$$M_x = -\frac{\delta^2 z}{\delta x^2} = \frac{16\beta^2}{\pi^4} \sum_{1,3\cdots}^{m} \sum_{1,3\cdots}^{n} \frac{-(-1)^{\frac{m+n}{2}} m}{n(m^2+\beta^2n^2)^2} \cos mx \cos \beta ny \qquad (49)$$

and

$$M_y = -\frac{\delta^2 z}{\delta y^2} = \frac{16\beta^4}{\pi^4} \sum_{1,3\cdots}^{m} \sum_{1,3\cdots}^{n} \frac{-(-1)^{\frac{m+n}{2}} n}{m(m^2+\beta^2n^2)^2} \cos mx \cos \beta ny, \qquad (50)$$

and the torsional moment (according to (21) in Art. 6) to be

$$M_z = -\frac{\delta^2 z}{\delta x \delta y} = \frac{16\beta^3}{\pi^4} \sum_{1,3\cdots}^{m} \sum_{1,3\cdots}^{n} \frac{(-1)^{\frac{m+n}{2}}}{(m^2+\beta^2n^2)^2} \sin mx \sin \beta ny \qquad (51)$$

The moment coefficient at the center of a square slab is found by substituting $x = y = 0$ and $\beta = 1$ in (49) or (50), and it is

$$M_c = \frac{16}{\pi^4} \sum_{1,3\cdots}^{m} \sum_{1,3\cdots}^{n} \frac{-(-1)^{\frac{m+n}{2}} m}{n(m^2+n^2)^2}$$
$$= \frac{16}{\pi^4}\left[\frac{1}{1(1+1)^2} - \left(\frac{3}{1(9+1)^2} + \frac{1}{3(1+9)^2}\right) + \left(\frac{5}{1(25+1)^2} + \frac{3}{3(9+9)^2} + \frac{1}{5(1+25)^2}\right)\right.$$
$$\left. - \left(\frac{7}{1(49+1)^2} + \frac{5}{3(25+9)^2} + \frac{3}{5(9+25)^2} + \frac{1}{7(1+49)^2}\right) + \cdots\cdots\right]$$
$$= \frac{16}{\pi^4} \cdot 0.2245 = 0.0369, \qquad (52)$$

as shown on the diagram in Fig. 3(a). This calculation is typical; other coefficients shown in Fig. 3(a) were computed in the same way. It may be noted that in (52) the terms of the double-infinite series are arranged in

groups with $m+n=2,\ 4,\ 6,\ 8,\ 10\ldots\ldots$, respectively, and thus the double-infinite series is transformed into a single-infinite series.

The moment M_{diag} across the diagonal at the corner in a square slab is numerically equal to the torsional moment M_z at the point, defined by (51); that is,

$$M_{diag}=\frac{16}{\pi^4}\sum_{1,3\ldots}^{m}\sum_{1,3\ldots}^{n}\frac{1}{(m^2+n^2)^2}=\frac{16}{\pi^4}\cdot 0.282=0.0463. \tag{53}$$

The moment M_{diag} at the corner of a rectangular slab across a line making angles of 45 degrees with the sides, is determined by an expression similar to (53), but containing the ratio β of the long span to short span. In the limiting case in which $\beta=\infty$ (or, $\alpha=0$), this expression may be reduced to the form,

$$M_{diag}=\frac{2}{\pi^3}\sum_{1,3,5\ldots}^{n}\frac{1}{n^3}=0.0678, \tag{54}$$

which is the value shown at the left-hand edge in Fig. 3(a).

(b) *Infinitely long strip*, extending from $x=0$ to $x=\infty$ between the simply supported edges $y=\pm\frac{\pi}{2}$; fixed edge along the y-axis. This slab is a special rectangular slab with the spans $a=\infty$, $b=\pi$. Load $w=\frac{\pi}{4}$; $wb^2=\frac{\pi^3}{4}$. $K=0$; $EI=1$.

The solution of Lagrange's equation,

$$\Delta\Delta\, z=\frac{\pi}{4},$$

is written in the form

$$z=z_1+z_2$$

where z_1 is the deflection at the point (x,y) when the support at the y-axis is removed, so as to make the edge deflect freely. The remainder z_2 is the amount which is added when external forces applied at the free edge at the y-axis make the deflections and the slopes at this line again equal to zero. z_1 is the deflection of a simple beam with a span equal to π, and may be expressed as a polynomial in y, but may also be expressed by the Fourier series

$$z_1=\cos y-\frac{1}{3^5}\cos 3y+\frac{1}{5^5}\cos 5y-\frac{1}{7^5}\cos 7y+\ldots\ldots,$$

as may be verified by comparison with the expression for the load

$$w=\frac{\pi}{4}=\cos y-\frac{1}{3}\cos 3y+\frac{1}{5}\cos 5y-\frac{1}{7}\cos 7y+\ldots\ldots$$

The deflection z_2 must satisfy the following conditions: at all points, $\Delta\Delta\, z_2=0$; at the short edge, $z_2=z_1$ and $\frac{\delta z}{\delta x}=0$; at the long edges, $z_2=0$ and $\frac{\delta^2 z}{\delta x^2}=0$. These conditions are satisfied by

$$z_2=\sum_{1,3\ldots}^{m}(1+mx)e^{-mx}\frac{(-1)^{\frac{m+1}{2}}}{m^5}\cos my$$

Since $\frac{\delta^2 z_1}{\delta x^2} = 0$, the bending moment along the x-axis becomes

$$M_{ax} = -\frac{\delta^2 z_2}{\delta x^2}\Big|_{y=0} = \sum_{1,3,5..}^{m} \frac{(-1)^{\frac{m+1}{2}}}{m^3}(1-mx)e^{-mx} \tag{55}$$

When $x = 0$, this moment becomes $M_{ae} = \sum_{1,3..}^{m} \frac{+1}{m^3} = -\frac{\pi^3}{32}$. Since $wb^2 = \frac{\pi^3}{4}$, the corresponding moment coefficient becomes $\frac{M_{ae}}{wb^2} = -\frac{1}{8}$, as shown at left-hand edge in Fig. 6 (a). The series (55) converges rapidly. Values of M_{ax} were computed for $x = 0.5$, 1.0, 2.0, 3.0, and 4.0; the greatest positive value, 0.1339, which was found with $x = 2.0$, gives the coefficient $\frac{M_{ae}}{wb^2} = 0.0173$, as shown at the left-hand edge in Fig. 5 (a).

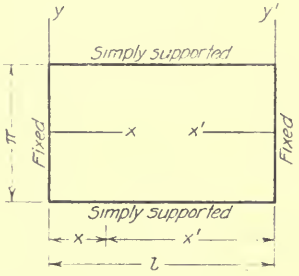

FIG. A1.—RECTANGULAR SLAB.

(c) *The rectangular slab shown in Fig. A 1.* Two parallel edges are fixed and two parallel edges simply supported Simple span $= \pi$; fixed span $= l$. Load $w = \frac{\pi}{4}$; when $l > \pi$, then $wb^2 = \frac{\pi^3}{4}$; when $l < \pi$, then $wb^2 = \frac{\pi}{4} l^2$; $EI = 1$; $K = 0$.

The solution given here is essentially Lévy's solution.* The procedure is essentially the same as in the preceding case, (b), which is the special case in which $l = \infty$.

Lagrange's equation

$$\Delta\Delta z = \frac{\pi}{4} \tag{56}$$

is solved by

$$z = z_1 + z_2 \tag{57}$$

where, as in case (b), z_1 is the simple-beam deflection, obtained when the

* See the historical summary, Art. 4, footnote 13, or A. E. H. Love, Mathematical Theory of Elasticity, Ed. 1906, p. 469.

edges y and y' are removed. z_1 may be expressed either by a polynomial in y or by the Fourier series

$$z_1 = \cos y - \frac{1}{3^5}\cos 3y + \frac{1}{5^5}\cos 5y - \ldots\ldots \tag{58}$$

The remaining part z_2 of the deflection must satisfy the following conditions:

$$\Delta\Delta z_2 = 0 \qquad \text{at all points;} \tag{59}$$

$$z_2 = 0, \frac{\delta z_2}{\delta y^2} = 0 \quad \text{at the simply supported edges;} \tag{60}$$

$$\frac{\delta z_2}{\delta x} = 0, \frac{\delta z_2}{\delta x^1} = 0 \text{ at the fixed edges;} \tag{61}$$

$$z_1 = -z_1 \qquad \text{at the fixed edges.} \tag{62}$$

The conditions (59) and (60) may be satisfied, as may be verified by differentiation, by an expression of the form

$$z_2 = \sum_{1,3\ldots}^{m} \frac{(-1)^{\frac{m+1}{2}}}{m^3} S_m \cos my \tag{63}$$

where

$$S_m = K_m \left[\left(e^{-mx} + e^{-mx'}\right) + mk_m\left(xe^{-mx} + x'e^{-mx'}\right)\right] \tag{64}$$

in which K_m and k_m are constants. This solution will satisfy the condition (61) when

$$k_m = \frac{1 - e^{ml}}{1 + (ml - 1)e^{-ml}}, \tag{65}$$

and it will satisfy the condition (62) when

$$K_m = \frac{1}{1 + (1 + mk_m l)e^{-ml}} \tag{66}$$

The deflections, then, are defined completely by equations (57) (58), and (63) to (66).

The bending moments in the x- and y- directions may be found by double differentiations of (57), (58), and (63). One finds

$$\begin{aligned} M_x &= -\frac{\delta^2 z}{\delta x^2} = -\frac{\delta^2 z_2}{\delta x^2} = \sum_{1,3\ldots}^{m} \frac{(-1)^{\frac{m-1}{2}}}{m^3} \frac{\delta^2 S_m}{\delta x^2} \cos my \\ &= \sum_{1,3\ldots}^{m} \frac{(-1)^{\frac{m-1}{2}}}{m^3}\left[S_m - 2k_m K_m\left(e^{-mx} + e^{-mx'}\right)\right]\cos my \\ &= \sum_{1,3\ldots}^{m} \frac{(-1)^{\frac{m-1}{2}}}{m^3} K_m\left[e^{-mx}\left(1 - 2k_m + mk_m x\right) + e^{-mx'}\left(1 - 2k_m + mk_m x'\right)\right]\cos my \end{aligned} \tag{67}$$

and

$$M_y = -\frac{\delta^2 z}{\delta y^2} = -\frac{\delta^2 z_1}{\delta y^2} - \frac{\delta^2 z_2}{\delta y^2} = \frac{\pi}{6}\left(\frac{\pi^2}{4} - y^2\right) - \sum_{1,3\ldots}^{m} \frac{(-1)^{\frac{m-1}{2}}}{m^3} S_m \cos my \tag{68}$$

The series (67) and (68) converge rapidly. When these series are used in connection with formulas (64) to (66) they are suitable for numerical

computations, and they were used in determining the points shown by small circles in Fig. 4(a), Fig. 5(a), and Fig. 6(a).

With $y = 0$ and $l = \infty$, formula (67) becomes the same as (55).

(d) *Slabs with four fixed edges.*

The approximate moment coefficients for square slabs, represented in Fig. 7 and Fig. 8 by points marked with circles, were determined by approximate expressions which contain trigonometric and exponential functions of x and y; they are somewhat similar in form to those applied in the preceding cases. Neither Navier's nor Lévy's solution applies directly to the slab with four fixed edges. Ritz's method, which was used, for example, by Nádai and Paschoud in analyscs of fixed slabs, is found to lead to suitable solutions of the problem.*

A2. *Theory of Ring Loads, Concentrated Couples, and Ring Couples.* Certain concentrated loads, each consisting of a group of forces within a small area, were introduced in Articles 8 and 9, where procedures of analyses of flat slabs were outlined, and where the results of these analyses were presented. The loads introduced are: the ring loads, which were defined in Art. 8, and which are used in the analysis of the normal square interior panel of a uniformly loaded flat slab; and the concentrated couples and ring couples, which were defined in Art. 9, and which are used in the study of unbalanced loads.

By the use of the concentrated loads in the analysis of flat slabs a procedure is followed which has general applicability, and which was used in one form in the preceding article (in cases (b) and (c)):

Lagrange's equation,

$$\Delta\Delta z = \frac{1 - K^2}{EI} w, \tag{12}$$

is solved, for the given loads and boundary conditions, by expressing the deflection in the form

$$z = z_0 + \Sigma z_m \tag{69}$$

where z_0 satisfies (12), without necessarily satisfying the boundary conditions, while each function z_m satisfies the equation

$$\Delta\Delta\, z_m = 0, \tag{70}$$

which is Lagrange's equation for $w = 0$.

The deflection z_0 in (69) may be, for example, the deflection of the point-supported slab under the load w. Then, z_m may be the deflection due to one of the concentrated loads, acting alone on the slab at a point of support, with the surrounding supports removed. By introducing one such concentrated load at each point of support or panel corner, and by adding the deflections due to all of the loads, one forms the series (69), which may be an infinite series, by differentiation of which one may obtain corresponding series for the moments. The concentrated loads must be so selected that all of the loads, including the applied load w, will cause the

* See the historical summary, Art. 4, footnotes 26, 34, and 36.

point-supported slab to deflect, outside the circles marked by the edges of the column capitals, exactly as the slab deflects which is supported on column capitals and loaded by w.

In the theory of the concentrated loads, now to be presented, it is assumed at first that only one concentrated load acts on the slab. Then, groups of loads are considered. The slab is assumed to extend indefinitely in all directions. Furthermore, let:

K = Poisson's ratio = 0, as before;

$r = \sqrt{x^2 + y^2}$ = radius vector measured from the origin of the coordinates.

(a) *Ring loads.*

Lagrange's equation

$$\Delta\Delta z = 0, \tag{71}$$

for the case in which $w = 0$, is satisfied at all points, except at the origin, by

$$z = C \, l \, r + c', \tag{72}$$

where C and c' are constants. The deflected surface, according to this equation, is a surface of revolution about an axis through the origin. A load, concentrated at the origin, and producing the state of flexure defined by (72), may be called, by definition, a ring load. The intensity of this ring load is measured conveniently by CEI, where EI is the usual stiffness factor of the slab. Since C is a distance, the ring load CEI may be measured in lb. in.^{2} units. One finds by differentiation of (72):

$$\frac{\delta z}{\delta x} = \frac{Cx}{r^2}, \quad \frac{\delta z}{\delta y} = \frac{Cy}{r^2}, \tag{73}$$

$$\frac{\delta^2 z}{\delta x^2} = \frac{C(y^2 - x^2)}{r^4}, \quad \frac{\delta^2 z}{\delta y^2} = \frac{C(x^2 - y^2)}{r^4}, \quad \frac{\delta^2 z}{\delta x \delta y} = -\frac{2Cxy}{r^4}, \tag{74}$$

that is

$$\text{that is } \frac{\delta^2 z}{\delta x^2} + \frac{\delta^2 z}{\delta y^2} = \Delta z = 0 \qquad \text{and} \quad \Delta\Delta z = 0 .$$

According to formulas (22) in Art. 6, the vertical shears are proportional to the derivatives of Δz; that is, the vertical shears are zero at all points except the origin. The moments in the directions of x and y are defined by the second derivatives in (74). The moment in the direction of radius vector, or the radial moment, is

$$M_r = -EI \frac{\delta^2 z}{\delta r^2} = \frac{CEI}{r^2} . \tag{75}$$

In a circular section with center at the origin and with radius r, there is, then, a uniformly distributed radial moment, defined by (75), but no torsional moment and no vertical shear. In the light of the state of flexure in the circular section with center at the origin and radius r_1, one may explain the nature of the ring load. Assume that the material is removed within the circle with radius r_1, and that a radial moment, determined by (75) is applied as an external load, uniformly distributed over the circumference of the circle. Then the slab, under the influence of this load alone,

will deflect according to formula (72), because thereby it satisfies all the boundary conditions. Now assume that the circle with radius r_1 is not cut out, but that instead some load within the circle produces at the circumference of the circle the state of flexure that was assumed before as a result of the external loads. On account of the identity of conditions at the circumference of the circle, the state of flexure outside the circle will remain unchanged, as determined by equation (72). More than one kind of load within the circle may produce this same effect: the load may consist of upward and downward loads $\pm P$, uniformly distributed over the circumferences or areas of two concentric circles; or it may consist of an upward load P at the origin combined with a down load P which is uniformly distributed over the area or the circumference of a circle with center at the origin and radius not larger than r_1. But whether the load is made up in one way or another, if the radius r_1 is small, the load may be considered as one concentrated load; namely, the ring load whose magnitude is measured by CEI, and whose effects are defined completely by equation (72).

It may be noted that, according to equation (72), the deflection at the origin is infinite. Since the origin lies always within the smallest circle containing the whole load, the infinite deflection at the center has only theoretical significance. When the ring load is applied at a point of support, then, in order to avoid the assumption of any infinite deflections, one may conceive of the support as being distributed over the circumference of a small circle whose center is at the original point of support and at a fixed elevation.

The expressions (74) are well suited for computations of such series as may be formed when a large number of ring loads are applied at the same time.

(b) *Concentrated couples.*

Lagrange's equation ((71))

$$\Delta\Delta z = 0$$

for $w = 0$ is satisfied at all points except at the origin by the solution

$$z = A\, x\, l\, .\, r + ax, \tag{76}$$

where A and a are constants. By differentiation one finds:

$$\frac{\delta z}{\delta x} = A\left(l r + \frac{x^2}{r^2}\right) + a \quad , \quad \frac{\delta z}{\delta y} = A\frac{xy}{r^2}\,; \tag{77}$$

$$\frac{\delta^2 z}{\delta x^2} = A\frac{x}{r^2}\left(l + \frac{2y^2}{r^2}\right) \quad , \quad \frac{\delta^2 z}{\delta y^2} = A\frac{x}{r^2}\left(l - \frac{2y^2}{r^2}\right), \quad \frac{\delta^2 z}{\delta x \delta y} = A\frac{y}{r^2}\left(l - \frac{2x^2}{r^2}\right), \tag{78}$$

$$\Delta z = A\frac{2x}{r^2} \quad , \tag{79}$$

this value of Δz is proportional to the value of $\frac{\delta z}{\delta x}$ in the preceding case, **(a)**, which gave $\Delta z = 0$; it follows, therefore, in the present case, that $\Delta\Delta z = 0$.

In the state of flexure just represented the y-axis remains undeflected. A circle drawn on the slab, with center at the origin of coördinates, remains

plane, but rotates about the y-axis, through some angle. On account of the anti-symmetry with respect to the y-axis, the resultant of the stresses in the cylindrical section $r = r_1$ is a couple about the y-axis. Now r_1 may be given any small value, that is, the couple must be transferred to the slab at the origin as a concentrated couple.

The magnitude of the concentrated couple may be found by considering the stresses in two sections parallel to the y-axis, on opposite sides of the origin. By formulas (22), in Art. 6, one finds the vertical shear per unit-width in a section parallel to the y-axis to be

$$V_x = -EI\,\frac{\delta \Delta z}{\delta x} = 2AEI\,\frac{x^2 - y^2}{r^4}$$

The total vertical shear in this section becomes, then,

$$\int_{-\infty}^{+\infty} V_x\,dy = 2AEI \int_{-\frac{\pi}{2}}^{+\frac{\pi}{2}} \frac{\cos^2\theta - \sin^2\theta}{\times}\,d\theta = 0$$

The total bending moment in a section parallel to the y-axis, with x positive, is equal to

$$\int_{-\infty}^{+\infty} M_x\,dy = -AEI \int_{-\infty}^{+\infty} \frac{x}{r^2}\left(1 + \frac{2y^2}{r^2}\right)dy = -AEI \int_{-\frac{\pi}{2}}^{+\frac{\pi}{2}} (1 + 2\sin^2\theta)\,d\theta$$
$$= -2\pi AEI$$

while a negative x gives $+2\pi AEI$. The resultant of the stresses in the two sections $\pm x$ is then equal to the concentrated couple $= 4\pi AEI$ (80), turning, when A is positive, in the direction from z to x.

A number of concentrated couples may be dealt with by computing series of the terms contained in equations (77) and (78).

(c) *Ring couples.*

The deflection due to two equal and opposite ring loads, close to the origin and to one another, and with centers on the x-axis, may be expressed as equal to a constant times the first partial derivative, with respect to x, of the deflection which is due to a single ring load, and is expressed by equation (72). This derivative was given in equation (73). Thus, when B is a constant, the function

$$z = \frac{Bz}{r^2}, \tag{81}$$

is the deflection due to a ring couple which is applied at the origin in the direction of x, and is measured in intensity by the quantity BEI. One finds by differentiation of (81):

$$\frac{\delta z}{\delta x} = \frac{B(y^2 - x^2)}{r^4}, \qquad \frac{\delta z}{\delta y} = -\frac{2Bxy}{r^4}, \tag{82}$$

$$\frac{\delta^2 z}{\delta x^2} = -\frac{\delta^2 z}{\delta y^2} = \frac{2Bx}{r^4}\left(1 - \frac{4y^2}{r^2}\right), \tag{83}$$

and

$$\Delta z = \Delta\Delta z = 0$$

(d) *Other types of concentrated loads.*

If the function $z = F(x,y)$ satisfies Lagrange's equation $\Delta\Delta\, z = 0$ at all points except at the origin, which is a singular point, then also the function

$$z = \frac{\delta^{m+n} F}{\delta x^m\, \delta y^n} \tag{84}$$

will satisfy the equation $\Delta\Delta z = 0$ at all points except at the origin; and z, like the original function F, will define some concentrated load at the origin. Other solutions may be formed by integration of F. Thus from the fundamental solutions (72) and (76), for ring loads and concentrated couples, and from the solution

$$z = D_1 \int r\, l.\, r\, dr + D_2 r^2, \tag{85}$$

which defines a single concentrated force proportional to D_1, at the origin, one may derive an infinite number of solutions, each defining a correspond-

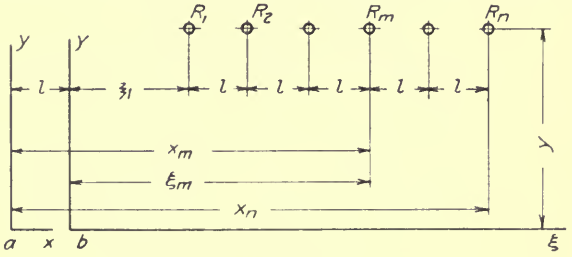

FIG. A2.—RING LOADS IN A ROW.

ing concentrated load. It is an example of this procedure, that the deflections due to the ring couple were derived by differentiation of the expression for the deflections due to the ring load.

(e) *The co-action of a number of ring loads.*

A number of equal ring loads, $R_1 \ldots\ldots R_n$, of intensity CEI, is assumed to act in a row parallel to the x-axis as shown in Fig. A2. The spacing is constant and equal to l. By using equations (73) and the relations $\xi_m = x_m + l$, one finds the change of slope between the two origins of coördinates, b and a at a distance of l, to be

$$S_b - S_a = C\Sigma\left(\frac{x_m}{x_m^2+y^2} - \frac{\xi_m}{\xi_m^2+y^2}\right) = C\left(\frac{x_n}{x_n^2+y^2} - \frac{\xi_1}{\xi_1^2+y^2}\right), \tag{86}$$

that is, the difference is expressed in terms of the coördinates of the first and the last load in the row.

In Fig. A3 ring loads of intensity CEI are applied at the points marked with small circles. The group of loads is symmetrical with respect to the lines $y = 0$, $x = \frac{1}{2}l$, and $x = \frac{1}{2}l \pm y$. According to (86) the change of slope between the points a and b may be expressed as follows, in terms of

the coördinates of the extreme loads in the first quadrant, that is, the loads on the line A:

$$s_b - s_a = 4C \sum_A \frac{x}{r^2}. \tag{87}$$

If the number of loads is very large, then the summation may be replaced by an integration. By making use of the axes of symmetry, one finds then

$$s_b - s_a = 4C \int_A \frac{x}{r^2} \cdot \frac{dy}{l} = \frac{2C}{l} \int_A \frac{x dy - y dx}{r^2} = \frac{2C}{l} \int_0^{\frac{\pi}{2}} \frac{r^2 d\theta}{r^2} = \frac{\pi C}{l} \tag{88}$$

This difference of slope may be reduced to zero if at the edge of the plate, which is assumed to be at infinity, a certain additional load is applied;

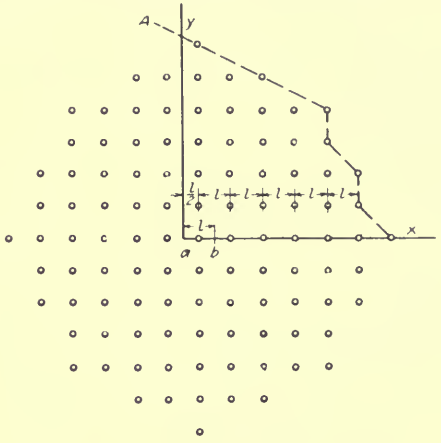

FIG. A3.—GROUP OF RING LOADS.

namely, a bending moment, uniformly distributed over the edge, producing a uniform bending moment in the slab in all directions, equal to

$$M_R = \frac{\pi CEI}{l^2} \tag{89}$$

With this additional moment present, small circles, drawn in the central portion of the slab, concentric with the ring loads, all with the same radius, will remain co-planar; and they will be contour lines of the deflected surface if one of them remains horizontal. On account of this relation to the ring loads the moment M_R is assumed, in the analysis of the uniformly loaded flat slab, to act with the group of ring loads.

(f) *The co-action of concentrated couples and ring couples.*

A concentrated couple $4\pi AEI$, and a ring couple BEI, whose effects are determined by equations (76) and (81), respectively, are assumed to act on the slab, at the origin, in the xz-plane. The circles r = const. remain plane under the influence of this combined load. The slope in the direction

of x varies, in general, from one point to another on the circle $r = \text{const.}$ The condition may be imposed, however, that all points of a certain circle, for example, the circle $r = \frac{c}{2}$ which marks the edge of a column capital, must have a common tangential plane. By comparing equations (77) and (82) one finds that all elements of the deflected surface at the circle $r = \frac{c}{2}$

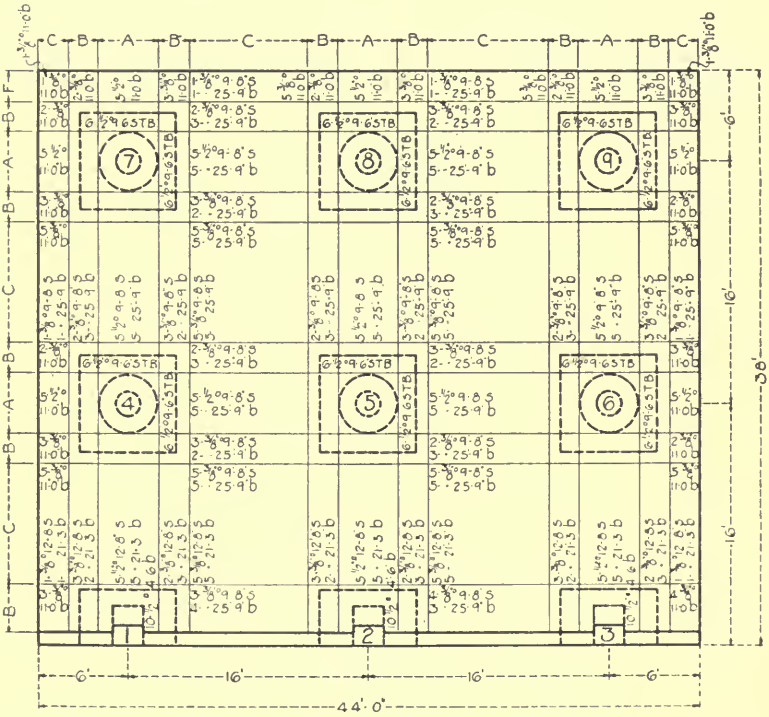

FIG. B1.—REINFORCING PLAN FOR SLAB J.

have a zero slope in the direction of y, and consequently have a common tangential plane, when

$$B = \frac{Ac^2}{8}. \tag{90}$$

Concentrated couples $\pm 4\pi AEI$ and ring couples $\pm BEI$ are used in the analysis of flat slabs with alternate rows of panels unloaded. The

rows considered are parallel to the y-axis. One concentrated load of each kind is assumed at each column center. The double signs, $\pm$, refer to alternate rows of columns. Because of the loads at the surrounding supports, equation (90) expresses in this case only approximately the condition that there is a common tangential plane at all points of the circle $r = \frac{c}{2}$. The following formula, which is a modified form of (90), and which is a close approximation, takes into consideration the concentrated

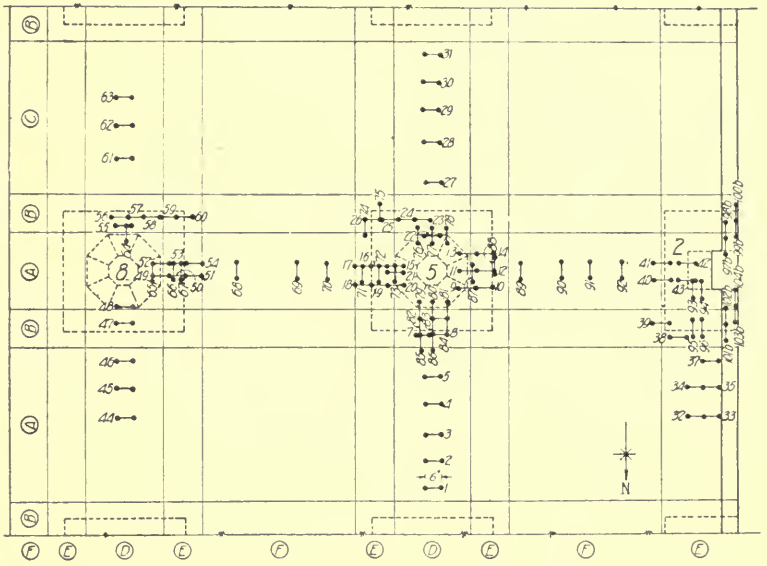

FIG. F2.—LOCATION OF GAGE LINES FOR TOP OF SLAB S.

loads at the nine points defined by the coördinates $y = -l$, 0, $+l$, and $x = \pm l$ (negative values of A and B) and $x = 0$ (positive A and B); this formula was derived by equating to one another the slopes in the direction of x at the points $\left(0, \frac{c}{2}\right)$ and $\left(\frac{c}{2}, 0\right)$:

$$B = \frac{Ac^2}{8}\left(1 + \left(\frac{c}{l}\right)^2\right) \qquad (91)$$

Formula (91) was used in computing values of B when alternate rows of flat slab panels are unloaded.

APPENDIX B.

TESTS OF SLABS AT PURDUE UNIVERSITY

By W. A. SLATER.

B1. *Description of Tests.* The tests referred to as the Purdue tests were made for the Corrugated Bar Co. under the direction of Prof. W. K.

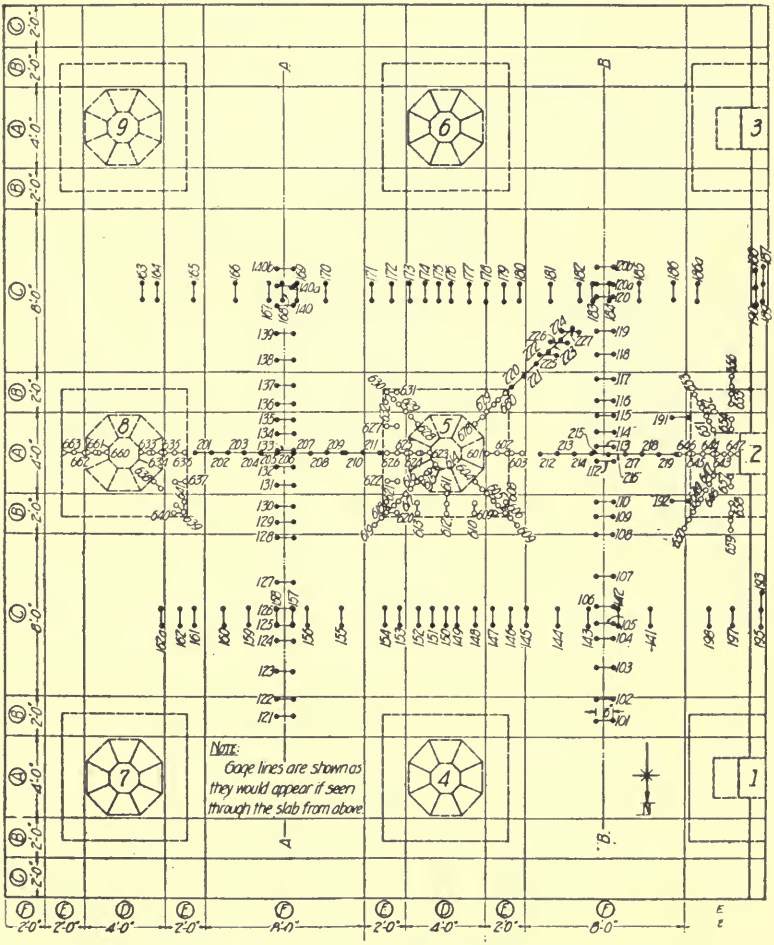

FIG. B3.—LOCATION OF GAGE LINES FOR BOTTOM OF SLAB J.

Hatt at Purdue University, Lafayette, Ind., on two test slabs, J and S, each of which had four panels 16 ft. square.

The dimensions of the concrete in the two slabs were the same, but the

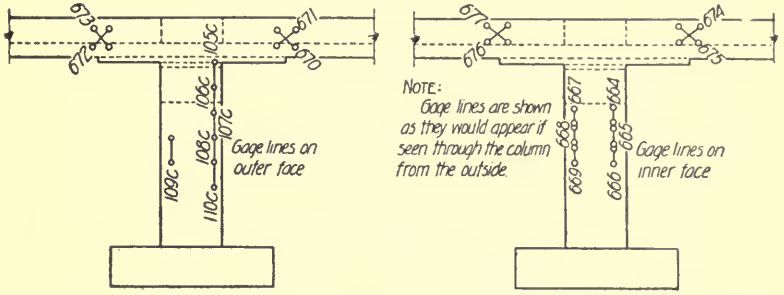

FIG. B4.—LOCATION OF GAGE LINES ON COLUMNS AND MARGINAL BEAMS OF SLAB J.

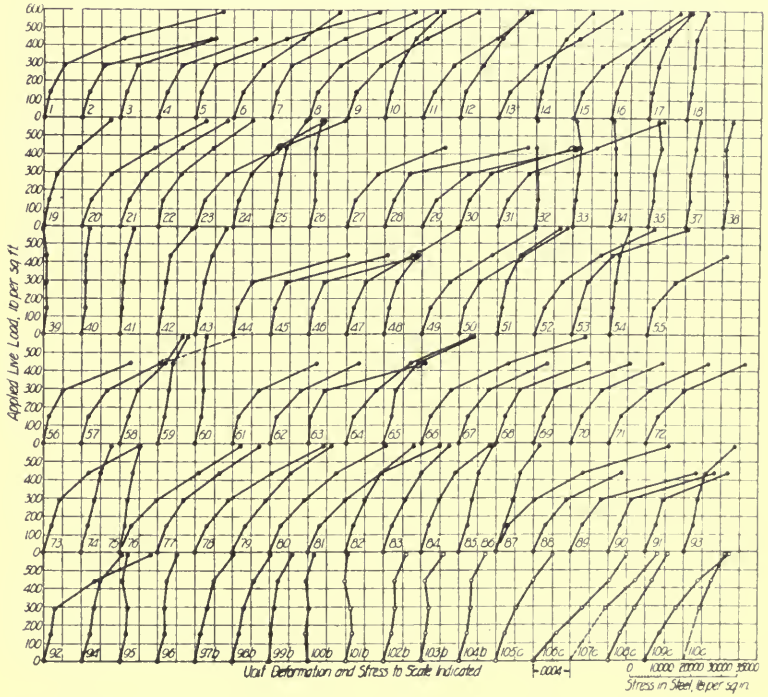

FIG. B5.—LOAD STRAIN AND LOAD-STRESS DIAGRAMS FOR TOP OF SLAB J.

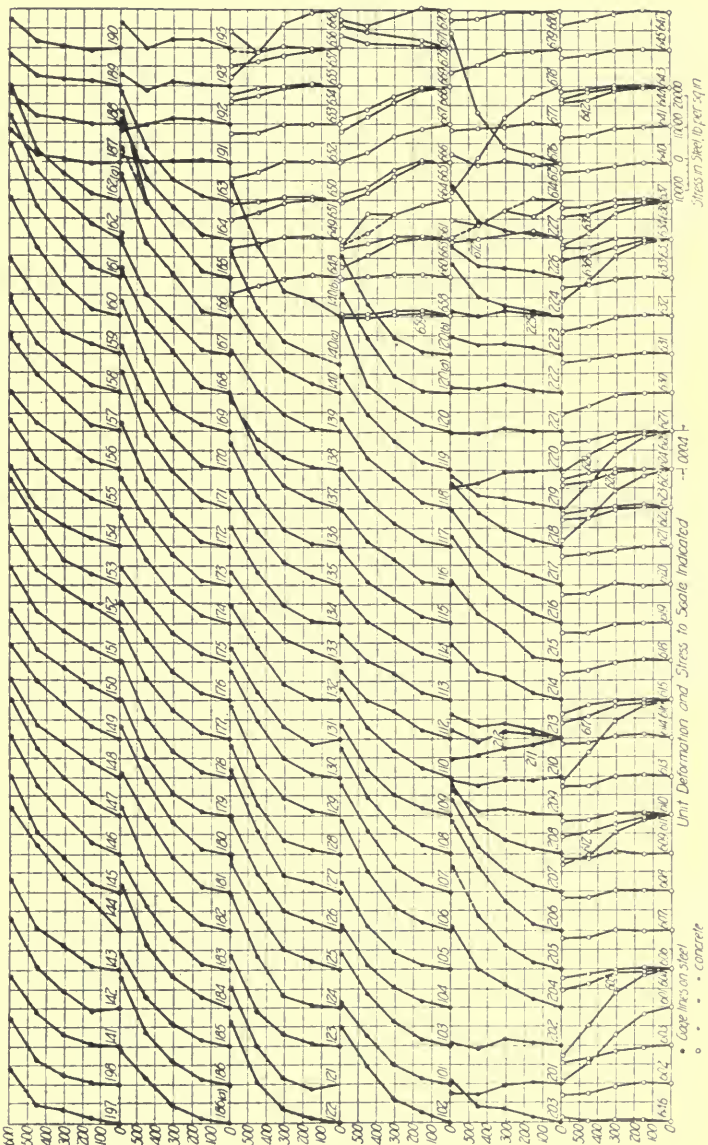
Applied Live Load - lb. per sq. ft.
Unit Deformation and Stress to Scale Indicated
Stress in Steel lb. per sq. in.
Edge lines on Steel
Edge lines on concrete

FIG. 136.—LOAD STRAIN AND LOAD-STRESS DIAGRAMS FOR BOTTOM OF SLAB J.

amount of reinforcement for slab S was considerably less than that for slab J. The latter fact will help to account for the smaller load which was carried by slab S than by slab J, but another important consideration is the fact that for slab S the average strength of the concrete control cylinders at 28 days was only 1215 lb. per sq. in. while the strength of the control cylinders for slab J was 2305 lb. per sq. in.

The methods of making the test are similar to those which have been described in reports of various tests on floors of buildings.*

The important dimensions of the slab are shown in Table XIII. The amount and distribution of the reinforcement are shown in Fig. B1 and B9.

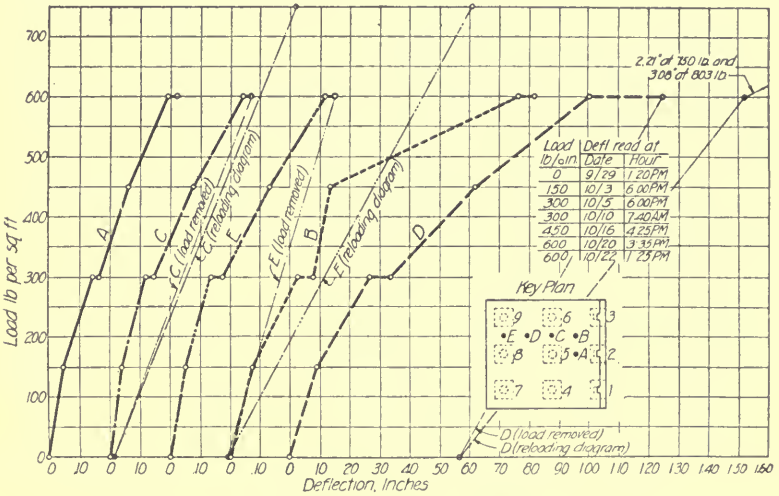
Load lb per sq ft
Deflection, Inches
2.21" at 150 lb. and 3.08" at 803 lb.
Load lb/sq in. | Defl read at Date | Hour
0 | 9/29 | 1.20 PM
150 | 10/3 | 6.00 PM
300 | 10/5 | 6.00 PM
300 | 10/10 | 7.40 AM
450 | 10/16 | 4.25 PM
600 | 10/20 | 9.35 PM
600 | 10/22 | 1.25 PM
Key Plan
A
B
C
D
E (load removed)
E (reloading diagram)
C (load removed)
C (reloading diagram)
D (load removed)
D (reloading diagram)

FIG. B7.—LOAD DEFLECTION DIAGRAMS FOR SLAB J.

The location of gage lines is shown in Fig. B2, B3, B4, B10, B11, and B12. The measured stresses in the reinforcement and deformation in the concrete are shown in Fig. B5, B6, B13 and B14. The deflections are shown in Fig. B7 and B8. Certain information concerning these tests has already been published† and reference to the published report will supply certain results of the test which are lacking in this paper.

In the tests of both slabs the load was applied as nearly uniformly as possible. In order to afford access to the gage lines on the top surface of the slabs, aisles were left in the loaded area. When the load was high enough these aisles were bridged over and sufficient load was placed immediately over them to give practically a uniform distribution of load.

---

* Univ. of Ill. Eng. Exper. Sta. Bulletins 64 and 84.

† W. K. Hatt, "Moment Coefficients for Flat-slab Design with Results of a Test," Proc. A. C. I. V. 14, p. 174 (1918).

B2. *Loading of Slab J.* In the test of slab J the highest load applied uniformly over the entire slab was 595 lb. per sq. ft. At this load the measured stress in the reinforcement was at the yield point in gage lines which crossed the mid-section of the slab (see Fig. 12 which shows location of sections), and the highest deflection reported for any panel was 1.1 in. After the load had been in place about two days longer the deflection had increased to 1.25 in. At this stage of the test it is reported that there was no evidence of crushing of the concrete. The entire load was removed from the slab and about 40 days later a load of 803 lb. per sq. ft. was applied "over one panel, the overhang, and into the adjoining panel, etc."* Failure occurred under this load by punching of the column* capital through the

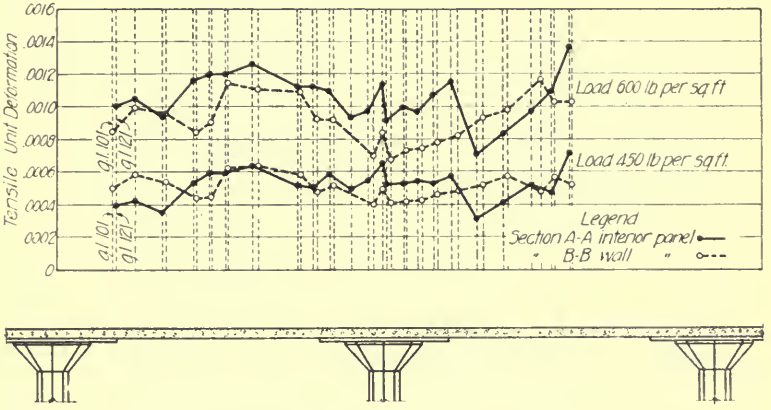

FIG. B8.—STRAIN DISTRIBUTION FOR REINFORCEMENT IN WALL PANEL AND INTERIOR PANEL OF SLAB J.

dropped panel. The fracture had the angle of a diagonal tension failure. Assuming the full live and dead load of an area 16 ft. square to have been carried on the central column, the computed shearing stress on the vertical section of depth *jd*, which lies at a distance *d* from the edge of the column capital, was 233 lb. per sq. in. Although the "failure of the slab . . . began with a feathering of the concrete on the dropped panel at the edge of the column capital"* this shearing stress is high enough that it seems that diagonal tension may have been a factor in causing failure.

B3. *Loading of Slab S.* The maximum load applied to slab S was 450 lb. per sq. ft. The official report of the test states that this load "was attended by complete failure of the concrete in compression and the stretching of the steel to the yield point."* The load-strain diagrams, Fig. B13 and B14, show that the reinforcement generally was highly stressed both at sections of negative moment and at sections of positive moment, and

* Proceedings A. C. I., Vol. XIV, pp. 182 and 183 (1918).

photographs of the slabs show the crushing of the concrete around the capital. However, the highest deflection reported was only 1.30 in. at the center of a panel, and when the load was removed the deflection decreased to 0.4 in. Relatively this deflection was small and the recovery was large and the test does not afford a conclusive answer to the question as to what load would have been required to cause collapse of the structure, or, in other words, as to what was the factor of safety against destruction of life and

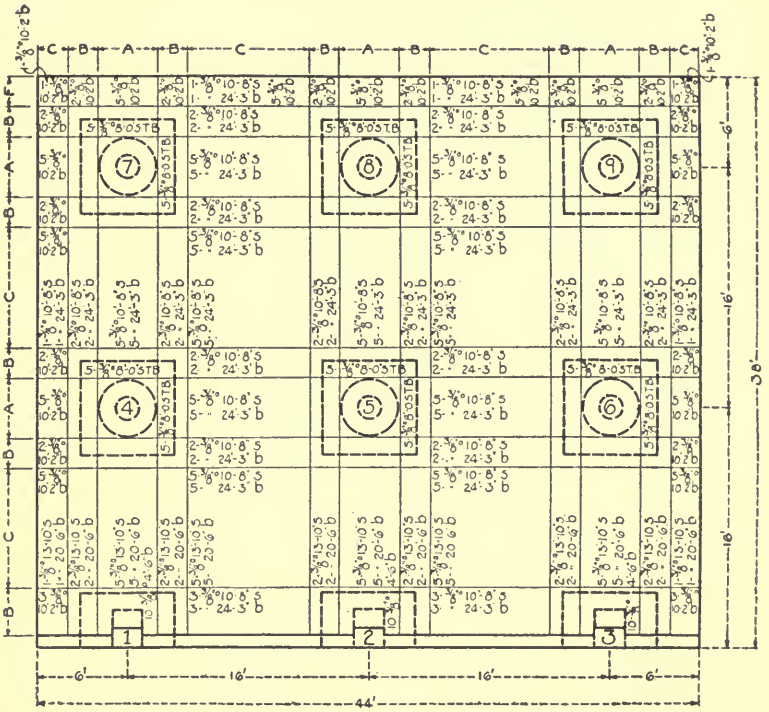

FIG. B9.—REINFORCING PLANS FOR SLAB S.

property. In view of the large load carried by the Waynesburg slab after the yield point of the negative reinforcement had been reached it does not seem unreasonable to believe that this slab might have carried more load without actual collapse.

B4. *Moments in Wall Panels.* In the design of slab J and slab S provision for greater positive moments in the wall panels than in the interior panels was made by using a larger area of reinforcement for the positive moment in the wall panels than in the interior panels. The same

number of bars was used at the two positions, but for the wall panels square bars were used and for the interior panels round bars were used. This gives 27 per cent more reinforcement for the wall panel than for the interior panel. Strains measured are shown in Fig. B8 and B16. For the lower loads the stresses were almost equal in the two panels of slab J, but were somewhat higher for the wall panel in slab S than for the interior panel. For the higher loads the stresses were higher for the interior panels in

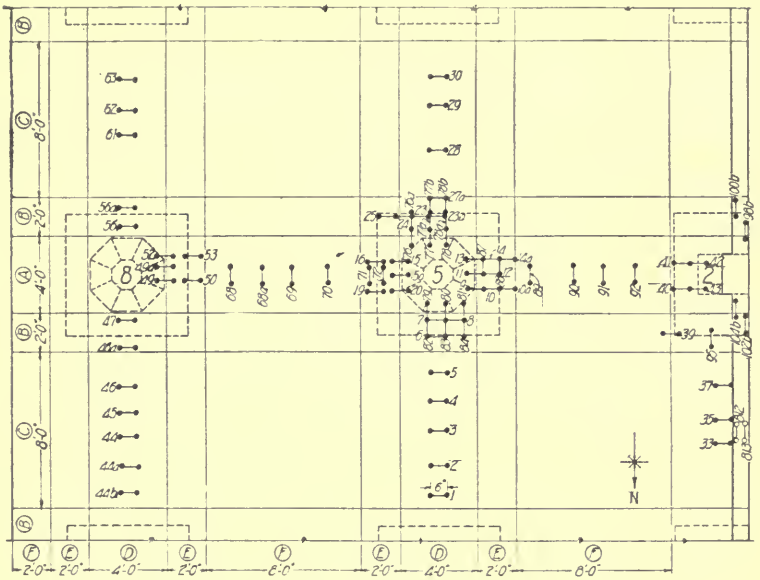

FIG. B10.—LOCATION OF GAGE LINES FOR TOP OF SLAB S.

both cases. The indication from this test is that the allowance of 27 per cent greater moment for wall panels than for interior panels was in excess of the requirement for wall panels. The moments in the wall panels will be dependent upon the moment of inertia of the wall columns and probably upon the manner in which the negative reinforcement at the edge of the wall panel is distributed, and for this reason the results in Fig. B8 and B16 should not be applied to other cases without taking into account the effect of these features of the design.

APPENDIX C.

BIBLIOGRAPHY.

References are made in the following list, to published results and to some unpublished results of tests on flat slabs or on slabs supported on beams which lie on the edges of the panels, but which have no intermediate beams.

In general the following sequence is used in references cited: Name or designation of structure tested, city, brief characterization of type of reinforcement, number of panels loaded, reference to periodicals by number in parentheses, date of publication.

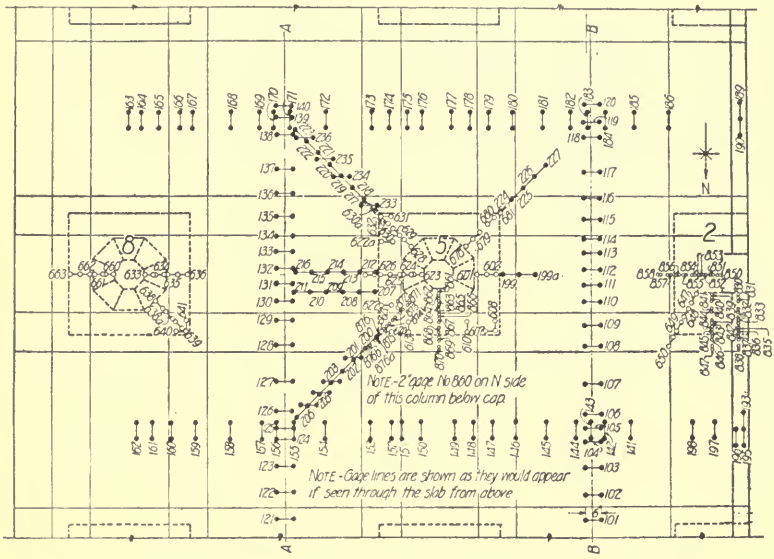
A
B
N
87
57
2
NOTE-2" gage No 860 on N side of this column below cap.
NOTE - Gage lines are shown as they would appear if seen through the slab from above.

FIG. B11.—LOCATION OF GAGE LINES FOR BOTTOM OF SLAB S.

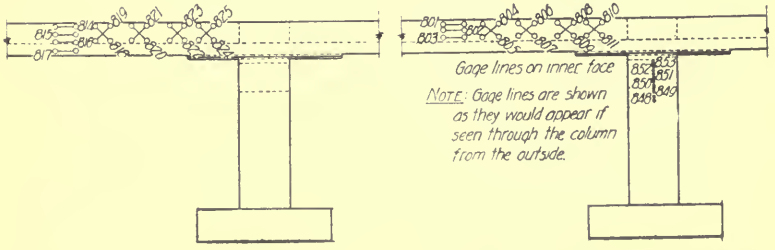

FIG. B12.—LOCATION OF GAGE LINES ON COLUMN Z AND MARGINAL BEAMS OF SLAB S.

The periodicals or institutions referred to in the bibliography are designated by the following numbers:

(1) Proceedings National Association of Cement Users and of its successor, the American Concrete Institute.

(2) University of Illinois, Engineering Experiment Station.

(3) Indiana Engineering Society.

(4) Proceedings Pacific Northwest Society of Civil Engineers.

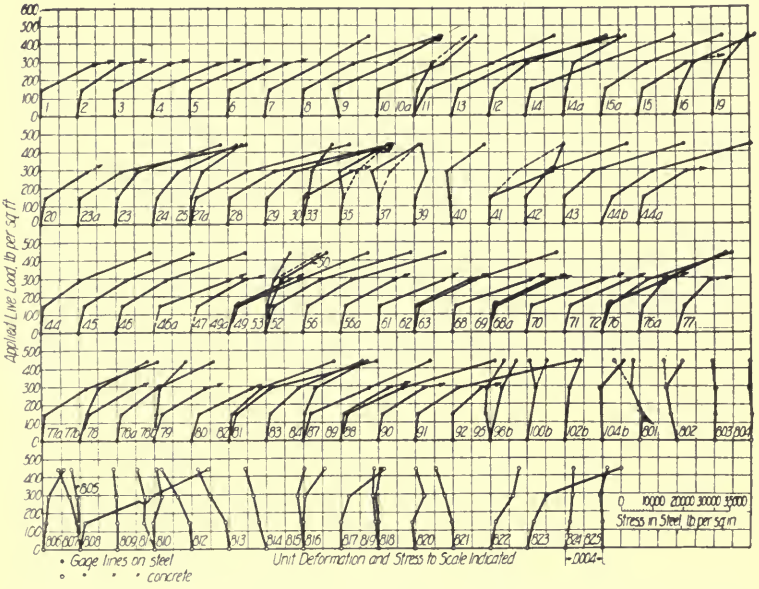
Applied Live Load, lb per sq ft
Gage lines on steel
concrete
Unit Deformation and Stress to Scale Indicated
Stress in Steel, lb per sq in
-.0004-

FIG. B13.—LOAD STRAIN AND LOAD-STRESS DIAGRAMS FOR TOP OF SLAB S.

(5) Transactions American Society of Civil Engineers.

(6) Journal of the Engineering Institute of Canada.

(7) Bulletin on Flat Slabs by Corrugated Bar Co.

(8) Engineering and Contracting.

(9) Engineering News.

(10) Engineering Record.

(11) American Architect.

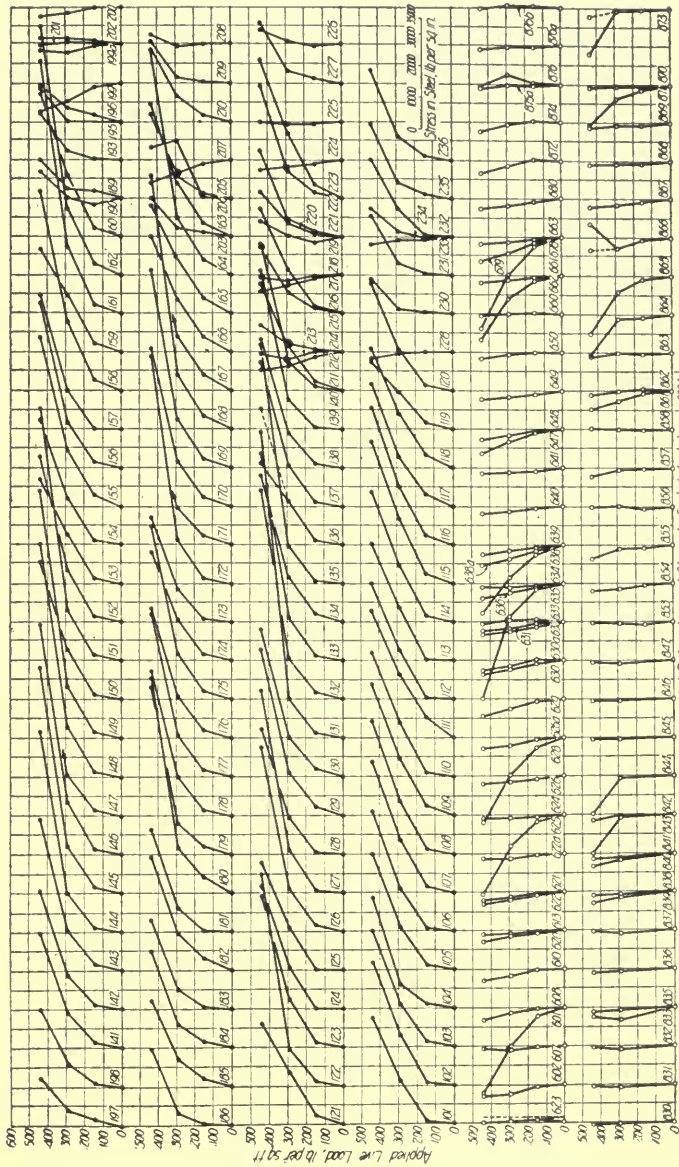
Applied Live Load, lb per sq ft
Unit Deformation and Stress to Scale Indicated
Stress in Steel, lb per sq in
Solid lines on steel
Dotted lines on concrete

FIG. B14.—LOAD STRAIN AND LOAD-STRESS DIAGRAMS FOR BOTTOM OF SLAB S.

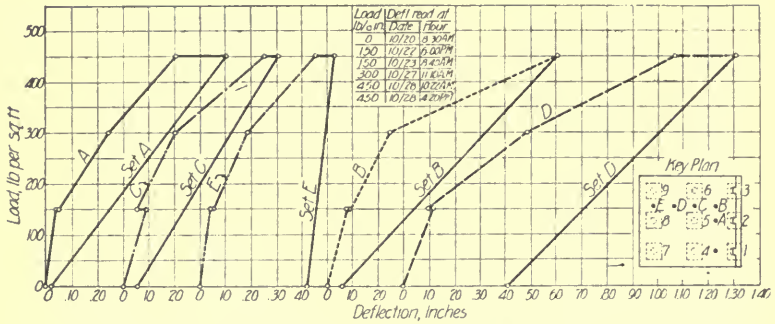

FIG. B15.—LOAD DEFLECTION DIAGRAMS FOR SLAB S.

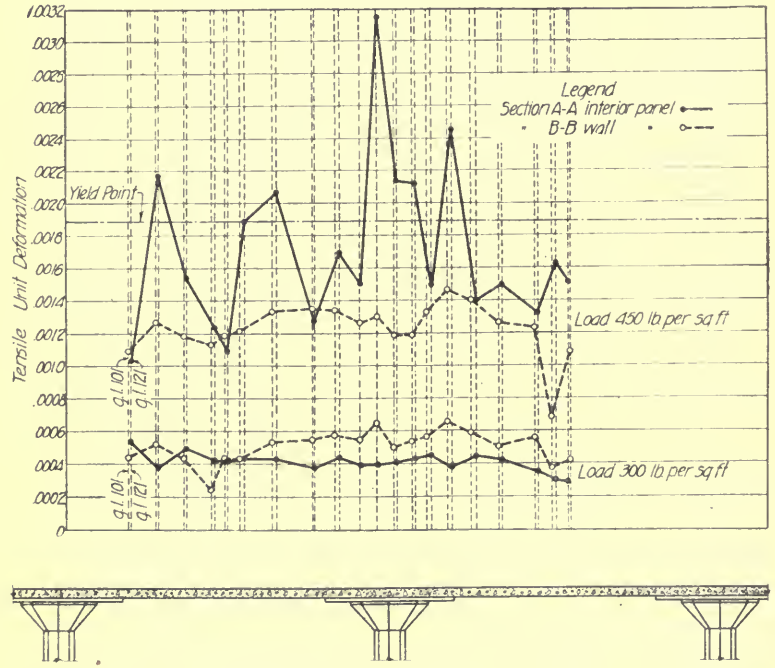

FIG. B16.—STRAIN DISTRIBUTION IN WALL PANEL AND INTERIOR PANEL OF SLAB S.

LIST OF TESTS.

1. C. Bach and O. Graf: Versuche mit allseitig aufliegenden, quadratischen and rechteckigen Eisenbetonplatten, Deutscher Ausschuss für Eisenbeton, v. 30, Berlin, 1915, 309 pp. These laboratory tests were made in Stuttgart, 1911 to 1914, under the direction of Bach and Graf. 52 slabs supported on four sides and 35 control strips supported as beams were tested to failure. The tests are reported in detail, without attempt, however, to explain or analyze the results. Analyses of the results have been made later by Suenson and by Nielsen; see E. Suenson, Krydsarmerede Jaernbetonpladers Styrke, Ingenioeren (Copenhagen), 1916, No. 76, 77, and 78; N. J. Nielsen, Krydsarmeredc Jaernbetonpladers Styrke, Ingenioeren, 1920, pp. 723-728.

2. Deere and Webber Building, Minneapolis, 1910, 4-way, 9 panels, (1) 1910, (2) Bull. 64, 1911, (9) 12-22-1910, (8) 12-22-1910.

3. Test of Rubber Model Flat Slab, 1911, 9 panels, (7) 1912, (1) 1912, p. 219.

4. Powers Building, Minneapolis, 1911, 2-way, 4 panels, (1) 1912, p. 61, (9) 4-18-1912, (10) 4-20-1912.

5. Franks Building, Chicago, 1911, 4-way, 4 panels, (1) 1912, p. 160.

6. Barr Building Test Panel, St. Louis, 1911, 2-way supported on beams, (1) 1912, p. 133.

7. St. Paul Bread Co. Bldg., 1912, 4-way, 1 panel, (5) 1914, p. 1376.

8. Larkin Building, Chicago, 1912, 4-way, 5 panels, (1) 1913, (10) 1-1913.

9. Northwestern Glass Company Building, Minneapolis, 1913, 4-way, 4 panels, (5) 1914, p. 1340.

10. Worcester (Mass.) Test Slab, 1913, (2) Bull. 84, 1916.

11. Shredded Wheat Factory, Niagara Falls, N. Y., 1913, 2-way, 9 panels, (1) 1914, (2) Bull. 84, 1916.

12. International Hall, Chicago, 1913, 4-way, 4 panels, (5) 1914, pp. 1433-1437.

13. Soo Line Terminal, Chicago, 1913, 4-way, 4 and 5 panels, (2) Bull. 84, 1916, (9) 8-16-1913.

14. Curtis Ledger Factory, Chicago, 1913, 2-way at columns, 4-way elsewhere, 4 panels, (2) Bull. 84, 1916.

15. Schulze Baking Co. Building, Chicago, 1914, 4-way, 4 panels, (2) Bull. 84, 1916.

16. Schwinn Building, 1914-15, long time test, 4-way, 1 panel, (1) 1917, p. 45.

17. Sears Roebuck Building, Seattle, 1915, 2-way, (4) Jan. and Feb., 1916.

18. Bell St. Warehouse, Seattle, 1915, 4-way, 4 panels, (4) 1916, (10) 5-13-16.

19. Eaton Factory, Toronto, Ont., about 1916, 4-way, 4 panels, (6) April, 1919.

20. S.-M.-I Slab, Purdue University (1917) circumferential reinf., 4 panels, (1) 1918.

21. Sanitary Can Building, Maywood, Ill., 1917, 2-way, 4 panels, (1) 1917, p. 172, and 1921, p. 500.

22. Shonk Building, Maywood, Ill., 1917, 4-way, 4 panels, (1) 1917, p. 172, and 1921, p. 500.

23. Western Newspaper Union Building, Chicago, 1917, 4-way, 4 panels, (1) 1918, p. 291, (2) Bulletin 106, 1918.

24. Slabs J and S, Purdue Univ., 1917, 2-way, 4 panels each, (1) 1918, p. 174, also 1921, p. 500.

25. Slab R, Purdue Univ., 1917, circumferential reinf., 4 panels, (1) 1917, p. 172.

26. Arlington Building, Washington, D. C., 1918, 2-way tile and concrete supported on beams. (Under preparation as Tech. paper of U. S. Bureau of Standards.)

27. Whitacre Test Slab, Waynesburg, Ohio, 1920, 2-way, tile and concrete, supported on beams, 18 panels, (11) 8-11-20 and 3-16-21 also under preparation as Tech. Paper U. S. Bureau of Standards.

28. Channon Building, Chicago, 1920, circumferential reinf. 4 panels, (1) 1921, p. 500.

29. Jersey City Dairy Company's Building, Jersey City, N. J., 1913, 2-way, 1 panel, tested by Corrugated Bar Co., Buffalo, N. Y., not published.

UC SOUTHERN REGIONAL LIBRARY FACILITY
A 001 293 368 5